A study of rock lenses in extensional faults, focusing on factors controlling shapes and dimensions

by

Merethe Lindanger

A thesis for the Candidatus Scientiarum degree
in petroleum geology/structural geology

Department of Earth Science
University of Bergen
April 2003

ACKNOWLEDGEMENTS

First of all I would like to thank my supervisor, Professor Roy H. Gabrielsen, for an interesting task for my thesis and for always being obliging. He has been an inspiring factor during this work through his enthusiasm for structural geology.

I would also like to thank all my fellow students, both geologist and non-geologists, for a great time at the university. A special thanks goes to my companions at 'Jomfruburet' for needful discussions and social activities. I would also like to thank Jill A. Clausen, Håkon Eliassen, Silje S. Berg and Tore Skar for constructive and pleasant companionship in the field.

Thanks are also expressed to Silje S. Berg, Jill A. Clausen, Rannveig Øvrevik, Jens Christian and Håkon Eliassen and for reading through and commenting upon my thesis in the final stages.

My utmost thanks go to Jens Christian who has always been there whenever needed, and for helpful discussions upon the thesis during these years.

Bergen, April 2003

Merethe Lindanger

ABSTRACT

The intension of this work has been to investigate the factors controlling the shapes and dimensions of horses, including the type of mechanism active in their generation and development, position of the horses relative to, or within, the fault core, the amount of displacement across a fault, and lithology. In addition it has been investigated if there is a linear relation between the three dimensions of the horses.

Rock lenses are carefully examined and measured in outcrops in three field areas, these being Frøya (island outside mid-Norway), Bornholm (Danish island) and Kilve (southern England), and in analogue plaster of Paris experiments. The rocks hosting the lenses consist of gneisses, nearly unconsolidated sandstones and limestones interbedded with shales, respectively.

The data of horses in this study support the proposal that the shapes and dimensions of horses are not completely arbitrary, but dependent on several factors. Horses occurring in fault cores tend to be thicker relative to length as compared to horses occurring in damage zones. Also the type of mechanism active in the generation of the horses is important for their shapes, where asperity bifurcation horses tend to be relatively thicker than horses generated as a result of segment splaying and amalgamation. Lithology seems to be a controlling factor upon the maximum sizes of the horses, where the largest horses are observed in ‘strong’ rocks, such as in gneiss and limestone interbedded with shales, whereas only relatively smaller horses are recorded in ‘weak’ rocks, such as nearly unconsolidated sandstones. The amount of displacement across a fault is another factor influencing the shape of the horses, where horses in faults with several meters vertical displacement tend to be thicker relative to length as compared to horses occurring in faults with less vertical displacement. The average horse in this study has a length that is ten times the thickness.

CONTENTS

Chapter 1

INTRODUCTION

1.1 Aim of the work

This thesis is part of the work for a Cand. Scient. degree in structural geology/petroleum geology at the Department of Earth Science at the University of Bergen. It presents the results of detailed measurements of horses (lensoid rock bodies) that appear in outcrops and in analogue plaster of Paris experiments. Professor Roy H. Gabrielsen has been my supervisor during this work.

The principal aim of this work has been to find out which factors influence the shape and dimensions of horses, including 1) the tectonic environment and 2) the type of mechanism active in generation and development of the horses. The latter is also related to a) the 'order' of the horses in context of their dynamic development, b) the position of horses relative to, and within, the fault core, and c) whether the horses occur in strain-hardening or in strain-softening fault zones. Furthermore, 3) the amount of displacement across the fault and 4) the lithology of the host rock are factors assumed to play an important role upon the shapes and sizes of horses. I will return to these factors in the discussion (chapter 5). The intension is to use the results obtained as input in numerical reservoir models.

Another aim has been to investigate whether or not there is a linear relation between the length and thickness of the horses. Hence, the horses are plotted in xy-diagram, and regression analyses have been performed. The measured length (l) has in some cases been projected parallel to the dip (a-axis) and/or strike dimension (b-axis; figure 1.2). In such cases the aim has been to investigate whether or not there is a difference between the shapes of the horses in these two dimensions.

Fieldwork includes measurements of horses on Frøya (central Norway, chapter 2.2), in Kilve (south-eastern England, chapter 2.4) and on Bornholm (Danish island south of Sweden, chapter 2.6). Measurements of horses generated in models of extensional faults in plaster of Paris have also been recorded (chapter 2.7).

1.2 The content of the thesis

The thesis has the following content:

Chapter 2: Description of each of the field areas together with the plaster of Paris experiments, emphasizing the description of the examined horses. Chapter 3: Presentation of the regression analyses and results obtained from the data of the horses. Chapter 4: Comparative analyses of the results obtained from the four datasets. Chapter 5: Discussion of the results in connection with the hypotheses. Chapter 6: The most important conclusions.

1.3 Previous work

The architecture of fault zones, in addition to related permeability structures, form primary controls on fluid flow in upper-crustal, brittle fault zones (Caine et al. 1996). The distinct components of fault zones are commonly that of a fault core, where most of the displacement is accommodated, and an associated damage zone that is mechanically related to the growth of the fault zone (Caine et al. 1996). However, elements such as segment splaying, linkage and ramping may cause both the damage zone and the fault core to be geometrically complex. Nevertheless, the intrinsic geometry of extensional faults is commonly dominated by lensoid rock bodies (horses), which may stack or overlap to constitute duplexes (Gibbs 1983, 1984) (figure 1.1). Horses are recorded from thrust regimes (e.g. Boyer & Elliot 1982) and strike-slip regimes (e.g. Woodcock & Schubert 1994), as well from extensional regimes (e.g. Gibbs 1983, 1984). Furthermore, horses are observed on all scales, from seismic scale, as first reported from extensional regimes by Gibbs (1983, 1984), and down to mm – cm scale (e.g. Gabrielsen & Clausen 2001). The horses may consist of undeformed to heavily fractured rocks (e.g. Koestler & Ehrmann 1991, Childs et al. 1996a), or may be entirely

dominated by fault rocks (Sibson 1977). The geometries of faults are recognized to be of importance due to the fact that they can control whether a fault zone act as a fluid conduit or barrier (e.g. Caine et al. 1996). To my knowledge a study of the dimensions of horses has not previously been presented in the literature.

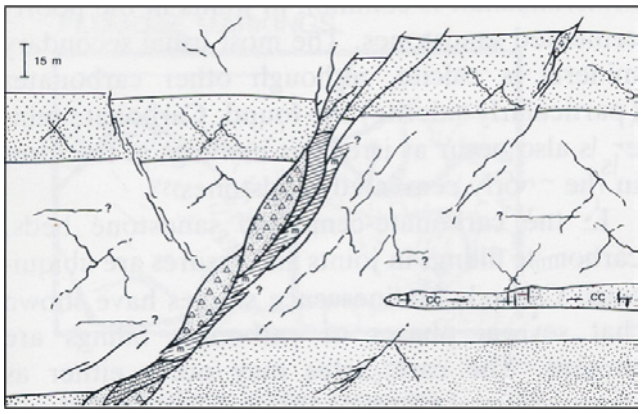

Figure 1.1 An example of an extensional fault where horses dominate the geometric elements. Modified from Gabrielsen & Koestler (1987).

1.4 Methods

The length and thickness of the horses are measured by use of a measuring tape. The length versus the thickness of each horse is then plotted in xy-diagrams, and regression analyses of the datasets are performed.

The intension of the work was initially to measure horses in three dimensions, these being the dip and strike dimensions and thickness. A record of three dimensions of the horses should make it possible to investigate whether or not horses have different shapes and sizes in the dip and strike dimensions. However, some horses are not exposed in neither of the dip or strike dimensions. In such cases, the length of the horses in the section was recorded, and the dip and strike dimensions were estimated. The thickness, on the other hand, is always measured. An exposed section of a horse is generally closer to one of the dip or strike dimensions than the other. The estimate of this dimension is then good, whereas the estimate of the other dimension is not. Due to this, the data of the horses are represented in three datasets.

In the first dataset both the dip and strike dimensions are estimated for horses exposed in sections between the two dimensions. As the estimate of one of the dimensions is generally poor, this dataset is considered the *least reliable*. The results of this dataset are presented in chapter 3.1.

The second dataset includes horses of which only one of the dimensions are represented. Because the other of the two dimensions, of which estimate is not satisfactory, is omitted, this dataset is considered *more reliable*. The results of this dataset are presented in chapter 3.2.

The third dataset include horses of which none of the dimensions are estimated. Instead the length of the horses, as it appears in the exposed section, is represented. Because no estimations have been done, this dataset is considered the *most reliable*. The results of this dataset are presented in chapter 3.3.

1.5 Terminology and definitions

A **horse** is a pod of rock completely bounded by two or more amalgamating faults (Dennis 1967, p.89). A horse most commonly has the shape of a lensoid body (Gabrielsen & Clausen 2001). Another definition is given by Nystuen (1989), who has defined a **horse** as a small thrust sheet bounded by thrust faults and located in broad movement zones between or within nappes.

A **duplex** is an array of overlapping horses (e.g. Gibbs 1983, 1984, Gabrielsen & Clausen 2001), shearing the same roof and floor faults (Boyer & Elliot 1982).

The **axes of the horses** referred to here are the **a-axis** (also referred to as the **dip dimension**), the **b-axis** (also referred to as the **strike dimension**), and the **c-axis** (**thickness**; figure 1.2). Sometimes the exposed section of the horses is neither in the dip or strike dimension. In such cases the **measured length (l)** of the horses is recorded. The angle between the a-axis and the studied section is then registered, and the a- and b-axes are estimated by use of the following equations:

$$\boxed{\begin{array}{l}\text{a-axis} = l \cos \alpha \\ \text{b-axis} = l \sin \alpha\end{array}}$$

If, however, α is less than 15^{o} to one of the axes, the measured length (l) is considered parallel to this axis (dimension). Further, the horses are assumed to be **symmetric**. Sometimes a horse is not fully exposed. Based on the assumption of symmetry, the considered half of the horses in such cases is then measured and thereafter multiplied with two.

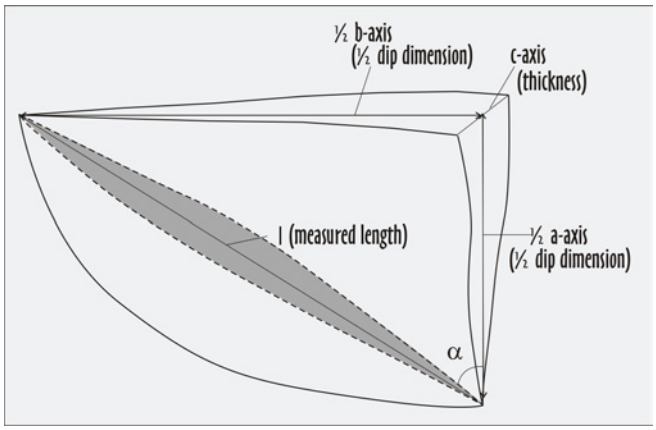

Figure 1.2 Sketch of the section of one fourth of a horse and the axes that are either measured or estimated. An example of how an exposed section of a horse may appear in the outcrop is shaded in grey. However, this section varies between the outcrops.

A set of horses often occurs within one larger horse, which is bounding them. This is because after establishment of a horse continued deformation may result in splaying of this into smaller horses. In such cases, the original horse is classified a **first order** horse, whereas the smaller horses it splits into are termed **second order** horses. Continued deformation may further splay the second order horses into third, and maybe fourth order horses and so on. I will return to this in the discussion (Chapter 5).

1.6 Uncertainties

In this thesis, the intension was to base the comparison between the horses on measures of the horses at their maximum dimensions. However, due to the fact that it is not always possible to know which section of the horses is exposed, one must assume that it is always minimum values of the axes that are measured (figure 1.3).

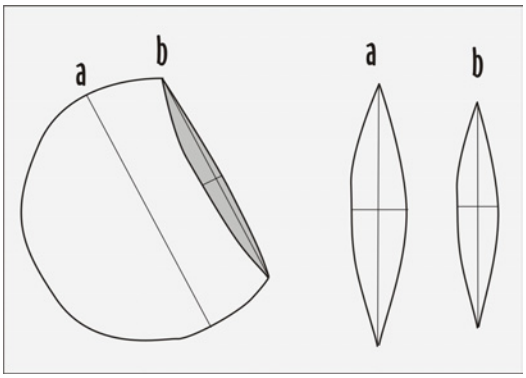

Figure 1.3 Sketch of a horse and two different sections, a and b, where a is a section of the full dimension of the horse, whereas b is an arbitrary section less than a.

Chapter 2

DESCRIPTION OF THE FIELD AREAS

This chapter presents a description of the localities, and more specifically the intrinsic architecture of the faults studied in field and in analogue gypsum experiments. I start with the description of the localities on Frøya, because the host rock for the horses (rock lenses) at these localities are the mechanically most competent of those treated in this study. Then follows a description of the localities in Kilve, where the host rocks are of medium mechanical strength, before I give a description of the localities and horses on Bornholm where the rocks are the mechanically less competent. Finally the gypsum experiments will be described, they represent the material of the absolutely weakest mechanical properties in this study. The aim of this chapter is to focus on how the horses appear in the field, and how their geometries differ according to the lithology in which they occur.

2.1 Regional geology of Frøya

The island of Frøya is situated outside the coast of Møre-Trøndelag, central Norway. The structural features on the island are assumed to be related both to deformations along the Møre-Trøndelag Fault Complex, a complex of which elements are identified between 61°40' – 64°20'N and 0° – 13°E (Gabrielsen et al. 1984, Blystad et al. 1995) (figure 2.1), and to deformations on the mid Norwegian shelf (Blystad et al. 1995, Grunnaleite & Gabrielsen 1995, Gabrielsen et al. 1999) (figure 2.1).

Geological development

The Møre-Trøndelag Fault Complex strikes ENE-WSW and parallels the coastline of mid Norway at its northeastern end. It continues offshore along the southern margin of the Møre Basin (Brekke & Riis 1987) and into the West Shetland Basin (Doré 1991,

Rattey & Hayward 1993, Doré et al. 1997). The complex is suggested to have originated in Precambrian (e.g. Seranne 1992), and since then acted as a zone of weakness separating the Møre Basin and Vøring Basin to the north and the northern North Sea to the south (Gabrielsen et al. 1999). Caledonian deformation led to N-S and NE-SW to ESE-WSW structural grain along the complex (e.g. Torsvik et al. 1989). Since Caledonian, the complex has been reactivated in several events, including WNW-ESE to NW-SE directed Devonian extension, which led to sinistral strike-slip movement along the complex and development of basins along the western coast of Norway (e.g. Anderson 1951, Oftedahl 1975), E-W to NW-SE directed extension in Carboniferous (e.g. Bukovics et al. 1984) and in Permo-Triassic (e.g. Færseth 1996), dextral strike-slip movement during late Jurassic – earliest Cretaceous (Grønlie & Torsvik 1989), and eventually two distinct phases of E-W to NW-SE contraction and inversion in Cretaceous and Tertiary (Gabrielsen et al. 1999) (figure 2.2). The complex is still tectonically active, and strike-slip faulting and contraction dominates the present activity (Fejerskov et al. 1995, Lindholm et al. 1995, Pascal & Gabrielsen 2001).

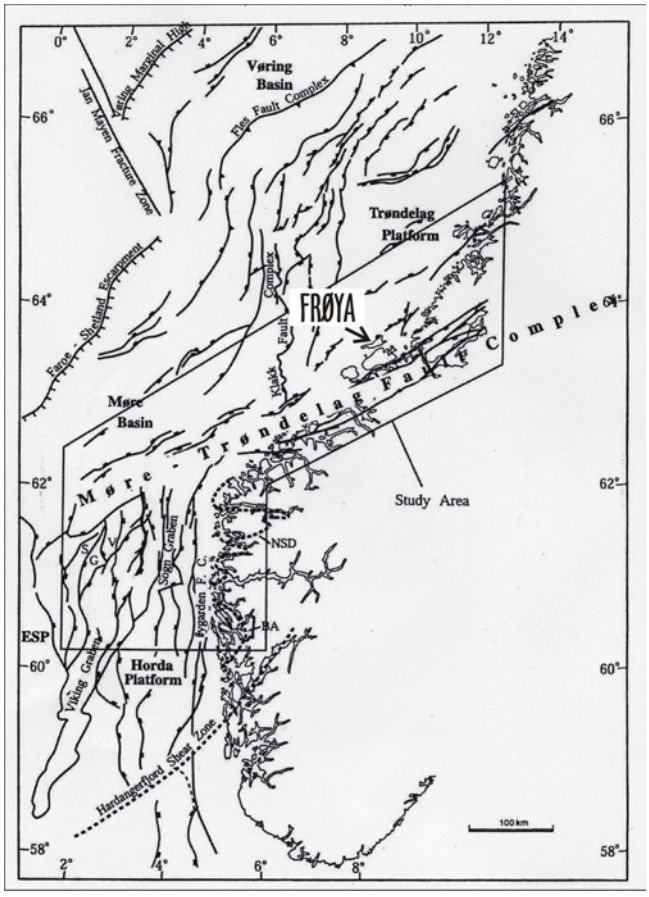

Figure 2.1 Main structural elements of the northern North Sea and the mid Norwegian shelf. Frøya is located at the border to the Møre-Trøndelag Fault Complex. After Gabrielsen et al. (1999).

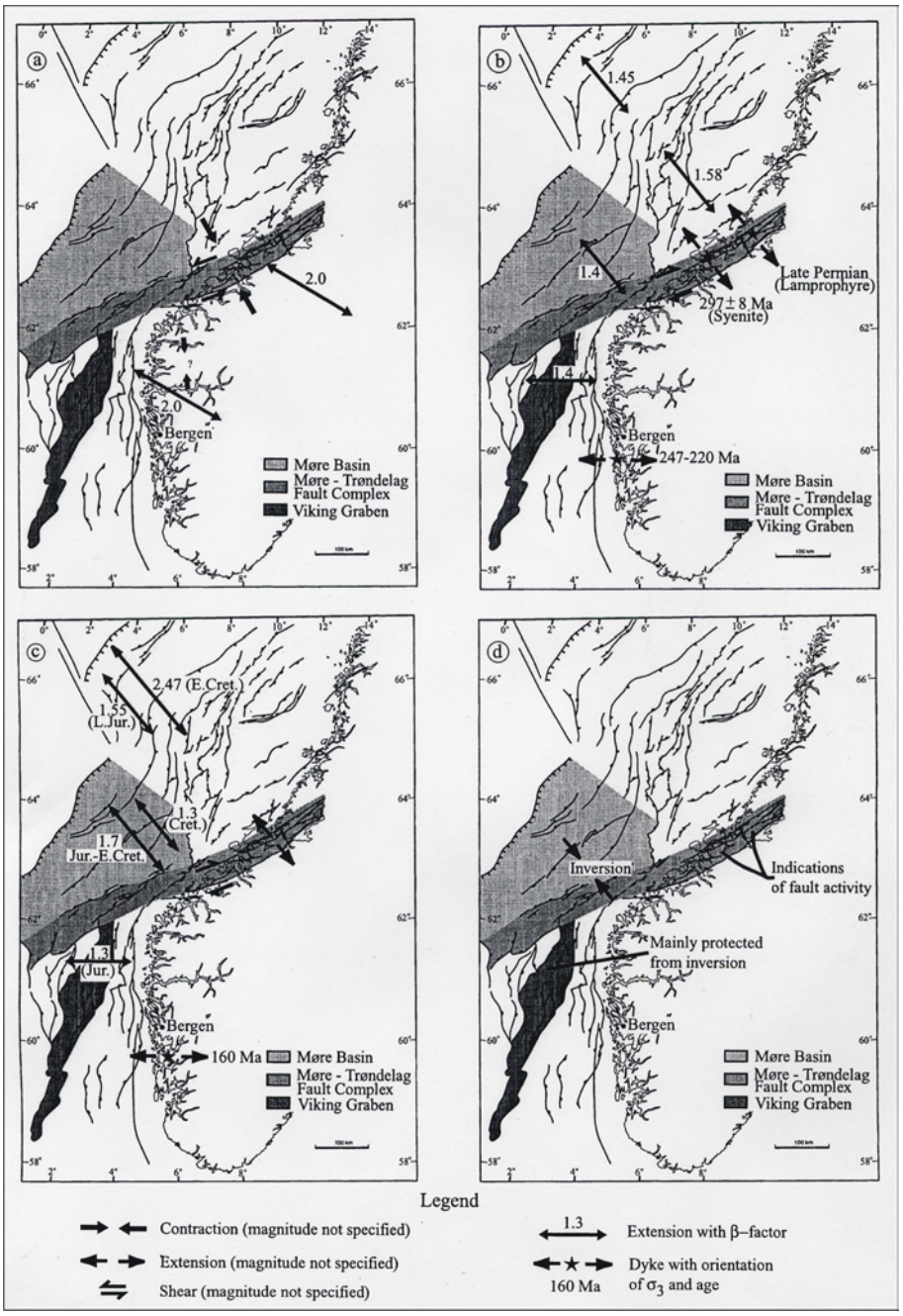

Figure 2.2 Stress situation and estimated stretching factors, northern Viking Graben, Møre Basin and Vøring margin for a) early Devonian, b) late Permo-Triassic, c) Jurassic-early Cretaceous and d) Tertiary. After Gabrielsen et al. (1999).

Lithology

The studied localities (figure 2.3) are situated within the Frøy Complex, where the rocks consist mainly of migmatitic gneisses intruded by granite/tonalite. The gneisses are

Precambrian, whereas the granites/tonalites are assumed to be of Caledonian age (Askvik & Rokoengen 1985).

Structural framework

Frøya is characterized by NE-SW to ENE-WSW oriented faults, that are part of the Møre-Trøndelag Fault Complex, in addition to NW-SE and WNW-ESE faults (Eliassen In prep). The faults generally show evidences for both normal and strike-slip movements.

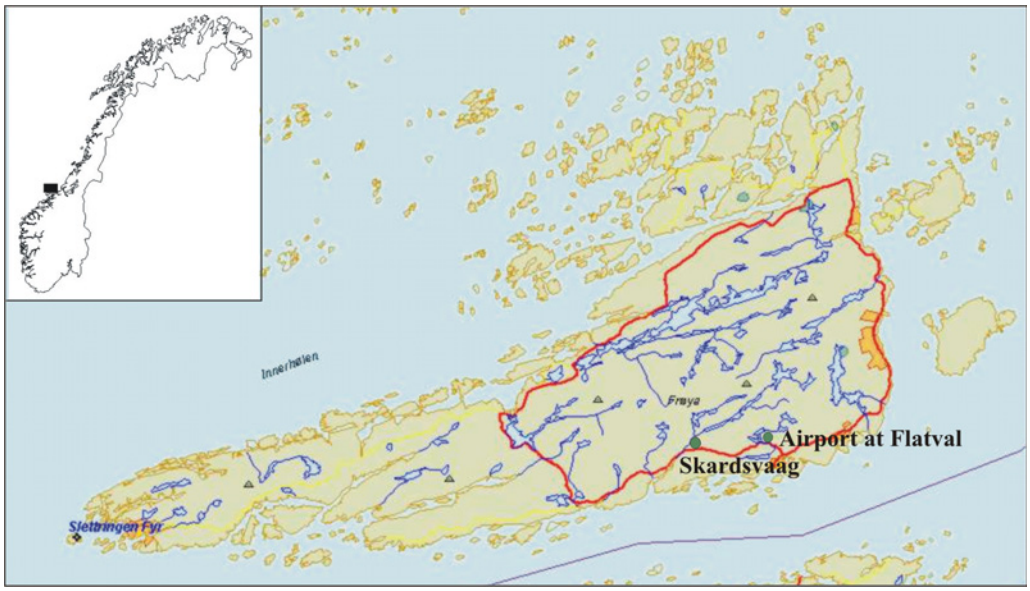

Figure 2.3 The island of Frøya, which is situated by the entrance to Trondheimsfjorden. The two localities on the island are situated at the local airport at Flatval and at Skardsvåg, respectively. Modified from Teleplan (2001).

2.2 Description of the localities on Frøya

The two localities studied on Frøya (Map sheet MR, zone 32) are both in road sections on the southeastern part of the island (figure 2.3), located within the same area mapped by Eliassen (In prep). In some areas the rocks are highly deformed and foliated, whereas the rocks in other areas are almost unaffected and the original grains are easy to identify. The foliation in the gneisses is ENE-WSW to NE-SW oriented (Eliassen In prep). The majority of the fractures are, on the other hand, NW-SE oriented.

Other work on Frøya includes Torske (1983) on studies of fluidization breccia in granite, Bering et al. (1986) on mapping of basement rocks, Gautneb & Roberts (1989) on petrochemistry, Nordgulen et al. (1995) on investigations of Caledonian granitoids, Braathen (1996) on mapping of fracture zones, Kyrkjebø et al. (2001) on the influence of transfer lineaments, fracture zones and basin master faults on the tectono-sedimentological development of the Mid-Norwegian shelf, and Eliassen (In prep) on mapping of lineaments and fractures.

2.2.1 Airport at Flatval

One of the localities on Frøya is situated near the local airport, about 1.5 km northeast of Flatval (UTM 878 632, see figure 2.3), a village at the southeastern coast of the island. The rocks in this locality are exposed along an approximately 100 m long E-W oriented road section. The studied section at this locality (figure 2.4) is about 7 m long and 1.5 m high, and exposes a N-S oriented system of fractures including two faults. Horses occur within one of these faults.

The rocks in the locality consist of a mixture of mainly foliated migmatitic gneisses and pegmatites that are highly fractured (figure 2.4). The fractures are nearly vertical and strike N-S. Some of the fractures are faults, showing normal displacement with a vertical displacement in the order of 0.5 m (figure 2.4). Due to the complexity in this outcrop it is hard to correlate marker horizons on each side of the fractures and it is therefore difficult to determine the vertical displacement across the fault. Unfortunately, no slickenlines have been observed on the fault plane, such that the direction of movement is also unknown.

The bulk fracture frequency along the section is about 15 per m, except for a pegmatite body where the fractures are more sparsely spaced and the frequency is about 4 per m (Eliassen In prep). There is no significant difference between the fracture frequency in the fault core and the rocks nearby. The fractures in this locality are planar to curviplanar and have caused the rocks to be sheetlike and tabular, and indicate that this is a shear zone where the rocks are more highly strained than the rocks in the vicinity of the zone.

There are two main faults in the locality. The one to the west is characterized by fault gouge and is assumed to have undertaken more movement as compared to the other main fault. Focus was attained to the other main fault. This fault is vertical and strikes N-S and displays a complex fault core. Lack of correlation markers across the fault and limited vertical exposure makes it impossible to establish the relative movement an the amount of throw of the fault. Nevertheless, due to the steepness of the fault it may be treated as a strike-slip fault. The horses seem to be constrained within the fault core.

The fractures in the road section extend beyond the studied section (figure 2.4), and it is likely that more than one fault branch contribute to the total damage zone. This makes it difficult to determine the width of the damage zone for this specific fault. Hence, the deformation seems to have been distributed along several planes, and irregularities affiliated with the different planes have caused the damage zone to thicken and to develop fault horses (rock lenses). Because of the thickness of the damage zone the fault zone seems to have undergone strain hardening (chapter 5).

Figure 2.4 Locality at Flatval, photo taken towards the south. N-S oriented systems of fractures, including two complex faults, one of which is characterized by horses, the other by fault gouge. The rocks in this locality mainly consist of migmatitic gneisses (dark grey) and pegmatite (pink). The arrows in the eastern part point at some small faults with vertical displacement of approximately 15 cm, showing normal displacement.

2.2.2 Studied horses in locality at Flatval Airport

The studied horses in this locality are constricted to the fault core (figure 2.4). The fault core is 1.3 m thick, and the rocks here consist of a mixture of migmatitic gneisses and pegmatites in accordance with the rocks outside the core. The thickness of the horses varies considerably across the core, and decreases from the more eastern parts of the

zone to the more western parts. In the eastern part of the core the horses are relatively thick (figure 2.5) with a thickness (c-axis) of about 20 cm and a length in the dip dimension (a-axis) of about 1 m (see chapter 1.5 for axis notation). In contraire to the horses in the eastern part of the core, the horses in the more western part are extremely thin and flattened (figure 2.6). The typical thickness of these horses is less than 10 cm. None of the horses in the western part of the core are exposed in full length in the dip dimension (a-axis), and even if they are measured to be at least 1.5 m, which is the length of the outcrop in the dip dimension that is exposed, the horses are probably considerable longer in this dimension, maybe as much as two-three times the mentioned length. Tabular fracturing often occurs in shear zones, which are more high-strained than the rocks adjacent to the zone. Most of the movement therefore seems to have occurred in the western part of the fault core, where the slimmer horses appear.

Figure 2.5 Detailed picture of the horses in the eastern part of the fault core marked in figure 2.4. The horses have a thick character compared to the horses in the opposite part (figure 2.6). Same scale as in figure 2.6.

Figure 2.6 Detailed picture of the horses in the western part of the fault core marked in figure 2.4. The horses are extremely thin and stacked in a shell-like manner. Hammer is used as scale.

Both the relatively thicker horses (figure 2.5) and the slimmer ones (figure 2.6) are exposed in a section that is vertical, i.e. parallel to the fault plane. The horses are fully overlapping each other and they are stacked in a shell-like manner. The dataset of the horses measured in the locality are plotted in figure 2.7. The R^2-value (see chapter 3.1 for explanation) for the plot, which is 0.36, indicates that the data points representing the horses are poorly constrained to the regression line. This further implies that there is a weak, but satisfactory relation between the length and thickness of the horses.

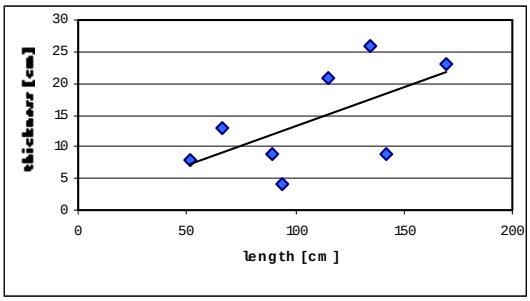

Figure 2.7 Plot of the length versus the thickness for the horses examined in the locality at Flatval. N = 8, and R^2 = 0.36.

2.2.3 Skardsvåg

The other locality (UTM 847 628) that is studied on Frøya is found about 3 km west of the first locality and is situated near a road cross leading to Skardsvåg, which is a village on the southern coast of the island. Similar to the first locality (figure 2.3) on Frøya, this second locality is also situated in a road section (figure 2.8). The fault transects rocks of similar type as in the locality at Flatval, consisting mainly of foliated migmatitic gneisses intruded by pegmatite. However, they are not as heavily fractured as the rocks in the first locality.

The outcrop in this locality exposes a large normal fault striking NW-SE with a dip of about 80^o towards the SW. The damage zone extends at least 5 m on each side of the fault. From correlation of possible marker layers on both sides of the fault a vertical displacement in the order of 5.3 m has been estimated (Eliassen In prep). Slickenlines found on one of the surfaces in the fault core indicates that the movement along the fault has been oblique.

The largest horses in the locality are up to at least 10 m measured in the vertical direction, and the maximum thickness is 2.5 m. These horses can best be seen when looking at the locality from the west (figure 2.9). Moving into the more central parts of the damage zone, the horses are smaller with lengths in the dip dimension varying between 2 and 4 m and with thickness up to about 1 m. These horses can best be seen when looking at the locality from the southeast (figure 2.11). Most of the horses associated with the fault are, however, found in the most central parts of the fault core. These horses are the smallest studied in this locality, with lengths in the dip dimension (a-axes) less than 4 m and with thickness less than 0.2 m (figure 2.11).

The largest (figure 2.9) and the medium sized horses (figure 2.10) appear in both the hanging wall and in the footwall of the fault, whereas the smallest horses studied in this locality appear within the fault core (figure 2.11). One of the medium-sized horses (horse 3, figure 2.10) fills the entire fault core, and is less than 1 m thick. The mentioned medium-sized horse consists of several small horses that contribute to the majority of the horses in the dataset from the locality.

The movement across the fault has been distributed on several planes, probably due to thickening of the zone during faulting because of irregularities on the fault planes and development of the horses (chapter 5.2). This thickness of the damage zone indicates that the rocks have undergone strain hardening during faulting (chapter 5.5).

Figure 2.8 Overview of the locality at Skardsvåg (UTM 847 628). The photo is taken towards northwest and shows an oblique fault striking NW-SE and dipping towards the SW. The rocks primarily consist of migmatitic gneisses (dark grey) intruded by pegmatite (pink).

2.2.4 The horses examined at Skardsvåg

Five of the horses in the locality at Skardsvåg are defined by fault planes striking E-W (figure 2.9). These horses are termed first order horses (chapter 1.5) and represent the largest horses studied at this locality. None of them are exposed in full length in the dip dimension due to vegetation and rock avalanches, but the majority must be at least 10 m in this dimension, which is the height of the outcrop in this locality. The thickness (c-axis) varies between 1 m and 6 m. Limited access to the horses due to their sizes and the steepness of the outcrop makes it difficult to measure the horses in the dip dimension (a-axis) and in thickness (c-axis). The horses were therefore measured from at distance using a measuring tape as an indicator. A system of fractures defining large lensoid bodies is present across the entire damage zone, and they cut through the fault core as well as the hanging wall and the footwall. However, because they are large compared to the rest of the horses in this locality and because the measures of them in the dip dimension (a-axis) and their thickness (c-axis) are not accurate, they are not included in the dataset representing the horses in this locality.

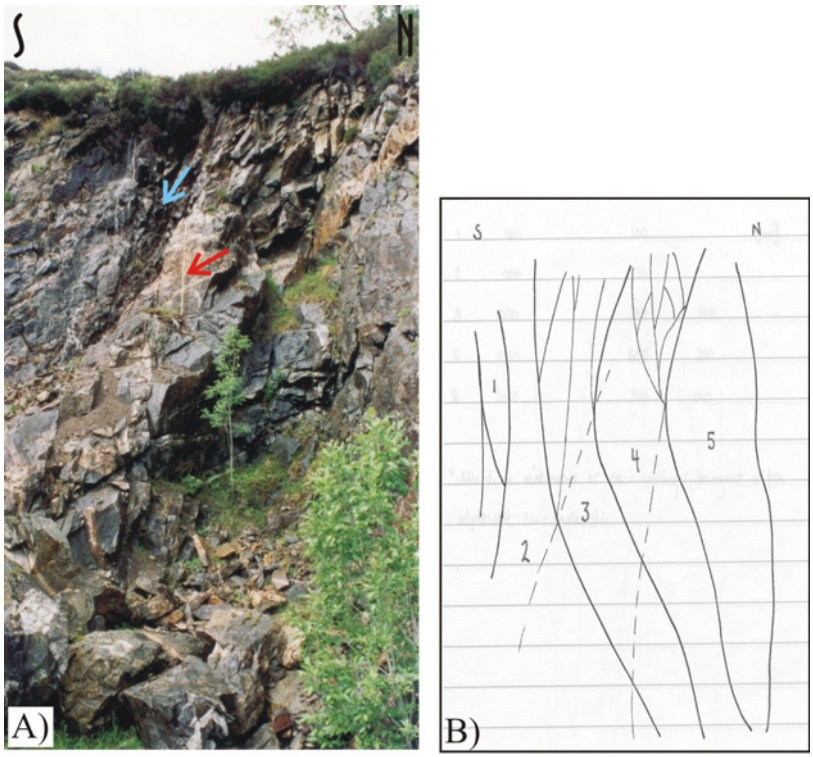

Figure 2.9 A) Large, first order horses in the locality at Skardsvåg, photo taken towards the west. The red arrow in the picture is pointing at a 2 m long measuring tape, the blue at the fault core. Fault planes striking E-W define the horses transverse to the wall of the cliff. B) Sketch of what is seen in A.

In the fault core several fault planes that further subdivide the large horses described in the previous section can be distinguished. These faults strike NW-SE and six medium sized, and over-lapping horses are seen (figure 2.10). The fault planes separating the medium-sized horses are oriented different than the fault planes defining the largest horses, cutting the largest horses into smaller ones. The medium-sized horses are best seen when looking in a northwestward direction. The horses are termed second order horses because they were probably initiated after the large, first order horses, sometimes cutting those into smaller units. The vertical dimensions of the medium-sized horses vary between 2 m and 4 m, and the thickness of these horses is less than 1.2 m. The medium-sized horses are stacked beside each other in a zone that is 3 m wide. The overall overlapping of the horses is generally right-stepping (figure 2.10).

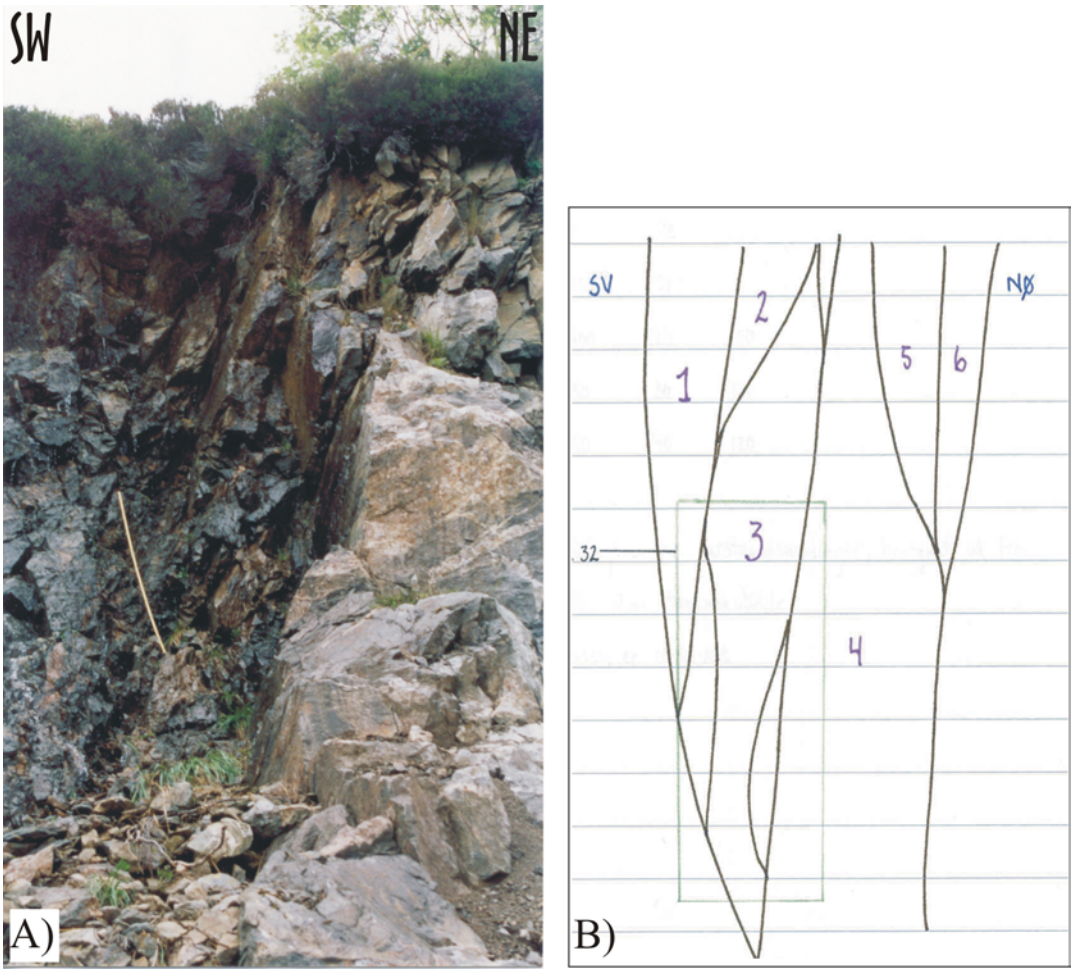

Figure 2.10 A) View of the medium sized horses in the locality at Skardsvåg. Photo is taken towards the NW and shows faults striking in a NW-SE direction defining horses of second order in this locality. A measuring tape of 2 m is placed in the fault core and is used as scale. B) Sketch of the six third order horses studied in the locality and the faults that define them.

As already mentioned, some of the horses in the locality at Skardsvåg are classified as first and second order horses. Following this hierarchy, however, the majority of the horses studied at this locality should be classified as fourth order horses. These horses occur in the fault core, within three horses classified as third order horses (figure 2.11), and they are the smallest horses to be distinguished in this locality. They are classified as third order horses because they probably developed after the establishment of the first and second order horses, and separating these into smaller units. The fractures or faults that are defining the third order horses are mainly striking WNW-ESE, although some strike in a more N-S direction. The measured length of the third order horses varies between 21 cm and 3 m. The thickness (c-axis) of these horses is between 4 cm and 22 cm. The geometrical stacking of the third order horses seems random, although the majority of the horses are right-stepping (figure 2.11B). In contraire to the horses of first and second order, the third order horses are less stacked beside each other and instead more distributed along the fault core, the zone in which they occur. Three third order horses (horse 1, 2 and 3) and fifteen fourth order horses (horse 4-18) were examined in the locality. A high R^2-value for the plot of the horses (figure 2.12) implies that that the horses, represented by the data points, are satisfactory constrained to the regression line. This further implies that there is a good relation between the length and the thickness of the horses.

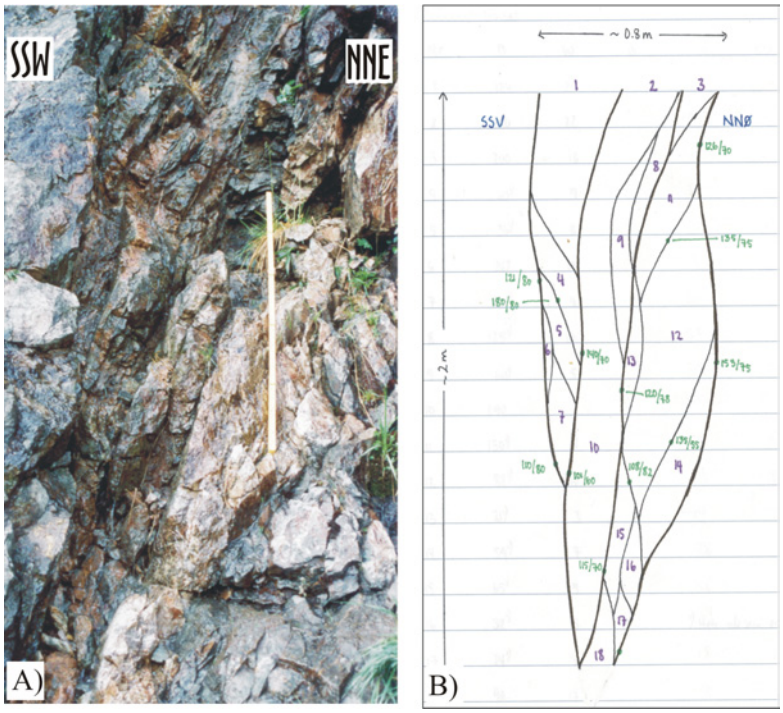

Figure 2.11 Overview of the smallest, third order horses that appear within the fault core of the fault in the locality at Skardsvåg. A) The picture is taken towards the WNW and show WNW-ESE striking faults defining the horses. The scale in the picture is 1 m. B) Systematic sketch of the lower part of the fault core and the horses appearing within the core as seen in the picture in A. Measures of the fault planes defining the faults are shown in green.

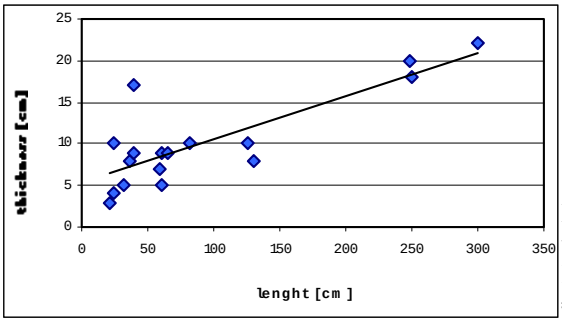

Figure 2.12 Plot of the measured length versus the thickness of the third and fourth order horses examined in the locality at Skardsvåg. N = 18, and $R^2 = 0.67$.

2.3 Regional geology of the Kilve area

Kilve beach is situated on the southern margin of the eastern branch of the Bristol Channel Basin (figure 2.13), a basin which forms part of a series of Mesozoic Grabens in southern England (e.g. Whittaker & Green 1983, Loyd et al. 1973, Kamerling 1979, Chadwick 1986).

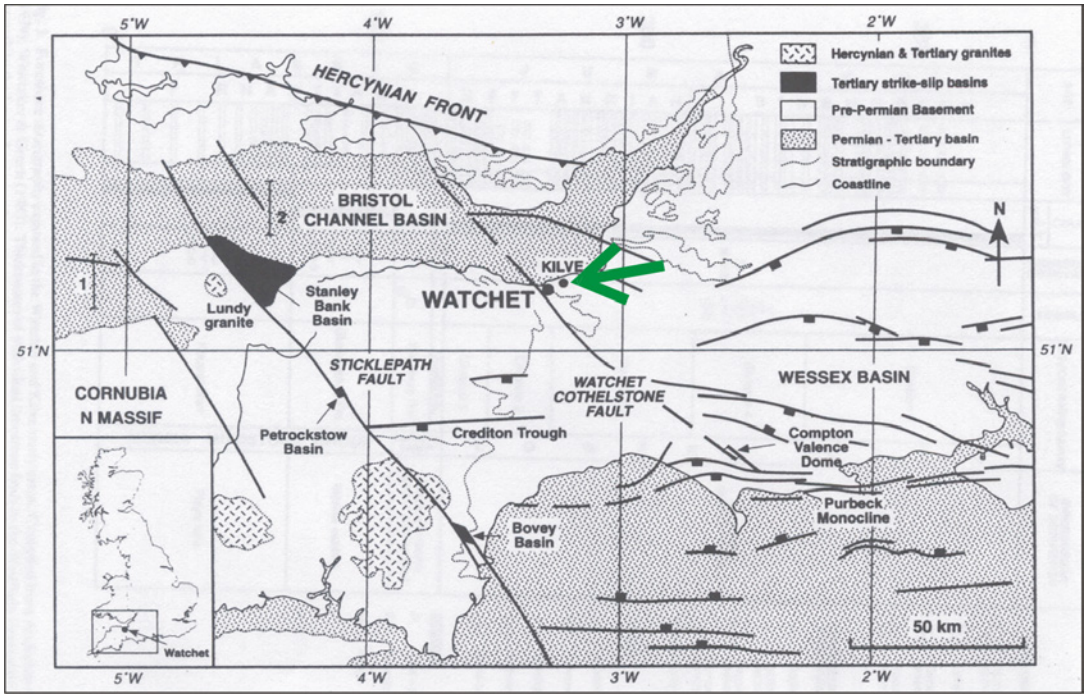

Figure 2.13 Structural framework of southwest England and the location of Kilve. The fieldwork was carried out on Kilve beach, about 2 km north of the center of Kilve. From Dart et al. (1995).

Geological development

There are no direct evidences for pre-Variscan structures within the Kilve district (Whittaker & Green 1983). Apart from possible strike-slip faulting during the Variscan orogeny due to compression (Holloway & Chadwick 1986), the area has been subjected to three main tectonic events. First there was three phases of N-S oriented extension during the Permian – Late Cretaceous, developing E-W oriented extensional faults. The first of these phases occurred in the Permian and the second in the Lower Jurassic (Hettangian – Sinemurian) (Kamerling 1979, Chadwick 1986). In between the first and second phase of extension there was a regional transgression at the end of Triassic. The third phase of extension took place during the Upper Jurassic (Kamerling 1979, Chadwick 1986). After the period of extension, some of the extensional faults in the Bristol Channel Basin were inverted during the Tertiary due to N-S compression (Dart et al. 1995). Finally, the partially inverted extensional faults were offset by NW-SE trending dextral, and NE-SW trending sinistral strike-slip faults, also in response to N-S oriented compression (Dart et al. 1995).

Structural framework

As a result to the tectonics in the area through time, extensional, contractional and strike-slip faults are present, exposed in cliffs and on the beach surface along the Somerset coast, which is almost parallel to the main fault trend of the basin. The faults are both of seismic and sub-seismic scale.

Lithology

The bedrocks in the study area consist entirely of Lower Jurassic Blue Lias strata, which are characterized by a cyclic pattern of sedimentation, which, in its fullest expression, is represented in upward order as shale, mudstone, limestone and mudstone (Whittaker & Green 1983). The shale, which has a sharp base, is deposited during rapid transgressions, the mudstones is caused by pulses of sediments, whereas the limestone is deposited in periods of shallow water conditions (Whittaker & Green 1983).

The Bristol Channel area with its excellent exposures and easy accessibility has been visited by several research groups. Earlier studies on the Kilve beach include e.g. Peacock & Sanderson (1991, 1993) on analysis of displacement, segment linkage and relay ramps, Peacock & Zhang (1993) on oversteps and bends along normal faults, Steen et al. (1998) on small faults for predicting fault distributions, Bixler et al. (1998) on the origin of magnetization and geochemical alteration in a fault zone, Kelly et al. (1998) on studies of conjugate strike-slip faults, Stewart & Argent (2000) on normal fault array polarity and detachments, and Peacock (1996) on fault patterns at different scales.

2.4 Description of the localities in Kilve

The localities studied in South-England are situated at the Kilve Beach, which is about 2 km north of the center of Kilve (Map sheet ST, zone 04/14). The beach is facing towards the north and the E-W oriented Bristol Channel Basin (figure 2.13). The rocks comprising the beach consist primarily of limestone benches, whereas the cliffs consist of organic-rich shales interbedded with argillaceous limestone. The area has numerous E-W striking normal faults as well as reverse-reactivated normal faults, reverse faults and strike-slip faults. Some of the faults can be studied in the dip, and sometimes in the strike dimensions, in the cliffs, and some may be studied in the strike dimension in horizontally exposed outcrops at the beach surface. Three faults are examined in the Kilve area in this study. The first two faults are examined in locality 1 and 2, respectively, whereas the third fault is found in locality 3, where it is exposed horizontally at the beach surface (figure 2.14). The localities are also examined by Skar et al. (In prep), and numerous other researchers (see introduction).

2.4.1 Locality 1 (Kilve Pill)

Locality 1 is situated about 10 m east from where the main path from the center of Kilve enters the beach (figure 2.14). The studied section in this locality is to be found within a cliff that is pointing towards the north (figure 2.15). The fault can be studied from both the eastern and the western side of the cliff. However, because the majority of the

horses that occur within the fault appear on the western side, focus was given this side. The outcrop in the locality is sub-vertical and the fault is exposed along a 10 m high and 15 m long section (figure 2.16).

The rocks hosting the fault and the horses associated with the fault consist primarily of organic-rich shales interbedded with limestone benches. The layers are dipping towards the south with an average angle of 15^{o} in both the hanging wall and the footwall, indicating that no significant rotation of the layers have occurred during faulting.

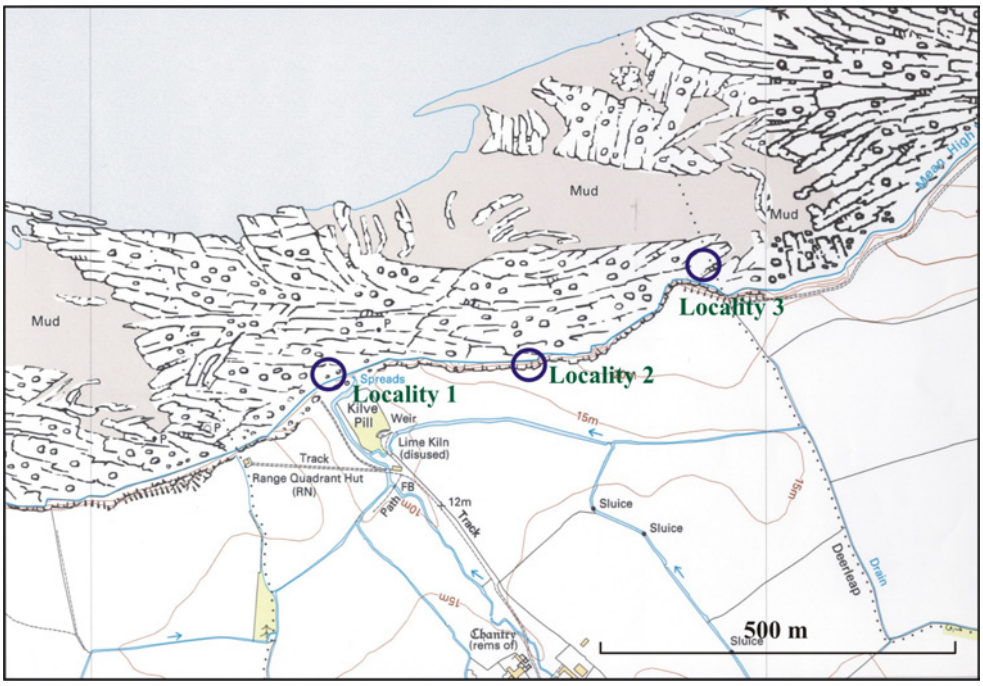

Figure 2.14 Map of Kilve Beach (1: 5000) showing the position of the three localities that were studied. Locality 1 and 2 are located within the cliffs, whereas locality 3 is located on the beach surface. Supplied by National Map Centre of Great Britain (2002).

The fault that appears in the locality strikes E-W and has an average dip of 40^{o} towards the north. Some of the limestone beds can be correlated across the fault, estimating the normal displacement of the fault is 19 m. Slicken-lines found on some of the fault surfaces show a pitch varying between 70^{o} and 90^{o}, indicating that movement has occurred sub-parallel with the dip direction and that the fault is a normal fault. Normal drag structures in both the hanging wall (figure 2.17) and in the footwall (figure 2.18) support that the fault is a normal fault. Indicators of reverse reactivation of the fault is found in the eastern side of the cliff, but is not observed in the western side examined in this study.

The damage zone of the fault is about 1 m thick in both the hanging wall and in the footwall, and is defined by numerous small-scale shear and tension fractures. The fractures vary in orientation, but two main directions can be distinguished, namely E-W and N-S (Skar et al. In prep). The displacement of the damage zone shear fractures is less than 10 cm, and most of the movement along the fault has therefore occurred along the main fault plane. A narrow fault core and damage zone as seen in this outcrop is typical of rocks having undergone strain-softening deformation.

Figure 2.15 Parts of The Kilve Beach where the fieldwork was carried out. The picture is taken towards the east and shows an overview of the tidal zone and the cliffs hosting the faults examined in this study. Locality 1 and 2 are sub-vertical sections within the cliffs, whereas locality 3 is at the tidal surface in a horizontal section.

The thickness of the fault core varies between 4 cm and 70 cm and is very distinct throughout the exposed cliff section (figure 2.17 and 2.18). The rocks comprising the fault core consist particularly of competent limestone in addition to organic-rich shales. In the upper parts of the section the fault core is considerably thinner and the limestone and the shale comprising the zone have a fabric parallel to the fault plane (figure 2.17). In the lower parts of the section two horses consisting of limestone are present within the fault core, and due to the two horses the fault core is thickest in this part (figure 2.18).

2.4.2 The horses examined in locality 1

The horses in locality 1 are evident throughout the fault, mainly in the footwall, but also in the hanging wall and in the fault core. The horses in the upper part of the section only occur in the footwall of the fault (figure 2.19). A limestone bed is present in the uppermost part of the section, though most of the rocks hosting the horses in the upper section consist of organic-rich shales. The horses comprise a part of the footwall that is about 0.5 m thick. The majority of the horses in this locality occur in the upper part of the section. Here, part of a horse is seen in the fault core, and this horse consists of limestone that is internally deformed. The horse is defining the fault core and occurs in the hanging wall of the main slip plane of the fault. The fault in the upper part of the section can be studied mainly in the dip dimension due to the steepness of the section.

Figure 2.16 Overview of locality 1 on The Kilve Beach. The picture is taken towards the east and shows an E-W striking normal fault dipping towards the north. Horses occur within the fault in the hanging wall and in the footwall as well as in the fault core. The rocks hosting the fault consist of organic-rich shales and beds of limestone. The layering is dipping towards the south, and show normal drag in both the hanging wall and the footwall.

Fewer horses are present in the lower part of the section, and they are evenly distributed in the hanging wall and in the footwall (figure 2.20). Horses also comprise the fault core, similar to the upper section. Contrary to the fault core in the upper part, one horse is present in the footwall of the main slip plane. The horses in the hanging wall are more evenly distributed and less overlapping as compared to the horses in the footwall, and

they are clearly left-stepping. The horses in the footwall comprise a wider zone compared to the horses in the hanging wall. A cave in the lower part of the section (figure 2.21) makes it possible to study some of the horses in the strike dimension (b-axis) in addition to the dip dimension (a-axis) and the thickness (c-axis).

Figure 2.17 Normal drag structures, especially visible in the limestone beds, seen in the hanging wall in the upper part of the section in locality 1. The fault core is thin compared to the lower part of the section, and the rocks comprising the core have a fabric parallel to the fault plane.

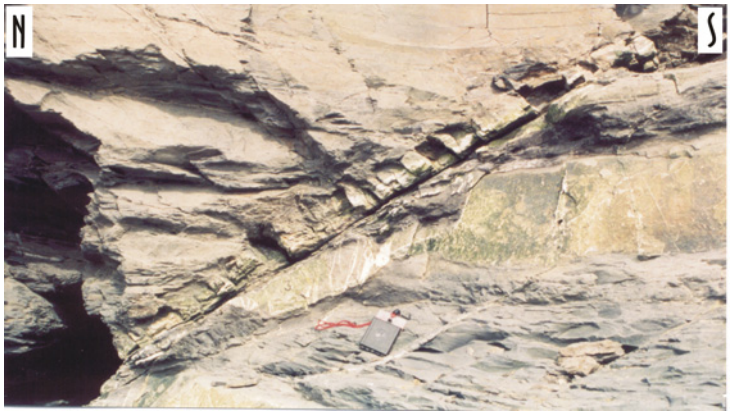

Figure 2.18 Normal drag structures in limestone bed in footwall. The fault core in the lower part of the section is thick compared to the fault core in the upper part due to the presence of limestone horses within the core. Compass used as scale.

Six of the horses in locality 1 are situated in the hanging wall (figure 2.20). These horses vary between 43 cm and 135 cm in the dip dimension, and are between 8 cm and 26 cm thick. The hanging wall horses are developed in the organic rich shale. However, as previously mentioned, the majority of the horses in locality 1 are located within the footwall (figure 2.19).

The footwall horses vary between 29 cm and 165 cm in the dip dimension, while their thickness varies between 4 cm and 29 cm. The footwall horses therefore cover a larger range than the hanging wall horses, both in thickness and in the dip dimension. The horses situated in the footwall cut mainly through organic rich shales, but they also cut through two limestone beds, which are 20-30 cm thick (figure 2.19).

Two horses can be recognized within the fault core. One of these horses can be seen in full, and the length in the dip dimension of this horse is 2 m and the horse is 17 cm thick. Only parts of the second horse in the fault core are visible, and the exposed length in the dip dimension is 3 m, and the thickness is 16 cm. Based on the assumption that the horses are symmetric (chapter 1.5), the second horse may be as long as 6 m in the dip dimension, which is twice the observed length. Compared to the thickness the horses in the fault core are considerably longer in the dip dimension than the horses appearing in the hanging wall and in the footwall. The horses in the fault core consist of limestone and display a high degree of internal deformation as evidenced by numerous cross-cutting calcite-filled fractures (Skar et al. In prep). The horses are probably parts of the limestone beds that have been cut of and dragged into the core, as seen in figure 2.22.

In view of the fact that the outcrop is nearly vertical, the horses in locality 1 are poorly exposed in the strike dimension. Nevertheless, three of the horses in the hanging wall and one of the horses in the fault core could be measured in the strike dimension due to the presence of a cave in the lower part of the section (figure 2.21). The three horses in the hanging wall vary between 43 cm and 102 cm in the dip dimension, whereas the same three horses vary between 125 cm and 304 cm in the strike dimension. The thickness of the horses vary between 6 cm and 26 cm. Based on these three horses, the horses thereby seem to be considerable longer in the strike dimension as compared to the dip dimension, maybe by an amount of 3 times the dip dimension. The fault core horse that can be measured in the strike dimension in the cave is minimum 3 m in the dip dimension, but may be as much as 6 m (see above). Half of this fault core horse is exposed in the strike dimension in the cave, but the total length estimated to 316 cm. Hence, the fault core horse seems to be longer in the dip dimension than in the strike dimension, which is contrary to the horses in the hanging wall that were measured in the strike dimension in the cave.

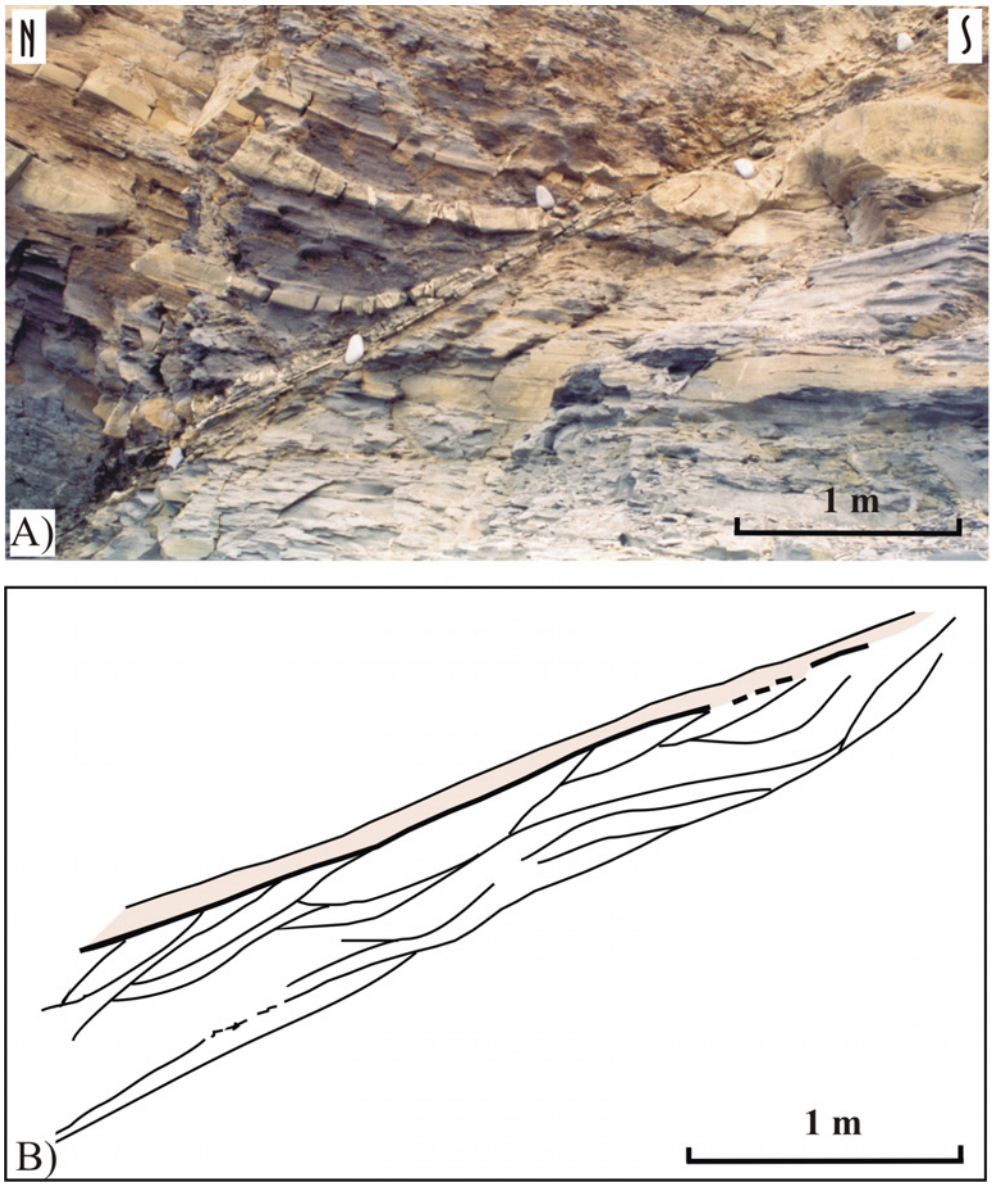

Figure 2.19 A) Picture of the upper parts of the exposed section in locality 1 on Kilve Beach taken towards the east. The horses occur only in the footwall where they comprise a zone that is 0.5 m. The horses cut through primarily organic rich shales, but also through a more competent limestone bed (upper right corner). B) Systematic sketch of what is seen in A. Fault core is shaded in pink.

The thickness of the fault core matrix that separates the horses in locality 1 is generally between 0.1 cm and 0.8 cm, both for the horses in the hanging wall and in the footwall. The horses commonly overlap by an amount of 20-50 cm in the dip dimension, which is 20-90% of the length of the horses in this dimension. The horses in locality 1 are more evenly distributed alongside the fault. The majority of the horses in the lower part of the section are left-stepping, except for the horses in the fault core, which are right-stepping with an overlap of ca. 1 m.

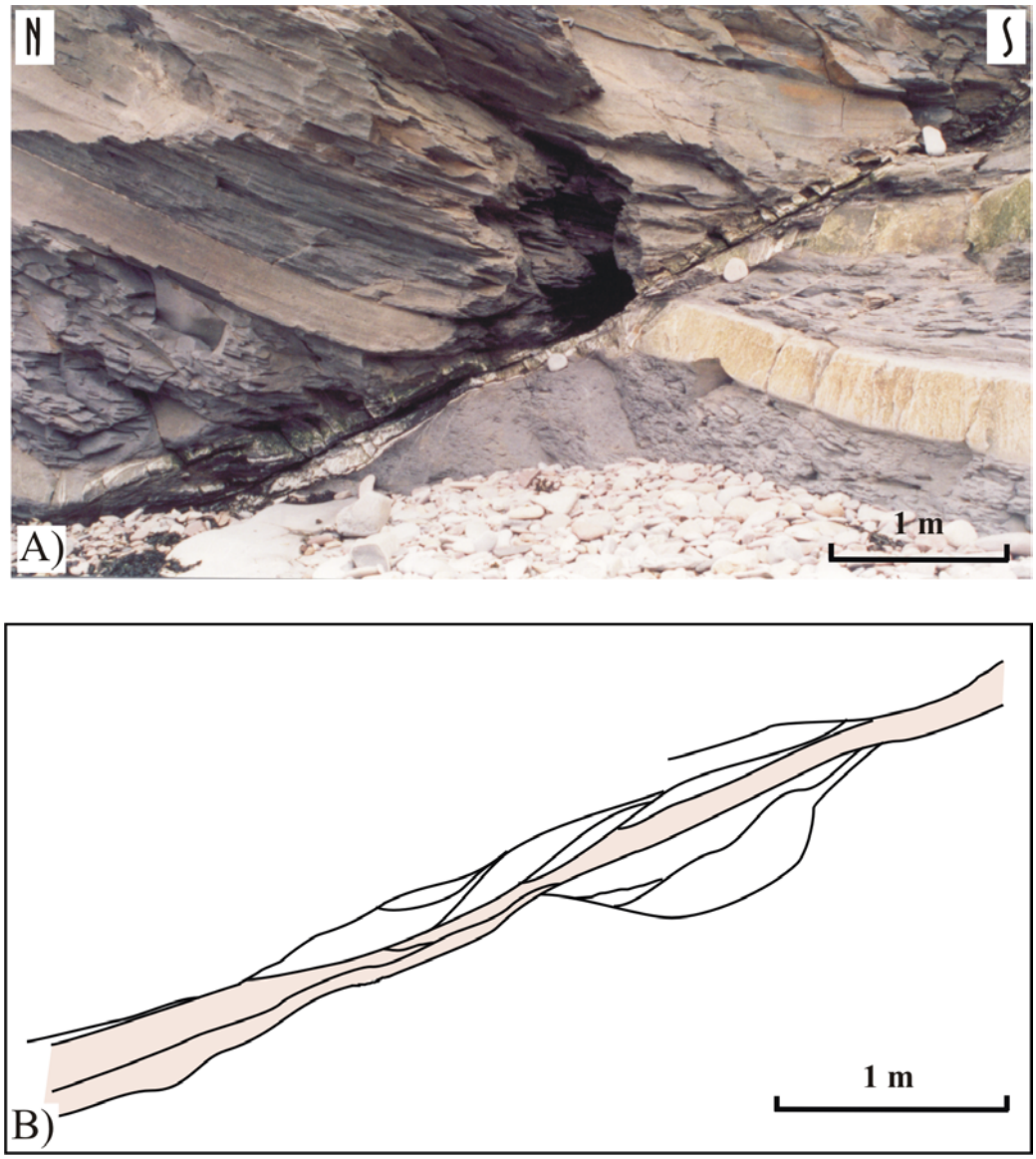

Figure 2.20 A) Picture of the lower part of the section exposed in locality 1 on Kilve Beach, taken towards the east. The rocks hosting the horses in the hanging wall consist of organic-rich shale, whereas the horses in the footwall cut through both organic-rich shale and a limestone bed. Two horses occur within the hanging wall, consisting entirely of limestone. B) Systematic sketch of what is observed in A. Fault core is shaded in pink.

The bulk of the horses seen in locality 1 are of the first order, and vary between 0.5 m and 2 m in the dip dimension, though two of the horses are more than 5 m in this dimension. The remaining four horses are classified as second order horses, having lengths in the dip dimension between 25 cm and 1 m.

The plot of the length versus the thickness of the horses measured in locality 1 is displayed in figure 2.23. An R^2-value of 0.27 implies that the data points representing

the horses are not well constrained to the regression line, such that the linear relation between the length and the thickness is weak.

Figure 2.21 Cave present in the lowermost part of the section making it possible to examine some of the horses in the strike dimension in addition to the dip dimension and thickness.

Figure 2.22 Part of the limestone bed in the lowermost part of the section has been dragged into the core and has segmented, thus defining a horse in the fault core.

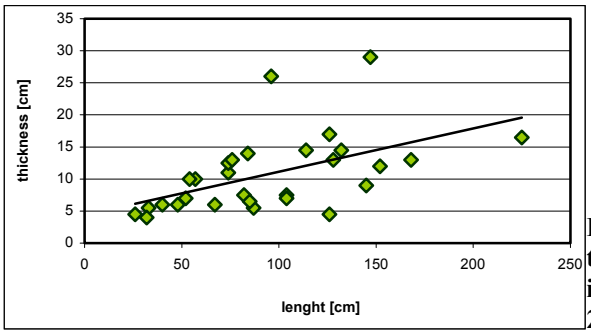

Figure 2.23 Plot of the length versus the thickness of the horses measured in locality 1 in Kilve, with the largest horses omitted. N = 29 and $R^2 = 0.27$.

2.4.3 Locality 2

Locality 2 is situated about 270 m east of locality 1 at Kilve Beach (figure 2.14). The studied section is about 6 m long and 10 m high (figure 2.24). Three faults are exposed

in this outcrop. These include one dominant fault with a normal displacement of 6.5 m and two minor faults with approximately 0.3 m normal displacement (figure 2.24 and 2.25). One of the minor faults is located in the hanging wall of the main fault, and is linked to the main fault both in the upper and lower part of the section, thus forming a large horse. Smaller horses do also occur within the large horse. The second minor fault is located in the footwall of the main fault. The majority of the horses in locality 2 are constrained by the main fault and this minor fault. The main fault is assumed to be linked to the fault examined at the previous locality. The exposed surface is plunging at various amounts across the section allowing the faults and the horses to be examined in the strike dimension as well as in a section between the dip and strike dimension.

The rocks hosting the fault consist of organic-rich shales interbedded with limestone beds, in accordance with the rocks in locality 1. The beds are oriented E-W, with an average dip of 20^{o} and 12^{o} towards the south in the hanging wall and in the footwall, respectively (data given by S. S. Berg), indicating that the hanging wall either rotated slightly during faulting or later, due to gravity sliding, or due to folding of the rocks during inversion.

As already mentioned the sediments in the locality host three faults, all of them normal faults. The main fault strikes E-W and has an average dip of 30^{o} towards the north. Four distinct limestone beds can be correlated across the main fault (figure 2.25) displaying a vertical displacement of 4 m. Slickenlines on the main fault surface have a pitch of 90^{o}, indicating dip-parallel movement during faulting.

The fault is characterized by a discrete fault core, similar to the fault in locality 1. The rocks within the core consist of organic-rich shale mixed with limestone, where the limestone is highly deformed and lighter in color than the limestone in the vicinity of the fault. In most part of the fault core the shale and the limestone have a fabric parallel to the fault plane, making the fault core relatively slim (figure 2.26). In other parts of the core the rocks are mixed to a greater extent. Here, limestone is forming horses within shale or shale form horses within limestone, and some horses are mixtures of both limestone and shale (figure 2.27). The fault core is distinct in this locality, similar to the fault core in locality 1. However, the horses in the core in this locality are considerably smaller, varying between 8 cm and 77 cm in the strike dimension and

between 0.4 cm and 8 cm in thickness. The thickness of the fault core varies between 10 cm and 20 cm, and is thickest in the parts were horses occur.

Figure 2.24 Overview of locality 2 on Kilve Beach, photo taken towards SE. A main fault with a well-developed fault core is present in the locality. The fault is striking E-W and dips 30° towards N. The rocks consist of argillaceous limestone interbedded with organic rich shales, and the beds are dipping towards S. Horses in the locality occur in the hanging wall, but mainly in the footwall and within the fault core. Though a bit camouflaged, Silje is representing the scale in the center of the photo, and she is caught measuring the orientation of the main fault.

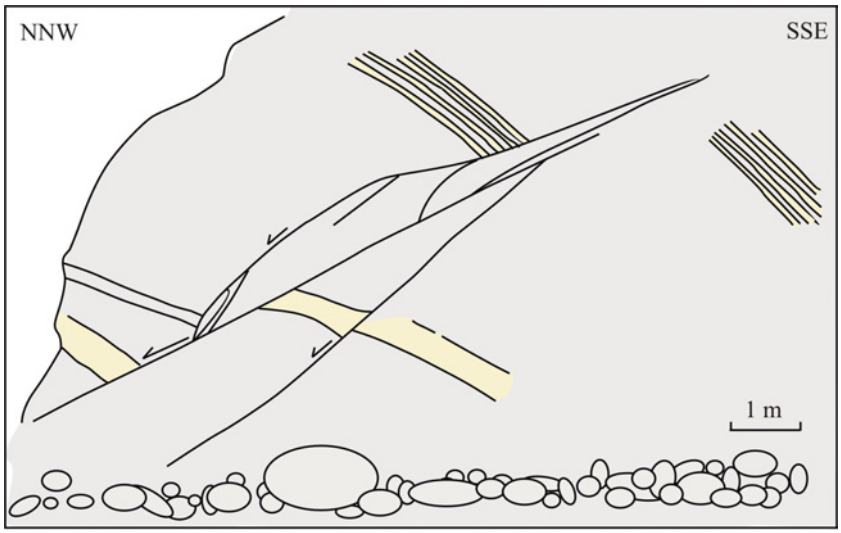

Figure 2.25 Sketch showing the main elements in locality 2 on Kilve Beach. The most prominent limestone beds are marked as yellow. One main fault and two minor faults are present in the locality. One of the minor faults is splitting from the footwall of the main fault, whereas the other occur in the hanging wall and is linked to the main fault in both the upper and lower part of the outcrop.

Highly fractured rocks in the vicinity of the fault make it difficult to estimate the damage zone of the fault. However, there is no significant displacement of the minor faults or fractures in the section, and it is therefore clear that most of the movement has occurred in the fault core of the main fault. The rocks seem to have undergone fluid-related strain softening during deformation.

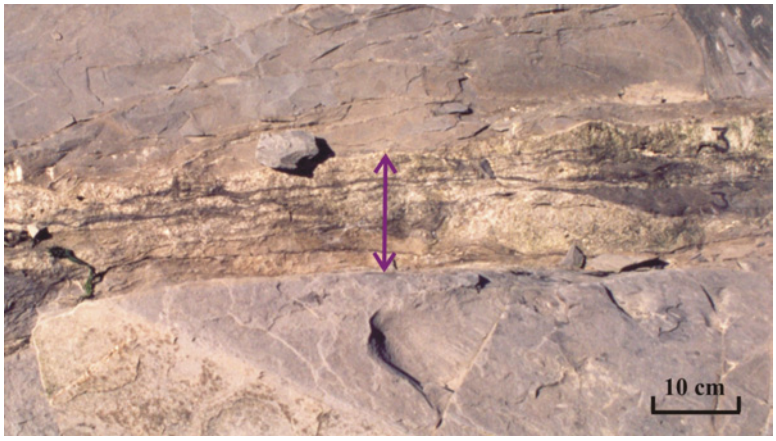

Figure 2.26 A slim part of the fault core in the strike dimension. The paler limestone is more dominant than the dark shale. Both of them are deformed within the fault core. Even if some horses are present the rocks generally have a fault-parallel fabric.

2.4.4 The studied horses in locality 2

Opposite to locality 1 the surface of the exposed section in locality 2 is more inclined. This makes it possible to examine the horses in the strike dimension in addition to the dip dimension and the thickness. However, since the surface is less vertical than the surface in locality 1, the horses are less well exposed in the dip dimension in locality 2. Except for the examined horses within the fault core the rest of the horses in the section are approximately equally exposed in the strike dimension and in the dip dimension. The examined horses within the fault core (figure 2.27) are exposed entirely in the strike dimension.

A few of the examined horses appear in the hanging wall, whereas the majority of the horses appear within the fault core (figure 2.27) and in the footwall (figure 2.28) of the fault. Two horses are extremely large compared to the rest of the horses in the locality. They both occur in the hanging wall and they are fully exposed in the strike/dip dimension and in thickness (figure 2.25). Both of the horses have a length in the strike/dip dimension of about 10 m, whereas the thickness of the two horses is 70 cm and 175 cm, respectively. A third horse may exist in the footwall, defined by the main

fault and the minor fault (figure 2.25). The uncertainty of this horse is due to the fact that only half of its length is exposed, maybe less. If it really is a horse, the exposed length of it is 7 m, and based on the theory of symmetric horses (chapter 1.5) this would imply that the horse is at least 14 m long. The thickness of the horse is 1.5 m. The two horses in the hanging wall, and the possible horse in the footwall, have probably developed early during faulting, and are therefore classified as first order horses (chapter 1.5). In addition to the two large horses in the hanging wall, three smaller horses are observed within one of the first order horses, two of them exposed in full (figure 2.25). The three horses are thought to have developed after the development of the mentioned first order horses, and are therefore classified as second order horses, varying between 61 cm and 340 cm in the dip/strike dimension and between 8 cm and 25 cm in thickness. The horses in the hanging wall mainly cut through organic-rich shales, but also through limestone beds (figure 2.25). The three second order horses are fully overlapping, whereas the two first order horses are overlapping by an amount of 1 m. All of the observed horses in the hanging wall are consequently left-stepping.

A large amount of the horses contributing to the dataset from locality 1 occur, as already mentioned, within the fault core of the main fault. Different from the horses within the fault core in locality 1 (figure 2.17 and 2.18) the equivalent horses in locality 2 (figure 2.27) are considerably smaller and more numerous. In addition they are exposed only in the strike dimension (b-axis) in a horizontal section of the outcrop, contrary to the fault core horses in locality 1, which are exposed merely in the dip dimension (a-axis). The fault core horses in locality 2 vary between 8 cm and 168 cm in the strike dimension, and between 0.4 cm and 8 cm in thickness.

The rocks in the studied section of the fault core consist of limestone and organic-rich shales, but dominantly the latter (figure 2.27). The limestone mostly occurs in the upper part of the studied section of the core, and in this part three limestone horses exist. All the three horses are floating within a larger horse consisting dominantly of shale. The limestone horses are the slimmest horses within the studied section, with a maximum thickness of 1.8 cm. The rest of the limestone contributes to horses together with the shale, or limit horses consisting entirely of shale. Two of the shale horses are, however, surrounded by, and seem to be floating within, part of the limestone, also in the upper part of the studied section of the fault core. These shale horses surrounded by limestone

highly resemble the equivalent limestone horses surrounded by shale, with a maximum thickness of 2.2 cm and an extension in the strike dimension of about 10 cm. Horses made of entirely shale dominate the lower part of the studied section. Darker bands of shale define these shale horses, which are relatively large, having a maximum expansion in the strike dimension of 77 cm and a thickness between 5 cm and 10 cm. The fault core itself in the studied section is lens-shaped, and may be a horse established prior to the horses inside. This horse may therefore be classified as a first order horse, whereas the horses inside the horse may be classified as second order horses, established secondary to the mentioned first order horse. Two of the limestone horses in the upper right corner of the studied section are clearly right-stepping. This also seems to be the case for majority of the rest of the examined horses within the fault core, even if some horses are found to be left-stepping. Except the horses surrounded entirely of opposite material, the horses are overlapping by an amount of one half of the strike dimension.

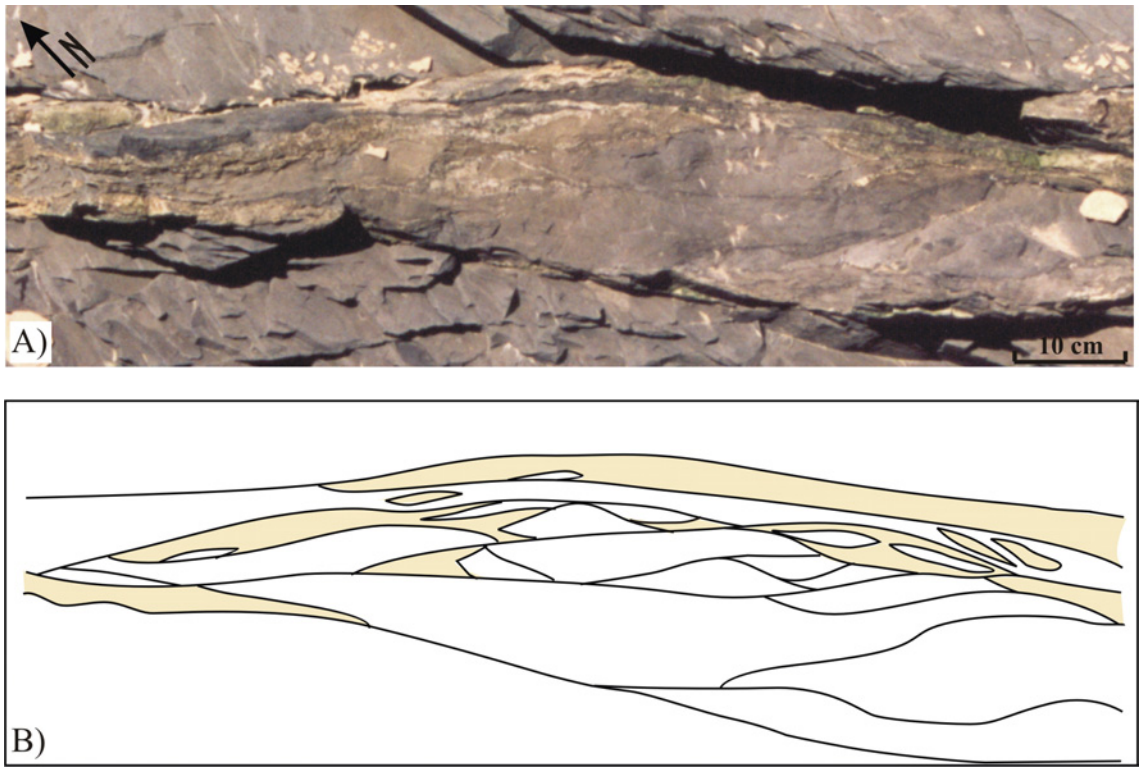

Figure 2.27 A) Excerption of the fault core in locality 2 in the strike dimension. Horses consisting of shale, limestone or both dominate the geometry, and maximum thickness of the core is 20 cm. B) Systematic sketch of the fault core as seen in A) where limestone is marked in yellow.

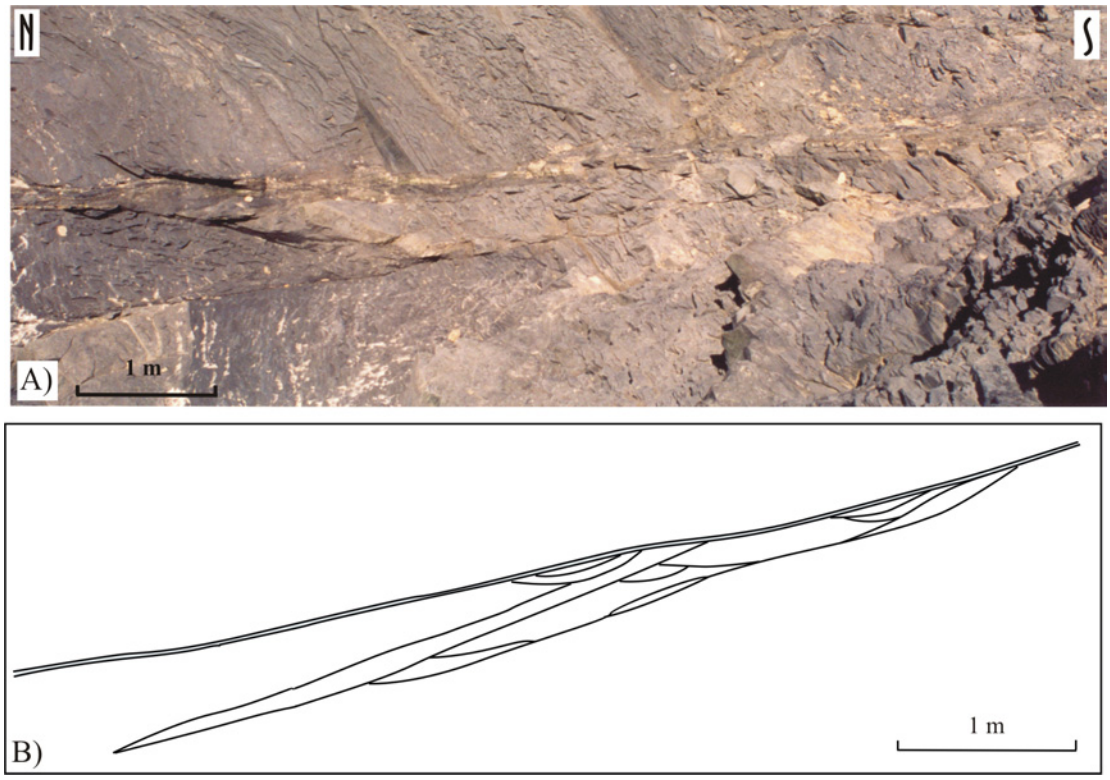

Figure 2.28 A) Section of the middle part of the outcrop in locality 2 on Kilve Beach. A minor fault splits from the main fault in the footwall. The majority of the horses in this locality occur either within the fault core or in the footwall of the main fault, the latter horses constrained by the main fault and the minor fault. B) Systematic sketch of what is seen in A. The fault core is shaded in blue.

The remaining horses studied in locality 2 occur in the footwall of the main fault, limited vertically by an underlying minor fault (figure 2.28). The section exposing the footwall horses has an angle of 50^{o} to the dip direction (chapter 1.5). This implies that the footwall horses are exposed approximately equally in the dip dimension (a-axis) and in the strike dimension (b-axis) in addition to the thickness (c-axis). The measured length of the horses is therefore mainly an indication of how the horses appear in the dip dimension and in the strike dimension. The footwall horses vary between 13 cm and 222 cm in the dip dimension and between 15 cm and 265 cm in the strike dimension. The thickness of the horses varies between 1 cm and 24 cm. The rocks hosting the horses consist primarily of organic-rich shales, and the original layering is vaguely present (figure 2.28). The original layering in the horses is oriented with an altered orientation as compared to the original layering in the protolith (figure 2.29). That is, the dip direction changes from south in the rocks in the hanging wall towards the north within the horses, indicating that the rotation of the horses is caused by normal movement along the main fault. The stepping of the horses seems random, though

slightly more than half of the horses are right-stepping. The minor footwall horses are probably established after the formation of the large horse they occur within, and they are therefore classified as second order horses.

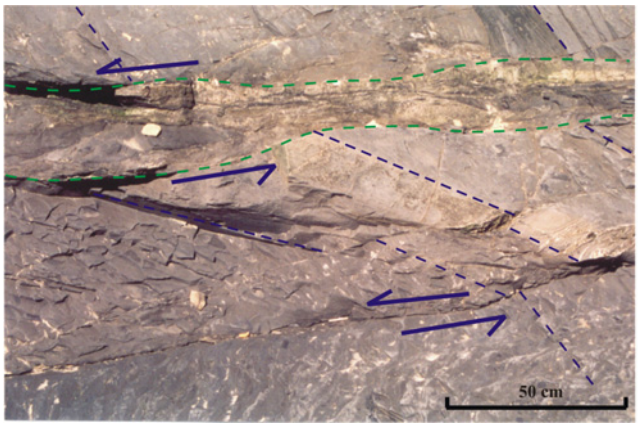

Figure 2.29 Layering of the rocks in the fault core is rotated towards north as compared to the rocks in the footwall, indicated by blue lines. Green lines indicate the fault core. Photo is taken down towards NE and shows a part of the fault core and the horses in the center of the exposed section in locality 2.

The plot of the length versus the thickness of the horses examined in this locality is displayed in figure 2.30. The data points representing the horses are well constrained to the regression line, implying that there is a strong relation between the length and the thickness of the horses.

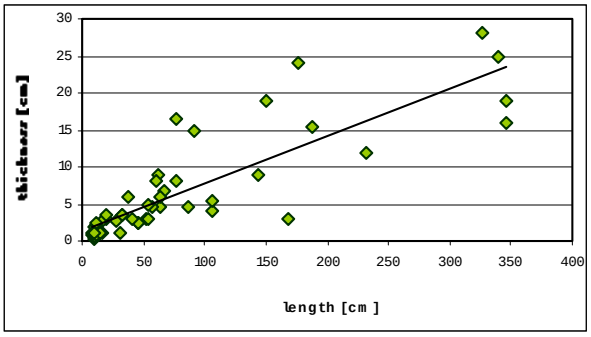

Figure 2.30 Plot of the length versus the thickness for all of the horses examined in locality 2 in Kilve. The three large first order horses are omitted because these are only partly exposed. N = 48 and $R^2 = 0.72$.

2.4.5 Locality 3

The third locality is situated approximately 500 m to the east of locality 1 (figure 2.14 and 2.15). However, the locality is to be found on the beach surface and it therefore deviates from the previously described localities, which are situated within the cliffs. The surface exposes a horizontal section of the hanging wall, the footwall and the fault core of a normal fault (figure 2.31). In this study a 3 m long section of the fault core was examined (figure 2.32).

In accordance to the previously described localities, the rocks hosting the fault in locality 3 consist of limestone and organic-rich shale. The exposed part of the hanging wall consists of shale with an overlying limestone bed, whereas the exposed part of the footwall consists of limestone. Both shale and limestone is present in the fault core, where particularly the limestone is highly deformed (figure 2.32).

Similar to the studied faults in locality 1 and 2, the fault in locality 3 strikes E-W, and is dipping about 40^{o} towards north. The amount of displacement was not possible to measure.

Limited vertical exposure of the fault makes it difficult to examine the hanging wall and the footwall in the dip dimension. The movement across the fault seems to have been constrained to the fault core, which is reasonable when considering the faults studied in the area that have a similar fault core appearance as the fault in this locality. The deformation seems to have been constrained to the fault core of the fault. The rocks may seem to have undergone fluid-related strain softening.

Figure 2.31 Photo of the fault core of the exposed fault in locality 3 on Kilve Beach, taken towards south. The darker shale in the upper part of the fault core represents the hanging wall, whereas the paler limestone in the foreground represents the footwall. The fault has a well-developed fault core consisting of deformed rocks. Horses are numerous within the core and dominate the architecture.

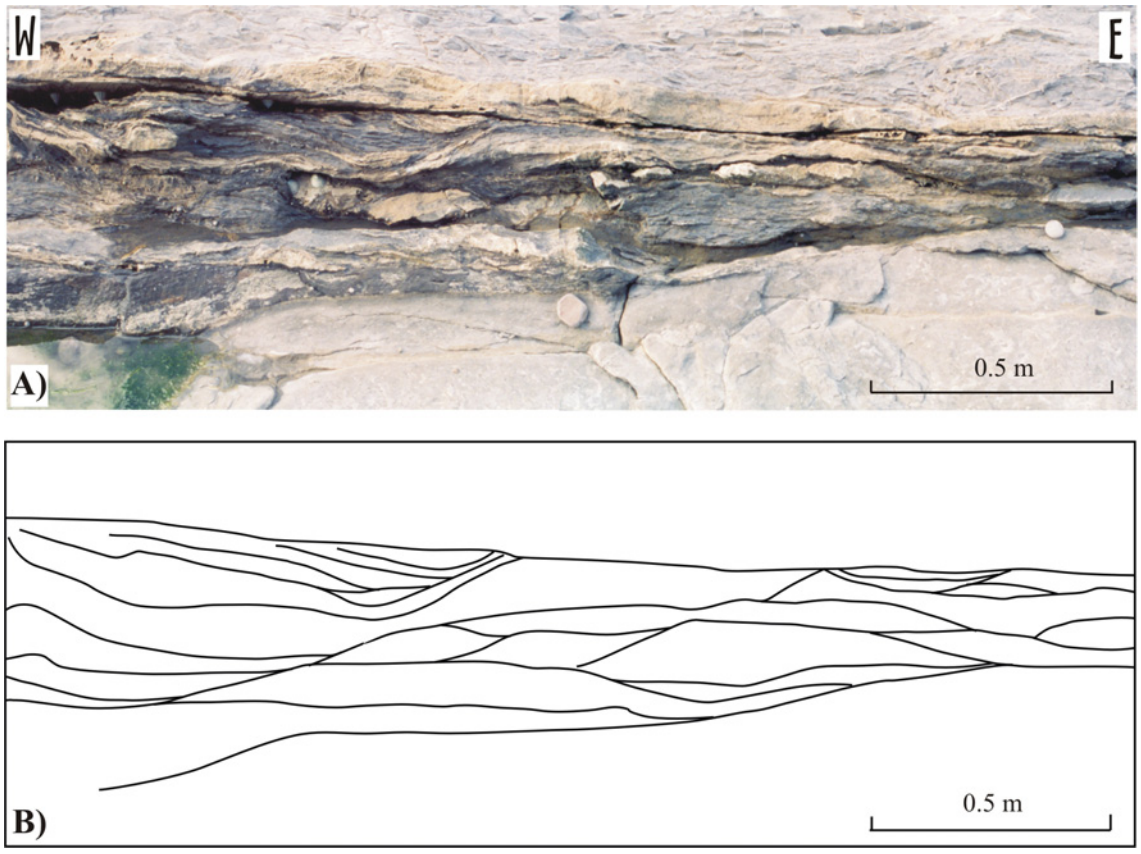

Figure 2.32 A) The examined part of the fault core, picture taken towards the south. Rocks within the fault core have undergone ductile deformation in addition to faulting. Horses consist of limestone (light colour) surrounded by shale (dark colour), of shale surrounded by limestone, or of both limestone and shale. B) Sketch of the horses examined within the core. Different from the horses in locality 1 and 2, the horses in this locality are defined by less planar faults/fractures.

The fault in the locality has a distinct and complex fault core, varying between 20 cm and 60 cm in thickness. Both limestone and shale are present in the core, and are some places highly deformed. In some part of the fault core the rocks display ductile deformation structures and the shale seems to be smeared along the fault plane (figure 2.33). Horses occur in the entire part of the fault core exposed at the surface, but is especially numerous in the western part where the shale content is high. The fault core is thickest in the western part where the shale content is high, and the majority of the horses occur and the core is most complex (figure 2.33). The fault core is slimmer in the eastern part of the studied section, where the architecture is less complex (figure 2.34).

2.4.6 The horses examined in locality 3

The examined horses in locality 3 are within the fault core. Horses are likely to be present in the hanging wall and the footwall as well, but due to the limited horizontal

exposure of the fault they are more difficult to locate. Similar to the fault core horses in locality 2 they are small and numerous compared to the fault core horses in locality 1. The horses are well exposed in the strike dimension (b-axis) and in thickness (c-axis) only. Measurements show that the horses vary between 22 cm and 196 cm in the strike dimension and between 3 cm and 22 cm in thickness. Both limestone and shale is present within the core and some of the horses consist entirely of shale, whereas others consist entirely of limestone. However, the majority of the horses are a mixture of both limestone and shale. The horses examined in locality 3 in this study are located within the thickest part of the fault core where the shale content is high. The fractures/fault defining the horses are uneven and considerably curviplanar, and most of the time follow the transitions between limestone and shale (figure 2.32).

The plot of the strike dimension versus the thickness of the horses examined in the locality is displayed in figure 2.35. The data points representing the horses are well constrained to the regression line, confirmed by the R^2-value. Hence, there is a strong relation between the strike dimension and the thickness of the horses.

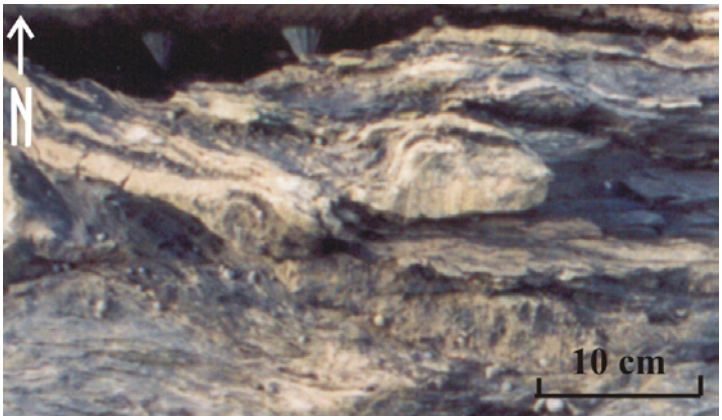

Figure 2.33 Rocks having undergone ductile deformation. Observed folding of the limestone in the upper left corner of the photo.

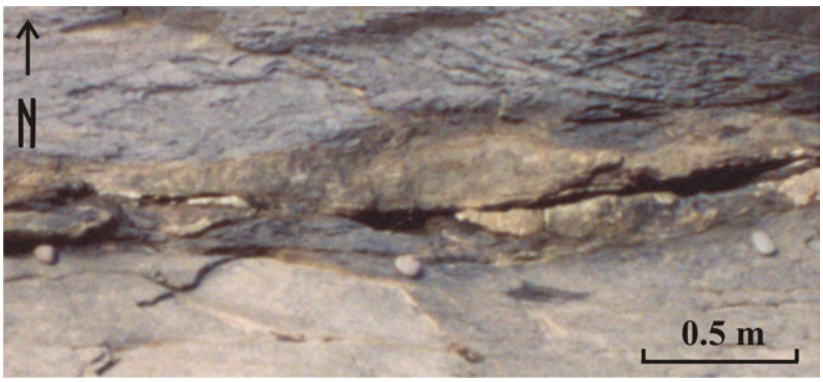

Figure 2.34 Slim part of the fault core where the architecture is less complex, and less shale is present.

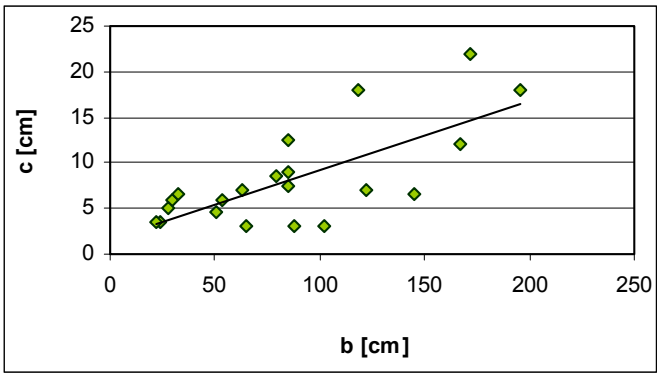

Figure 2.35 Plot of the strike dimension (b-axis) versus the thickness (c-axis) for the horses examined in locality 3 in Kilve. R^2 = 0.51 and N = 21.

2.5 Regional geology of the Fennoscandian Border Zone

Geologic development

The island of Bornholm belongs to Denmark and is sited in the Baltic Sea, about 40 km south-east of southern Sweden (figure 2.36). The island is positioned within the south-eastern part of the Fennoscandian Border Zone (figure 2.37), a zone which has been tectonically active from the late Palaeozoic to recent time (Liboriussen et al. 1987).

Little is known about the tectonic evolution in the Early Palaeozoic time, due to tectonically overprint in the Late Palaeozoic and Mesozoic (Liboriussen et al. 1987). Nevertheless, the zone has been argued to exist since the Precambrian (Strömberg 1976). The zone has been subjected to numerous tectonic events. In the Bornholm area this includes uplift and erosion during Silurian, dextral wrench tectonics during latest Carboniferous and early Permian that resulted in pull-apart basins (such as the Rønne Graben), extension during Triassic, Jurassic and early Cretaceous, and a post rift phase dominated by late Cretaceous and early Tertiary inversion tectonics (Liboriussen et al. 1987, Vejbæk et al. 1994).

Figure 2.36 The island of Bornholm, Denmark is situated about 40 km south of southern Sweden in the Baltic Sea. Map is downloaded from http://geography.about.com

Structural framework

The island of Bornholm is characterized by a complex mosaic of rotated fault blocks that are separated by strike-slip, reverse- and normal faults (Deeks & Thomas 1995). The blocks can be grouped into three large units, namely the Bornholm Horst, the Rønne Graben and the Sose Platform. The faults strike approximately NW-SE and NNW-SSE (e.g. Gravesen et al. 1982).

Lithology

The oldest sediments found on the island are Palaeozoic, deposited during Cambrian, Ordovician, and Silurian as dominantly coastal to deep oceanic deposits, and are exposed on the southeastern part of the island (e.g. Gravesen 1996).

The Mesozoic sediments are exposed in the west and in the south on the island, and consist of sediments deposited during the Upper Triassic, Jurassic and Lower Cretaceous. The sediments consist of clay, sand and gravel, and were deposited on the Bornholm Horst, in the Rønne Graben and the Sose Platform. Deposition mainly kept pace with subsidence of the blocks, and the sediments consist of coastal to shallow oceanic deposits (Gravesen 1996). Mesozoic was a tectonically active period, and tectonics together with sea level changes (eustasy) and climatic fluctuation, controlled the deposition during Triassic to early Cretaceous (Gravesen et al. 1982, EUGEON-S Working Group 1988, Gravesen 1996).

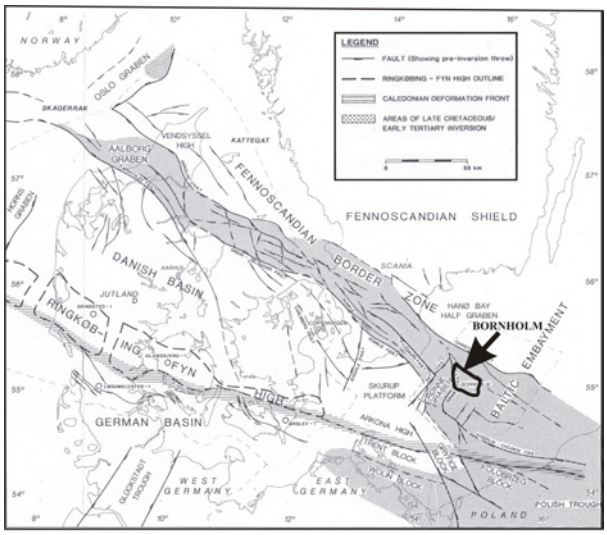

Figure 2.37 Structural map showing the location of Bornholm and the Fennoscandian Border Zone. After Liboriussen et al. (1987).

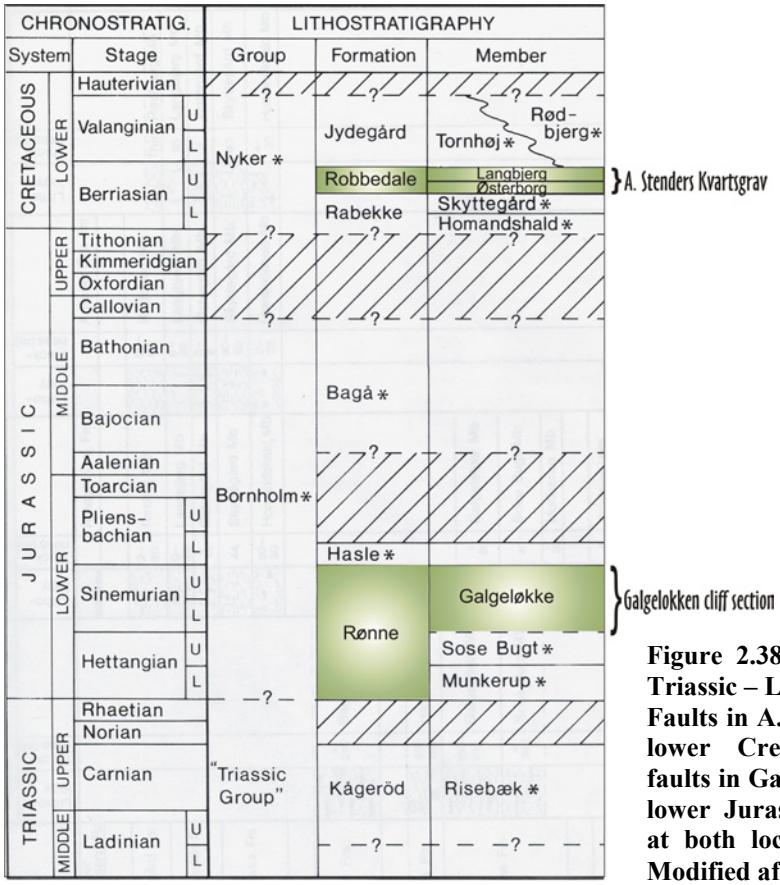

Figure 2.38 Stratigraphic column of the Triassic – Lower Cretaceous of Bornholm. Faults in A. Stenders Kvartsgrav occur in lower Cretaceous sediments, whereas faults in Galgeløkken cliff section occur in lower Jurassic sediments. Sediments are at both localities nearly unconsolidated. Modified after Gravesen et al. (1982).

2.6 Description of the localities on Bornholm

The island host two of the localities in this study, both of them situated in the south-west (Map sheet 1822 III NW). The first locality to be described is within A. Stenders

Kvartsgrav, a sand pit in the Robbedale area, whereas the second is within the Galgeløkken Cliff section (figure 2.39). Common for the two localities is that they each expose faults hosted by nearly unconsolidated sand interbedded by various amounts of clay. Earlier studies in A. Stenders Kvartsgrav include Nielsen et al. (1996) on sedimentology and ichnology, and Johnsen (1998) who performed an analysis of fault seal potential, and in Galgeløkken cliff section earlier studies include Sellwood (1972) of sedimentation, Arndorff (1993) and palaeosoils and Johnsen (1998) and analysis of fault seal potential. Earlier studies of both of the localities also include Clausen et al. (2003) on fault geometry and clay smear. The fieldwork was executed in cooperation with Jill A. Clausen.

2.6.1 A. Stenders Kvartsgrav

One of the study areas on Bornholm is situated within A. Stenders Kvartsgrav, a sand pit in the Robbedale area. The sand pit is located 3.5 km southeast of Rønne, which is the main city on the island (figure 2.39).

The sand pit is situated in the Arnager-Sose Block and occurs within the Lower Cretaceous Robbedale Formation of the Nyker Group, and the sediments consist of fine-grained intertidal flat, coastal lagoon and beach sand (Østerborg Member) and medium and coarse-grained subtidal, intertidal, barrier and sand-wave sand (Langbjerg Member) (Gravesen et al. 1982) (figure 2.40). The sediments are exposed along an approximately NNW-SSE oriented section. However, the section is some places covered by sediment avalanches and the formations and the structures are therefore only partly exposed.

Focus was given a complex fault zone, located in the central part of the pit (figure 2.40). The fault zone can be studied in three different sections. One section is in the upper part of the outcrop, another in a horizontally exposed surface on the ground along strike, and eventually the third section is in the lower part of the outcrop (figure 2.40 and 2.41). Some of the upper sediments on the ground had to be removed to expose the part of the fault zone in the horizontal section (figure 2.41). Six fault branches could be distinguished, all of them related to the fault zone. In this study the fault branches are named fault A, B, C, D, E and F (figure 2.40) and can be studied in different parts of the

outcrop. Fault A, B, C and D are exposed in the upper part of the outcrop (figure 2.40 and 2.41), fault E in the horizontal section on the ground surface (figure 2.41), and fault F is exposed in the lower section.

The sediments consist of nearly unconsolidated medium to coarse-grained sand that is interbedded with various amounts of clay. The beds are tilted and dip averagely 20^{o} towards the southwest in both the footwall and in the hanging wall, indicating no significant rotation of the layering due to movement across the fault zone.

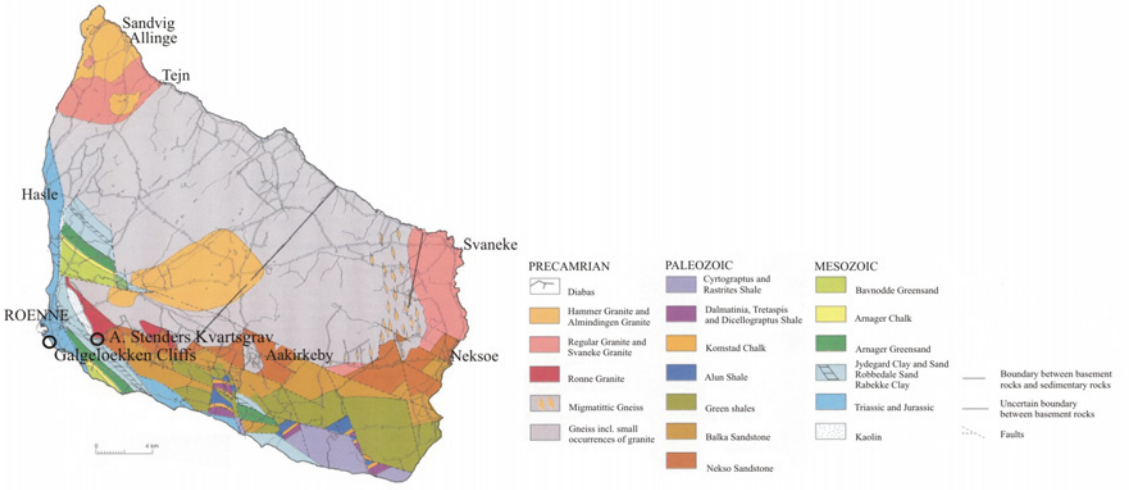

Figure 2.39 Geologic map of Bornholm, showing the localization of the two studied areas on the island. A. Stenders Kvartsgrav is situated within Lower Cretaceous sediments, whereas the Galgeløkken cliffs are situated within Lower Jurassic sediments. Modified after VARV (1977).

An extensional fault zone occurs in the central part of the pit. Within the fault zone six discrete faults branches can be distinguished, and in this study these six faults branches are termed fault A, B, C, D, E and F (figure 2.40). Each of the faults strikes NE-SW. Fault A and F are the main faults within the fault zone, and the two faults are dipping towards the SW. Fault B and D are synthetic, whereas fault C is antithetic to the two main faults. Fault B, C, and probably fault D, are linked to fault A in the upper part of the zone (figure 2.41). Fault F has a different orientation than fault A, and is therefore suggested to either be a wrenched part of fault A or a distinct fault segment that is connected to the fault zone, for instance via a relay structure, underneath the sediment cover. Fault E was revealed after removing some of the sediments on the ground between the upper and lower exposure of the outcrop and may not actually be a distinct fault, but more likely a section that exposes the fault zone in the strike dimension

(figure 2.41). The horizontal section is considerably complex and may show the interference between fault A and F, and maybe between fault D.

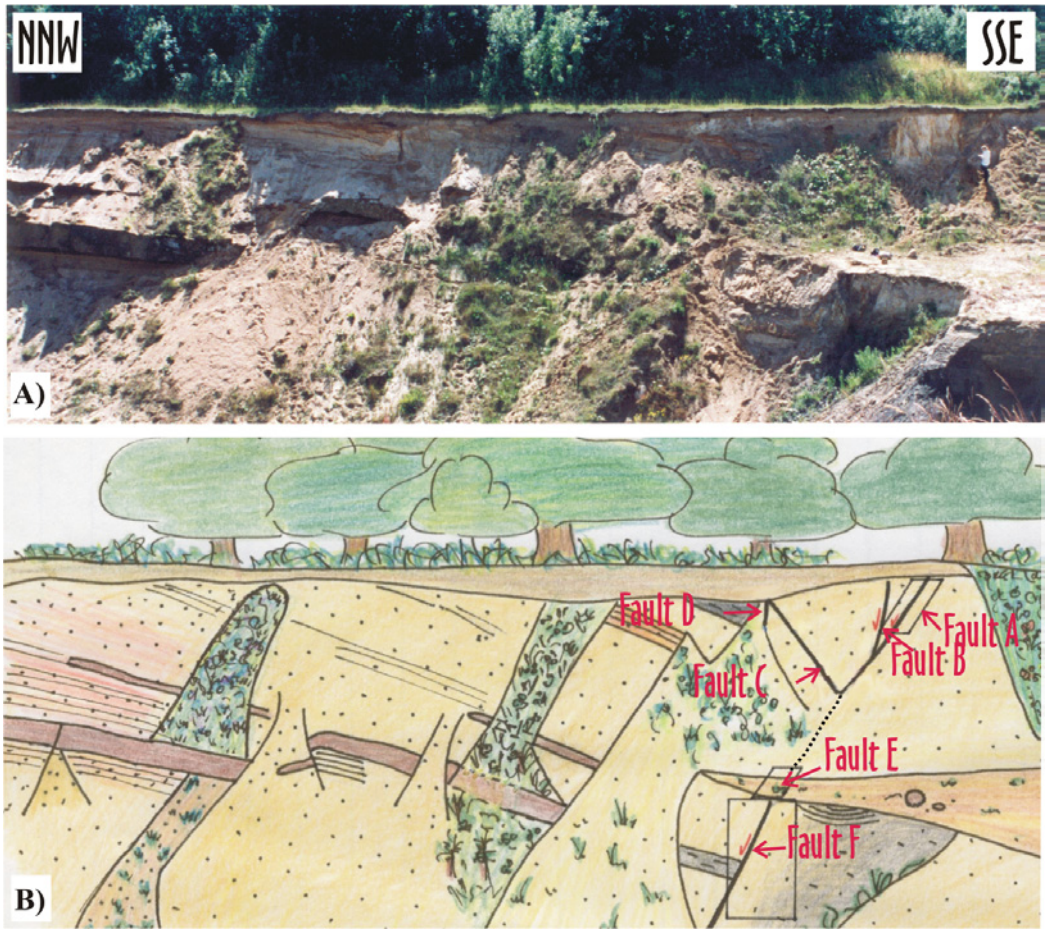

Figure 2.40 A) Overview of the locality within A. Stenders Kvartsgrav on Bornholm. Continuous beds of sand and clay are gently dipping towards the NE. Sediment avalanches largely cover the outcrop. A complex fault zone comprised by six discrete fault branches occurs to the right, where Jill is used as scale. B) Sketch of what is seen in A.

None of the beds could be correlated across the fault zone, but considering the height of the vertical exposure of the formation and the inclination of the layering, the throw must be at least 13 m. The movement across the fault is suggested to be normal (Clausen et al. 2003). However, reverse drag structures of some of the layers in the fault block between fault A and B indicates that the fault zone has been inverted (Clausen et al. 2003) (figure 2.42). The fault zone can be divided into a fault core and a damage zone. Horses occur mainly within the fault core of fault A and F, but three horses were also found in fault C. Focus was given fault A and F due to the fact that these two faults had the most interesting fault core and damage zone, and because they seem to be the main faults within the fault zone.

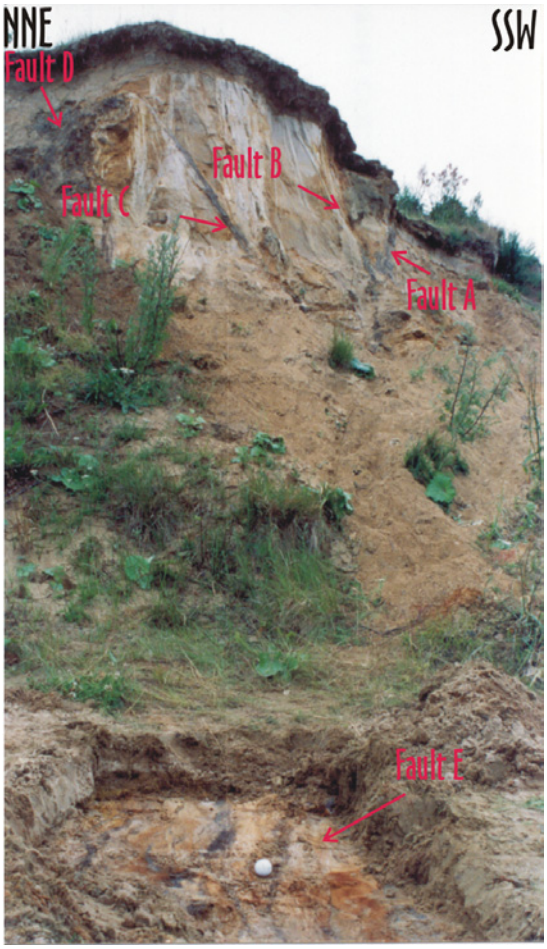

Figure 2.41 The upper part of the outcrop, including a part of the section on the ground surface departing the upper exposure from the lower. Fault B, C, and most likely fault D, are linking up to the main fault A in the upper parts of the exposure. Fault E is probably a section exposing the complex fault zone along strike.

The damage zone is defined by deformation bands and comprises a part of the fault zone that is at least 4 m thick in the hanging wall in the upper part of the exposed outcrop. Sediment avalanches cover most parts of the footwall, but the damage zone is probably thicker than the 1.5 m that is exposed in the upper part of the section (figure 2.42). The hanging wall is dominated by steeply dipping (70^{o}-85^{o}) deformation bands, varying in width between 0.1 cm and 2-3 cm, whereas the deformation bands in the footwall are less dipping (45^{o}-60^{o}) (Clausen et al. 2003). Although some of the deformation bands in the hanging wall of fault A are single, the majority are clustered (Clausen et al. 2003). The deformation bands in the footwall are, however, single, indicating that the footwall suffered less intensified deformation during faulting. The single deformation bands are further away from the fault core than the clustered deformation bands, and they are suggested to have developed prior to the clustering, representing an early stage in the development of the fault zone (Clausen et al. 2003). A narrowing of the fault zone during faulting is associated with strain softening. The damage zone consists primarily of coarse sandstone, and no clay is interfering the

deformation bands. Horses may also occur within the damage zone, but are hard to define due to the incoherency in the sandstone and the lack of clay defining them.

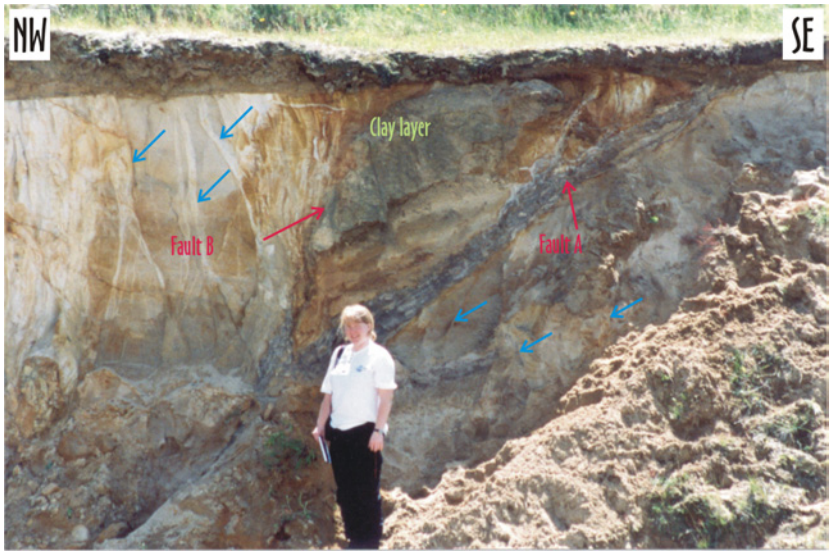

Figure 2.42 Clay layer in the fault block between fault A and B showing reverse drag. Blue arrows are pointing towards some of the deformation bands occurring in the damage zone of the fault zone.

Each of the faults has a well-developed fault core, which is characterized by a high content of clay. Within fault A in the upper section of the exposed fault zone the fault core is varying between 15 cm and 30 cm in thickness. The fault core in this particular fault can be divided in two, where the part closest the hanging wall is chaotic and contain a higher amount of clay than the part closest the footwall. In the less chaotic part more sand is present, and the clay membranes are considerably thinner, defining horses consisting of medium to coarse-grained sand (figure 2.43).

The fault core within fault F consists, in accordance to the fault core within fault A, of horses of sand bounded by clay membranes (figure 2.44). However, the fault core of fault F is considerably wider than the fault core of fault A, varying between 30 cm and 80 cm in thickness across the exposed section. In addition, the clay membranes separating the horses are also thicker.

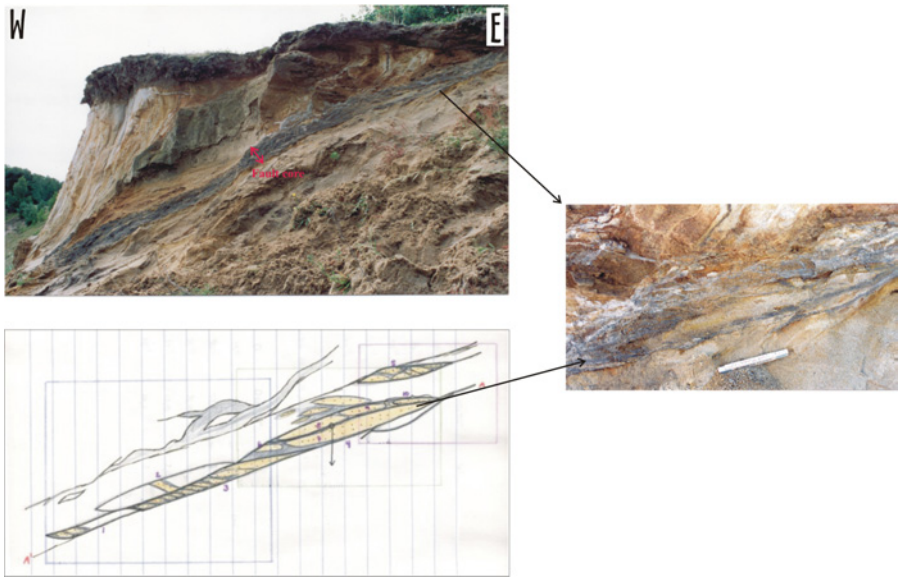

Figure 2.43 A) The exposed part of fault A in the upper part of the outcrop, photo taken towards the north-west. Fault A is one of the main faults in the fault zone and has a well-developed fault core. Clay has been smeared along the fault core, and has separated horses of sand. B) Sketch of the upper part of fault A. The part of the fault core closest to the hanging wall is highly chaotic, whereas the part closest the footwall shows distinctive horses of sand separated by clay membranes. C) Example of small horses occurring within a larger horse.

Fault cores with the highest amounts of clay, i.e. the fault cores in fault A and F, probably represent the fault planes were the majority of the movement across the fault has been taken up.

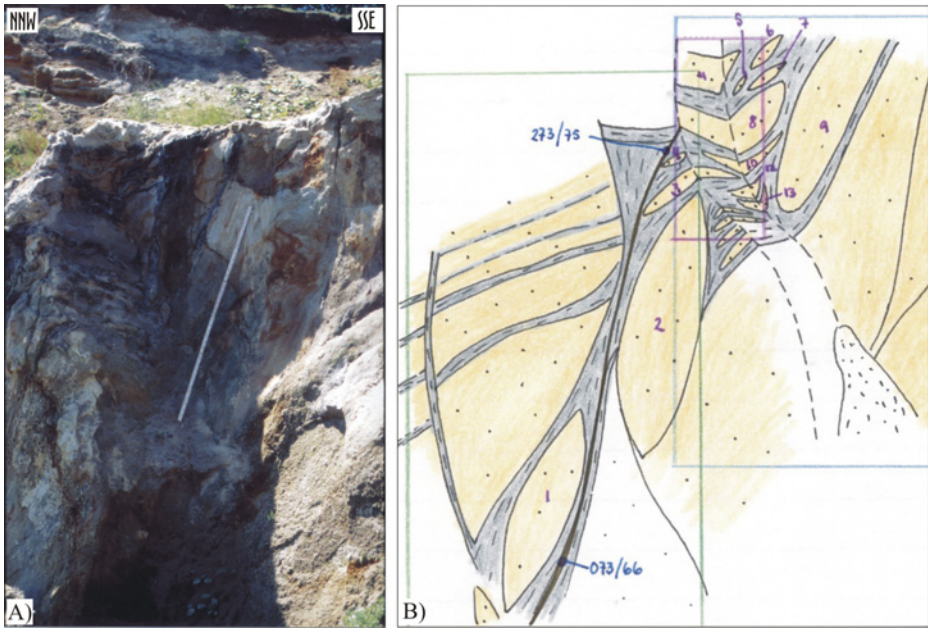

Figure 2.44 A) The lowermost fault in the locality, photo taken towards the west-southwest. B) Systematic sketch of the fault. Horses of sand separated by clay membranes occur within the fault core Due to the section of this fault, horses could be studied in three dimensions.

2.6.2 Studied horses within A. Stenders Kvartsgrav

The observed horses in this locality are located within the fault cores of fault A, C, E and F. Commonly the horses consist of medium to coarse-grained sand, separated by clay membranes of various thickness. The horses within the pit range between 4 cm and 80 cm in the dip dimension (a-axis), between 5 cm and 180 cm in the strike dimension (b-axis), and they are between 1 cm and 25 cm thick.

Fault A is exposed in the upper section of the outcrop, and the horses in the fault are located within the fault core. The upper part of the fault core is chaotic, and therefore are the majority of the examined horses in fault A located in the part of the core that is nearest the footwall (figure 2.43). The horses consist entirely of medium to coarse-grained sand, and are separated and defined by clay membranes that contain coarse-grained sand as well. The clay membranes are generally 0.5 cm to 2 cm in thickness. The horses comprise a part of the fault core that is 10-20 cm thick. The surface exposing the horses is inclined such that the horses are approximately equally exposed in the dip dimension and in the strike dimension in addition to thickness. The horses within fault A vary between 7 cm and 80 cm in the dip dimension and between 6 cm and 96 cm in the strike dimension. The thickness is varying between 2 cm and 15 cm. The majority of the horses are prominent right-stepping, and they overlap by an amount that is between one fourth and one third of the length of the horses. Some of the smaller horses occur within larger horses. The horses overlap each other, and the smaller horses overlap by a larger amount than the larger horses. The large horses are suggested to have developed prior to the horses appearing within them, and they are therefore classified as first order horses. The small horses have probably developed in later stage of the faulting, and are classified as second order horses.

Five horses were found within the fault core of fault C (figure 2.45). They were revealed after removing some of the sediment cover in the lower part of the upper section, and hence exposed fully in all the three dimensions, except for one horse. They are all made of sand, and surrounded by clay membranes. In the dip dimension the horses vary between 30 cm and 52 cm, whereas they vary between 21 cm and 36 cm in the strike dimension. Their thickness varies between 1.5 cm and 4.5 cm (data given by Roy H. Gabrielsen). Except for one of the horses, they are exposed in full (figure 2.45).

The horses are mainly left-stepping and are overlapping by an amount of one third – one fourth of the length of the horses.

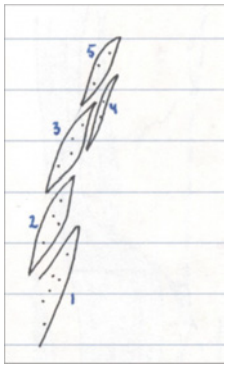

Figure 2.45 Sketch of the five horses observed in fault C. They were revealed after removing some of the loose sediments in the upper section of the outcrop. The horses consist of sand and are separated by clay membranes. Sketch redrawn from R. H. Gabrielsen.

Fault E is probably not a distinct fault segment, but likely fault A or F, or the linking between the two seen in strike dimension. The two sections were dug out from the ground surface, and together they exposed a part of the fault zone that was 4 m long and 0.6 m wide (figure 2.46 and 2.47). The geometries in the section are complex and the section seems to expose a part of the fault zone where different fault segments are crosscutting. Similar to the horses within fault A and C the horses in the section consist of sand, except for two horses that consist of clay (figure 2.46). One of the clay horses is hosting smaller horses consisting of sand. Clay membranes are separating the horses and are up to 10 cm thick, even if some of the membranes are only vaguely present between some sand horses. Due to the fact that the horses were dug out from the ground the horses are only exposed in the strike dimension in addition to the thickness. However, the horses are exposed in full in this dimension and the measures of the horses in this section are closer to the true length of the horses in the strike dimension than the measures of the horses in fault A and C. The horses in the section vary between 5 cm and 180 cm in the strike dimension and between 1 cm and 16 cm in thickness. The horses are distributed throughout the section, and both the amount of overlapping and the way the horses step seem random.

As mentioned earlier in this chapter fault E is exposed in the lower section of the outcrop, just underneath the section exposing the fault zone in the strike dimension (figure 2.46 and 2.47). The section is nearly vertical, but the surface is irregular such that some of the horses can be examined in both strike dimension and dip dimension, as well as and the thickness (figure 2.47). In accordance with the rest of the horses in the

fault zone, the horses in fault F occur within the fault core, and they are present in the entire core. The horses consist entirely of sand and they are swept in by clay membranes of various thickness. The horses range between 4 cm and 85 cm in the dip dimension and are between 2.5 cm and 25 cm thick. The horses that could be examined in the strike dimension were between 20 cm and 140 cm. Unlike the rest of the horses in the sand pit, the horses in fault F are less distributed along the fault core. Instead the horses are stacked beside each other in a higher degree. None of the horses occur within larger horses and they were probably developed during the same stage in the faulting. This implies that they are all classified as first order horses.

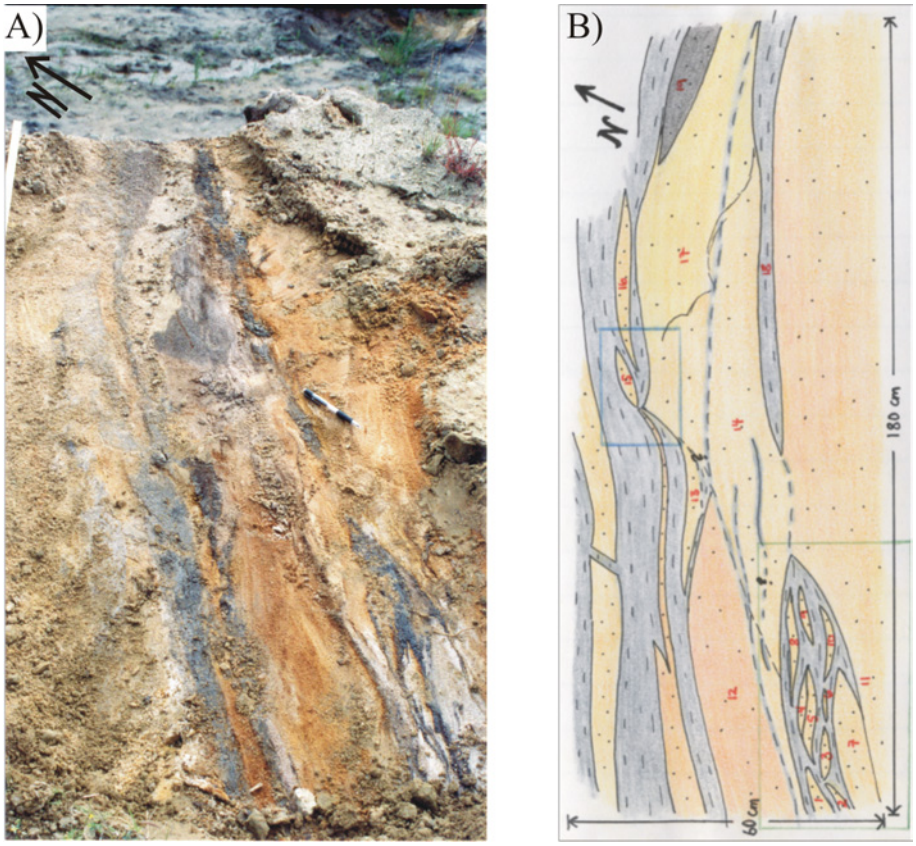

Figure 2.46 A) The first exposed section of fault E, showing a part of the fault zone in the strike dimension. The section was exposed after removing some of the hardly packed sediments on the ground surface between the upper and lower exposed section in the outcrop. The section is chaotic and is suggested to present a part of the fault zone where some of the fault branches are crosscutting. Horses could still be identified, consisting mainly of sand separated by clay membranes of various thickness. B) Systematic sketch of the observed section shown in A.

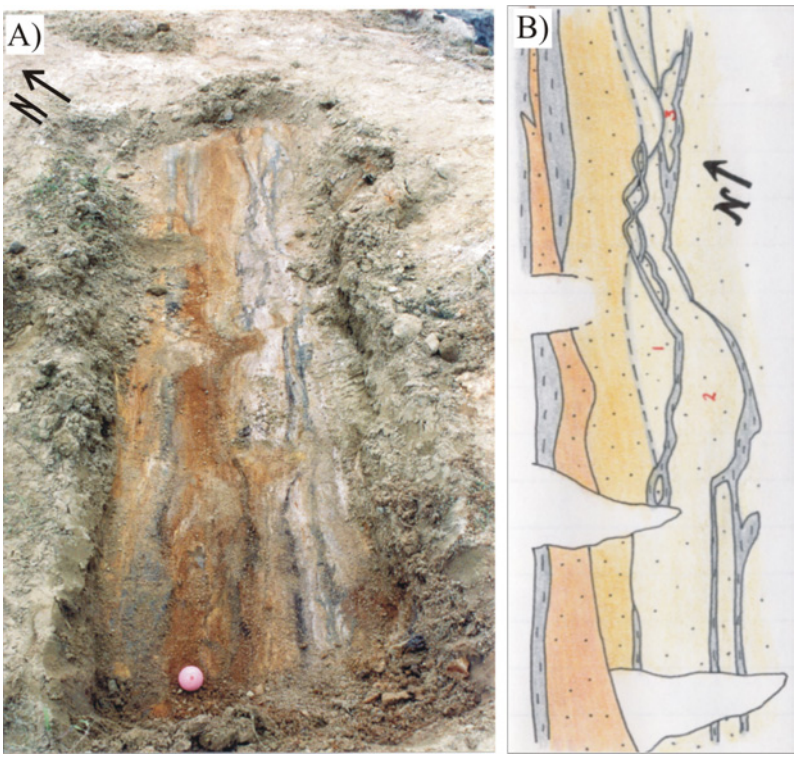

Figure 2.47 A) The second part of the exposure of Fault E. B) Systematic sketch of was is observed in A). In accordance to the previous section of the fault, the horses in this part consist of sand separated by clay membranes. However, the section is less chaotic as compared to the first part of the fault (figure 2.46) and only three horses could be distinguished. Pink golf ball as scale.

The plot of all of the horses studied in the locality is displayed in figure 2.48. An R^2-value of 0.51 implies that the data points representing the horses are well-constrained to the regression line. Hence, there is a satisfactory relation between the length and thickness of the horses.

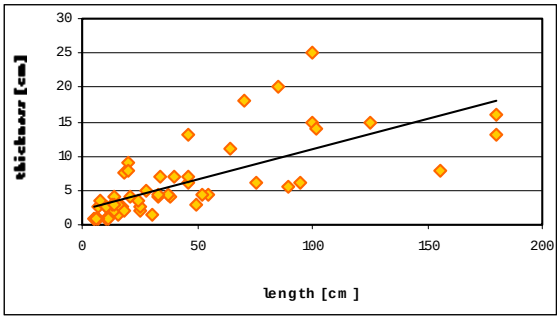

Figure 2.48 Plot of the length versus the thickness for the horses examined in fault A, C, E and F in A. Stenders Kvartsgrav. N = 53 and R^2 = 0.51.

2.6.3 The Galgeløkken Cliff section

The second study area on Bornholm is in a part of the Galgeløkken Cliff section, on the south-western coast on the island (figure 2.39). Lower Jurassic sediments are exposed in the outcrop, and the studied section is 4 m long and about 2 m high (figure 2.49). Five small faults can be distinguished, and horses relate to four of them. The horse related faults are numbered from 1 to 4 from east to west.

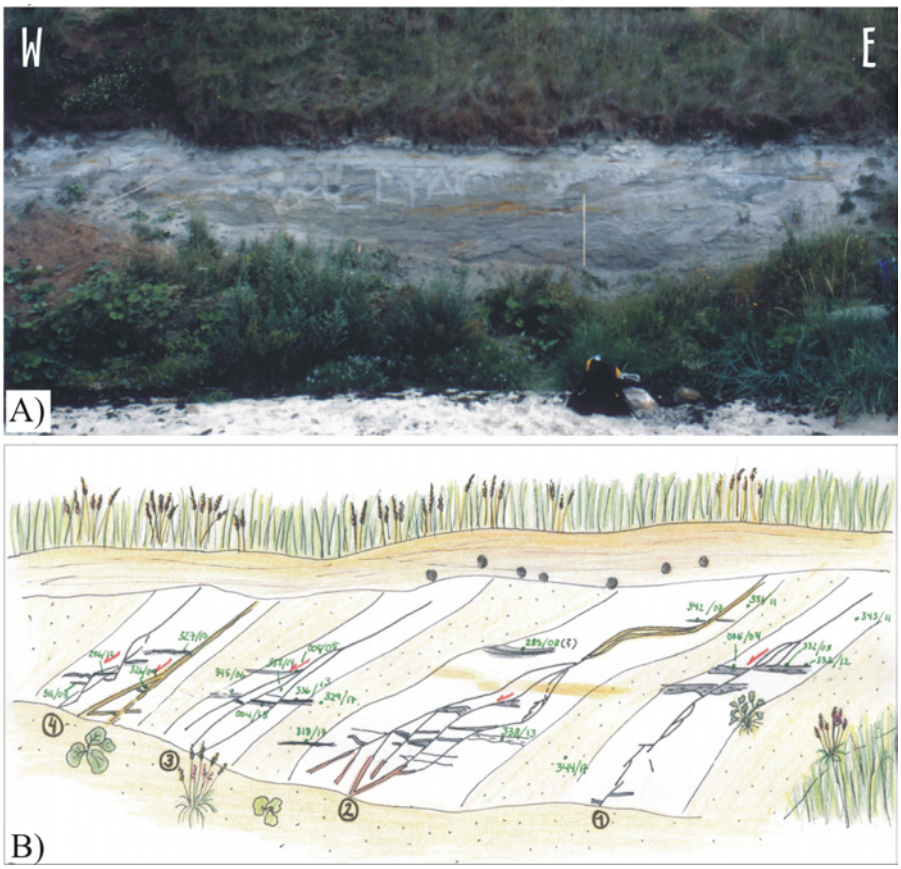

Figure 2.49 A) The examined part of the Galgeløkken cliff section on Bornholm, photo taken towards north. Four faults (1-4) were distinguished in this locality, all of them normal faults dipping towards the west and with a vertical displacement less than 5 cm. Horses are found within all of the faults, and they consist of fine to medium-grained sand separated by thin clay membranes. The horses are occurring within the hanging wall and footwall of the faults. B) Systematic sketch of what is seen in the photo in A).

Very fine-grained sand in cross-bedding draped by thin laminas of clay dominates the section. The original layering, S_o, is distinguished especially by use of the clay laminas, and dips gently towards the south. The throw across the faults are minor, and not surprisingly the orientation of the original layering of the sediments is the same in the hanging wall and the footwall of the faults. The sediments are almost unconsolidated,

making it possible to study the horses in three dimensions. On the other hand, the cliff section is a protected site and suffers enough already from tourists visiting the beach. For that reason mainly the loose sediment cover due to erosion was removed. Small amounts of throw across the faults have led to sparsely development of horses in the section.

As mentioned, five discrete normal faults were carefully examined in the cliff section (figure 2.49), four of them associated with horses. The faults are very similar and they strike NW-SE and dip towards NNE by an amount of 50°, although variations between 13° and 88° occur along the different fault planes. Clay laminas can be correlated across the faults, and the throws of the faults are recognized to vary between 0.4 cm and 4.5 cm, and the displacement between 1 cm and 12.8 cm (figure 2.50-53). Horses occur within the hanging wall and footwall, in what may be characterized as the damage zone. Common for each of the faults is that they have no developed fault cores and only poorly developed damage zones. The fault planes in fault 1 and 4 are discontinuous and are made up of small vertically linking segments (figure 2.50 and 2.53). Besides, the faults are diminutive compared to the faults examined in the sand pit.

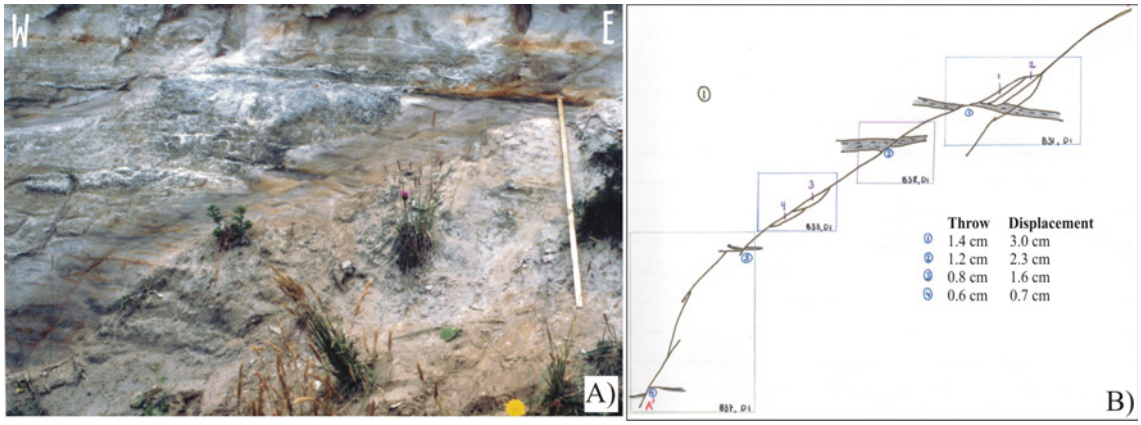

Figure 2.50 A) A close-up photo of fault 1, which is the first fault from the east in the section. Four horses occur within this fault, all of them within the footwall. B) Sketch of what is observed in A. The amount of throw and displacement were measured four different places along the fault.

The damage zones of the four faults are characterized by horses, and ranges from being barely present, as in fault 1 (figure 2.50), and up to 20 cm in thickness, as in fault 2 (figure 2.51). The damage zones of fault 2-4 are thickening towards the lower parts of the faults. A bit surprisingly, perhaps, is that the horses that define the damage zone in the different faults most frequently occur within the footwall, indicating that the

footwall has suffered slightly more deformation than the hanging wall. Although no more than four horses occur in fault 1, they all occur in the footwall (figure 2.50). The fault plane in fault 2 separates into two branches, marked as B-B' and C-C' (figure 2.51), where the branch B-B' seem to be the main fault plane. The damage zone of fault 2 is about as thick in the footwall as in the hanging wall if B-B' is the main plane, whereas if C-C' is the main plane every single one of the horses in the fault occur in the footwall. Similar to fault 2 the fault plane in fault 3 split into two branches, marked as D-D' and E-E' (figure 2.52), and both of the branches seem to have taken up equal amounts of movement. D-D' seems to be the main fault plane, and if that is the case the damage zone of fault 1 is about as thick in the hanging wall as in the footwall. Two small fault segments link to comprise fault 4 (figure 2.53). The damage zone in fault 4 is only present in the footwall of the upper segment, where it comprises a thickness of 4.5 cm.

2.6.4 Studied horses within the Galgeløkken Cliff section

The horses that were located within the Galgeløkken Cliff section all occur in either the hanging wall or the footwall of the four faults. The section exposing the horses is not very steep, having an angle of averagely 50^{o} between the section and the dip direction. This implies that the section gives an indication of how the horses appear in the dip dimension as well as in the strike dimension in addition to thickness. Common for all the horses is that they consist of fine-grained sand draped by thin laminas of clay. The fractures/faults defining the horses are usually smeared by clay.

Four horses are present in fault 1 (figure 2.50) and as mentioned earlier in this chapter they all occur in the footwall of the fault. The horses are very small, ranging between 6 cm and 14 cm in the dip dimension and between 11 cm and 26 cm in the strike dimension. The thickness of the horses is only 2-3 cm. The two horses occurring in the upper part of the fault almost fully overlap, whereas the two horses further down in the fault overlap by an amount of one third of the length of the horses. The two upper horses are left-stepping, and the two lower horses are right-stepping. A minor fault branch split from the main plane in the footwall of the upper part of the fault, just below

the two horses present in this part. The branching may represent an early stage in development of a new horse (figure 2.50).

The horses related to fault 2 vary more in size than the horses in fault 1. They vary between 1 cm and 80 cm in the dip dimension, and between 2 cm and 172 cm in the strike dimension, and they are between 0.3 cm and 14 cm thick. Two of the horses are present in the hanging wall of the fault, whereas the majority occurs within the footwall (figure 2.51). With the exception of two horses, the horses occur in the lower part of the fault, where they comprise a 20 cm thick damage zone. The mentioned two upper horses are left-stepping in accordance to the two upper horses in fault 1. Also both the large horses (labeled 1-3) and the tiny horses (labeled 4-7) have a preferred left-stepping manner. In accordance to the horses in fault 1 the horses in fault 2 are considerable distributed along the fault plane, and some of the horses occur as single horses. In addition, parts of the fault plane display no horses at all.

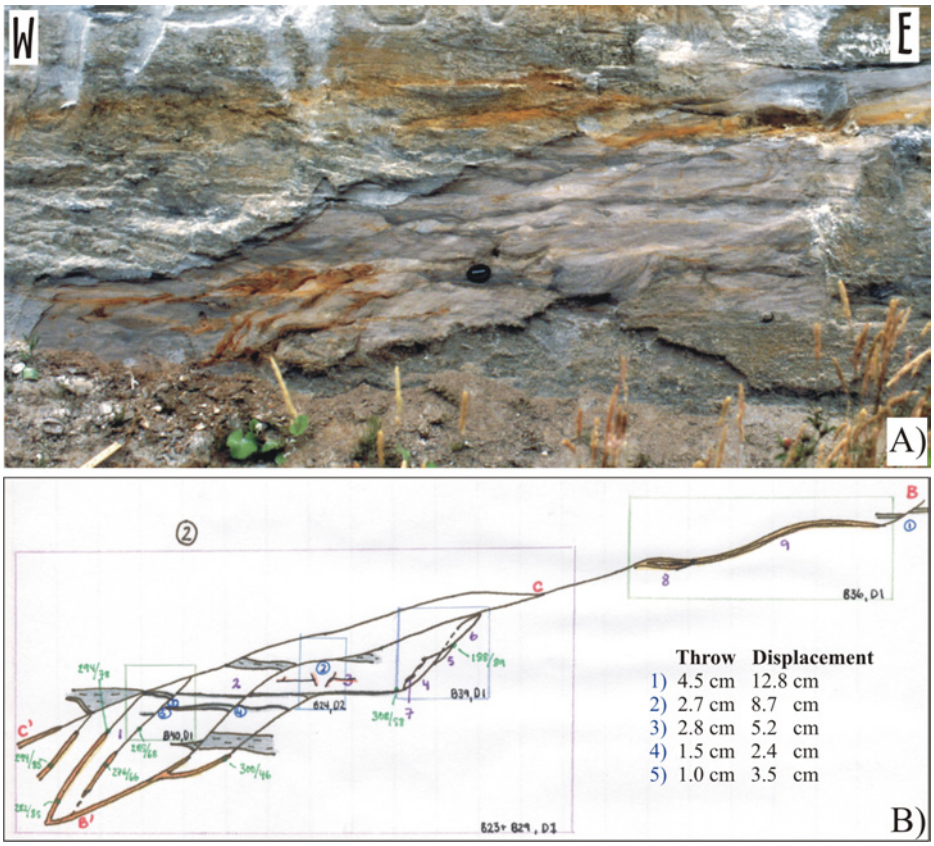

Figure 2.51 A) A close-up photo of fault 2, which is the second fault from the east in the Galgeløkken cliff section. Nine horses occur within the footwall and hanging wall of this fault. B) Sketch of what is observed in A. The amount of throw and displacement were measured five different places along the fault.

Fault 3 display horses of various sizes, similar to fault 2. The horses vary between 6 cm and 103 cm in the dip dimension, between 8 cm and 123 cm in the strike dimension, and between 0.5 cm and 18 cm in thickness. Three slim and small horses (labeled 8-10) are distributed along the fault plane in the upper part of the fault plane, none of them are overlapping each other (figure 2.52). The damage zone thickens in the lower part where the horses are larger and more abundant as compared to the upper part. Each and one of the horses in the lower part are pronounced left-stepping. The large horses (labeled 1-3) overlap by an amount of one half of the length of the horses. The small horses (4, 5 and 7) are less overlapping, and overlap by an amount of about one fourth to one third of the length of the horses.

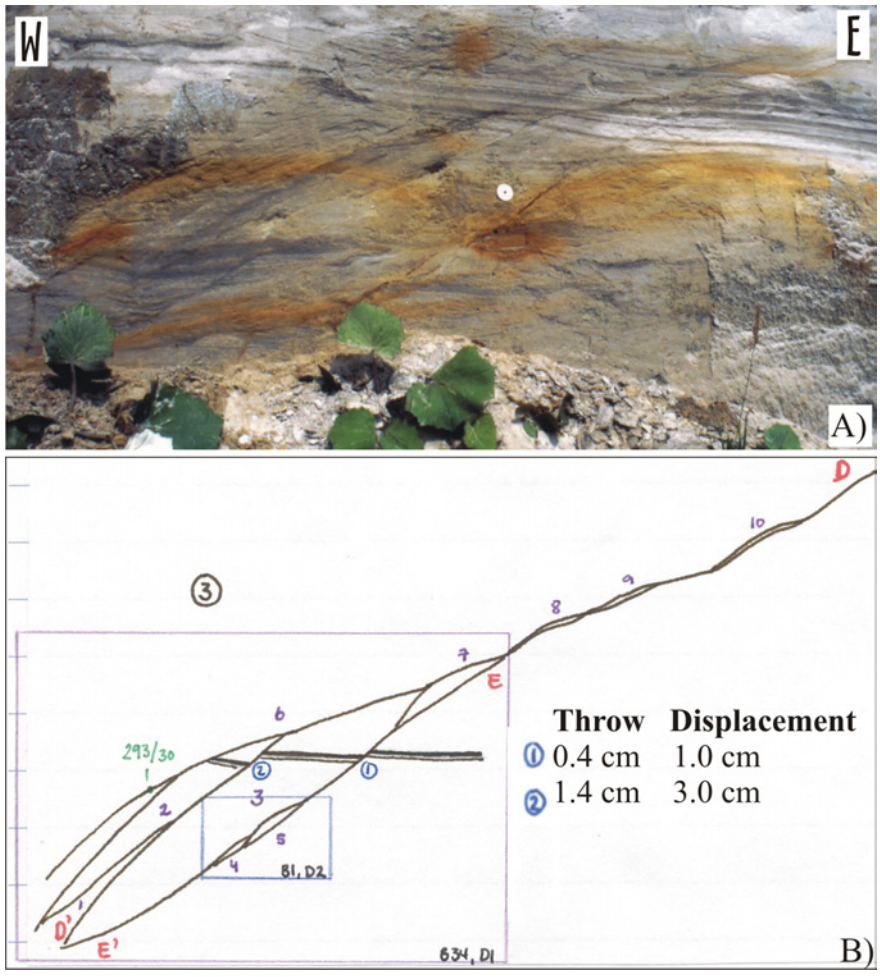

Figure 2.52 A close-up photo of fault 3, which is the third fault from the right/ east in the Galgeløkken cliff section. Ten horses occur within the footwall and hanging wall in this fault. B) Sketch of what is observed in A. The amount of throw and displacement were measured two different places along the fault.

Two horses (labeled 1 and 2) occur in the hanging wall of the lower fault segment in fault 4 (figure 2.53). A third horse (labeled 3) occurs between the two fault segments, and four horses occur in the footwall of the upper fault segment. The horses related to fault 4 are small compared to some of the horses in fault 2 and 3, having lengths in the dip dimension between 1 cm and 30 cm and in the strike dimension between 0.5 cm and 13 cm. Their thickness varies between 0.3 cm and 5 cm. The section exposing the horses in this fault has a lower angle (20^{o}) to the dip dimension than the rest of the horses in the locality. This implies that the horses are better exposed in the strike dimension than in the dip dimension. The horse occurring between the two fault segments (labeled 3) has most likely developed as a result of the linking of the two segments. The horses generally overlap by an amount that is one third of the exposed length of the horses, and all of them are left-stepping.

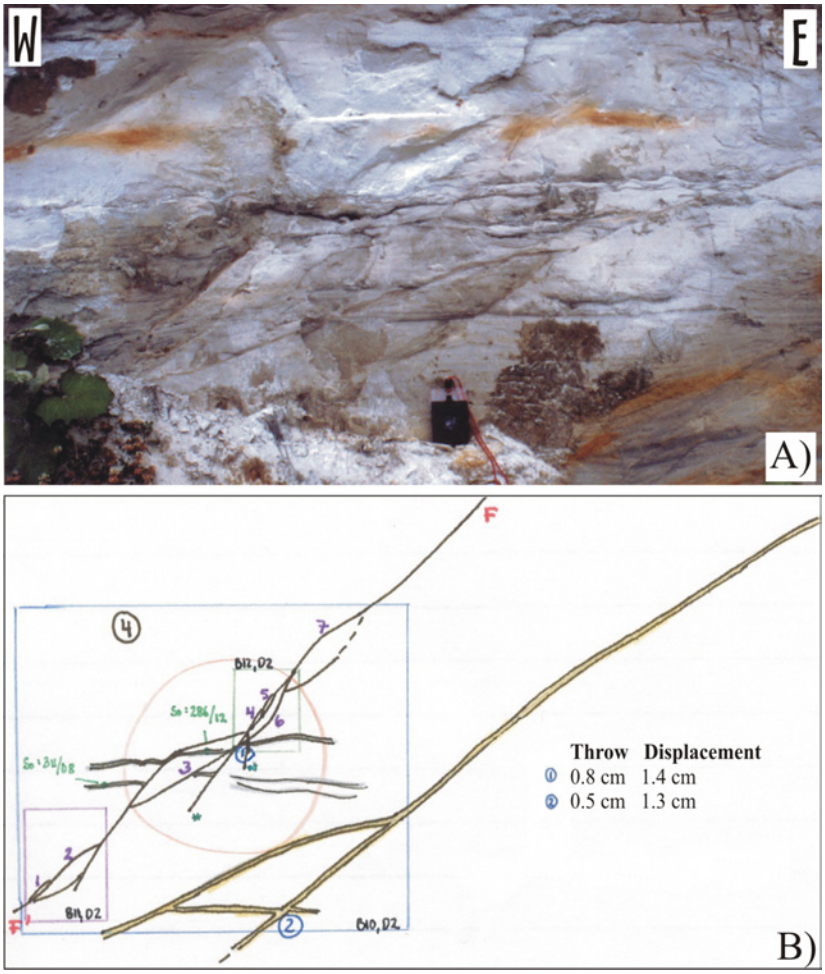

Figure 2.53 A close-up photo of fault 4, which is the first fault from the west in the Galgeløkken cliff section. Seven horses occur within this section. B) Sketch of what is observed in A. Horse 3 is interpreted as a result of linkage between to fault segments. The amount of throw and displacement were measured two different places along the fault.

The data points representing the horses in the plot of all the horses measured in the section (figure 2.54) are well constrained to the regression line, also confirmed by an R^2-value of 0.87. Hence, there is a strong relation between the length and the thickness of the horses.

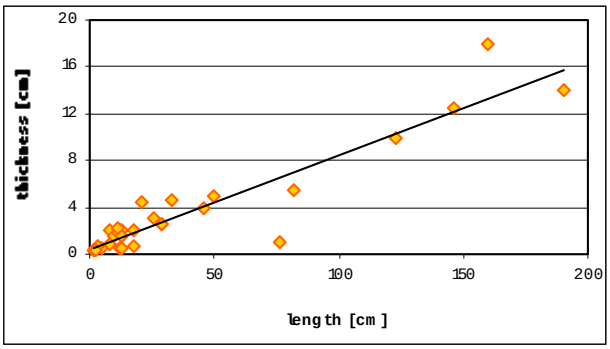

Figure 2.54 Plot of the length versus the thickness for the horses examined in the Galgeløkken cliff section. R^2 = 0.87 and N = 30.

2.7 Plaster of Paris experiments

Several experiments have been carried out at the university, the majority of them associated with horses. In my study I have studied five of them in detail (Experiment 1-5), in two of them (Experiment 2 and 3) horses were examined on both sides. All of the experiments examined are models of extensional faults. In two of the experiments (4 and 5) a ramp-flat-ramp geometry was used as basement, whereas no specific geometry was used in the latter three (1, 2 and 3). In four of the experiments (1, 2, 3 and 4) a wide setup were applied (21.5 cm), whereas a width of 11.5 cm was used in the fifth experiment (5).

A description of the procedure of the experiments is e.g. given by Fossen & Gabrielsen (1996) and Gabrielsen & Clausen (2001).

The faults in the plaster were generated by dragging a wooden wall in one end before the plaster solidified. The plaster represents the absolutely weakest material in which horses were measured in this study. One of the advantages of using the homogeneous and fine-grained plaster of Paris is that it has potential to develop very small details. Secondly, the plaster solidifies after deformation and thus preserves the details. The

disadvantages are that it rapidly changes physical properties during the experiment and the lack of internal marker horizons.

The horses generated in the plaster experiments are mainly measured along their a-axes (dip dimension) and c-axes (thickness). Nevertheless, some of the horses could also be measured along the b-axes (strike dimension) by studying the geometry on the top surface of the experiments.

2.7.1 Experiment 1

Four faults are associated with horses in the first plaster of Paris experiment that was studied (figure 2.55). The faults are dipping 30^{o}-40^{o} and have a vertical displacement varying between 1 cm and 4.5 cm.

Seven horses appear in one the vertical sections of the experiment. Horse 1 is exposed in three dimensions, whereas the rest of the horses are exposed in dip dimension (a-axis) in addition to thickness (c-axis). The seven horses vary between 2.3 cm and 11 cm in the dip dimension and between 0.4 cm and 3.5 cm in thickness. Horse 1 has a strike dimension of 9.5 cm. Horses 2, 3 and 5 are interpreted as a result of segment splaying, whereas the rest of the horses are interpreted as asperity bifurcation horses. The latter horses seem to be an early stage in the development of fault cores of the different faults.

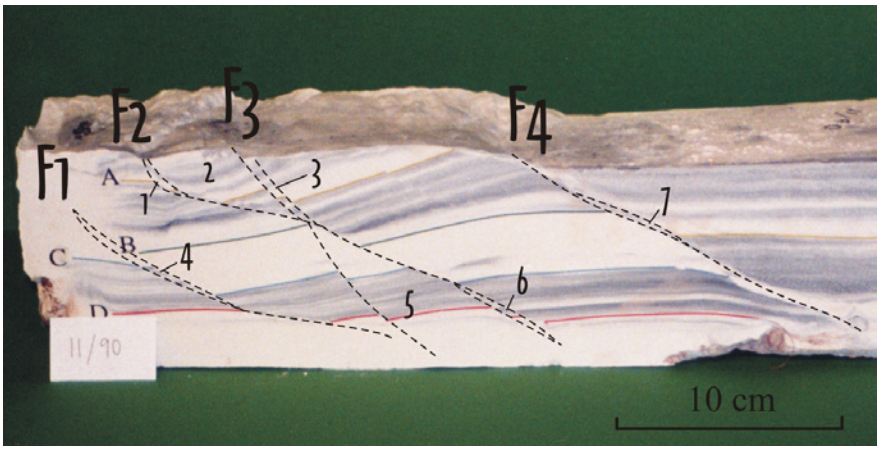

Figure 2.55 The first plaster of Paris experiment examined in this study. Four faults (F1-F4) are associated with horses (labeled 1-7).

The plot of the a- versus the c-axes for the horses is displayed in figure 2.56. An R^2-value of 0.97 implies that the data points representing the horses are well constrained to the regression line, and further that there is a strong linear relation between the two axes.

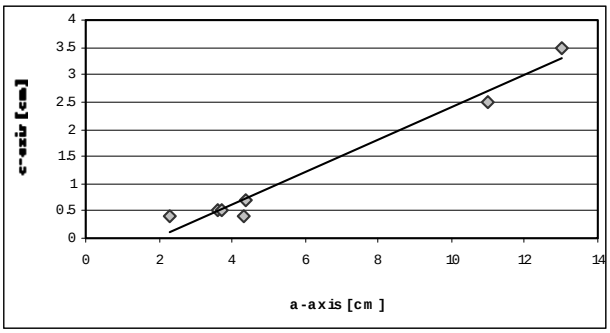

Figure 2.56 Plot of the a- versus the c-axes for the horses in plaster of Paris experiment 1. N = 7, and R^2 = 0.97.

2.7.2 Experiment 2

One fault is associated with horses in experiment 2. The fault has a dip of about 50°, and a vertical displacement of 10 cm (figure 2.57).

Ten horses occur within the fault, all of them in the hanging wall (figure 2.57). Seven of the horses were measured along their a- and c-axes (dip dimension and thickness). Six of these horses were seen in one of the vertical sections of the experiment (figure 2.57b), whereas the seventh was seen on the upper free surface. The remaining three horses were measured along their b- and c-axes (strike dimension and thickness), and were seen on top of the experiment. The horses vary between 3.4 cm and 7.3 cm in the dip dimension, between 5.0 cm and 7.6 cm in the strike dimension and between 0.3 cm and 2.0 cm in thickness.

Horses 1 and 3 are interpreted as asperity horses, whereas the rest of the horses are interpreted as a result of segment splaying and amalgamation. The horses are generally left-stepping, thus stepping the same way as the relative movement on the faults.

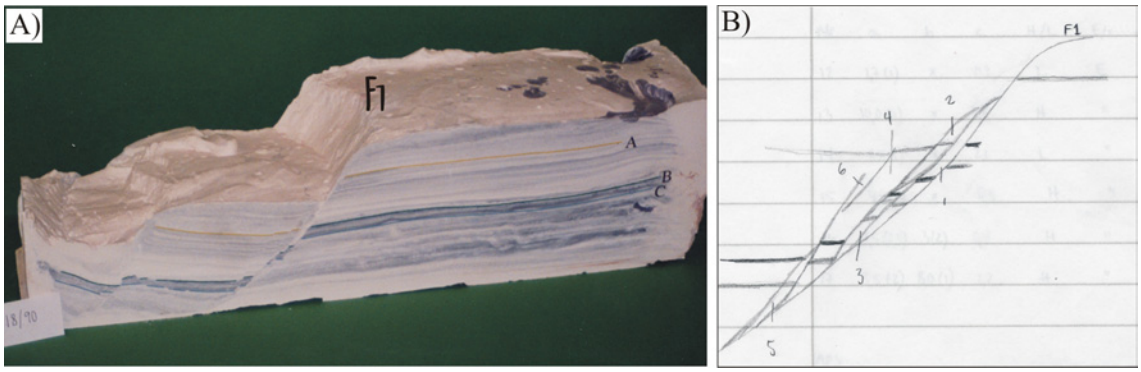

Figure 2.57 A) The second plaster of Paris experiment examined. All of the horses occur within the same fault, F1. Horses 1-6 were studied in the vertical section, whereas horses 7-10 were studied on the top. B) Sketch of the six horses studied in the vertical section.

The plot of the a-axes (dip dimensions) versus the c-axes (thickness) of the horses is displayed in figure 2.58. An R^2-value of 0.69 implies that the data points representing the horses are well constrained to the regression line, and there is a satisfactory linear relation between the a- and c-axes of the horses.

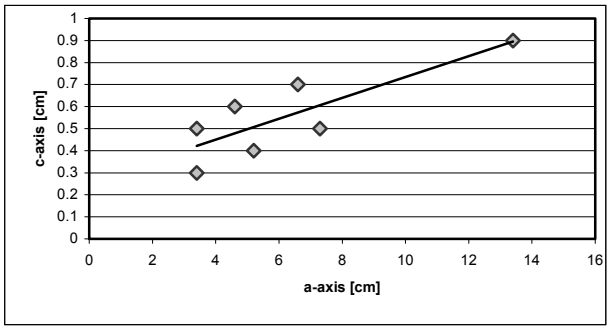

Figure 2.58 Plot of the a- versus the c-axes for the horses that occur in experiment 2. N = 7 and R^2 = 0.69.

2.7.3 Experiment 3

In experiment 3 both of the vertical sections were examined. Five faults (F1-F5) appear, each of them associated with horses (figure 2.59). F1 has a dip that decreases from 40° to 20° and a vertical displacement of 1.7 cm, F2 has a dip of 40° and a vertical displacement of 2.7 cm, F3 has a dip that decreases from 50° on the top to 10° towards basement and an average vertical displacement of 3.0 cm, F4 has a dip decreasing from 30° to 40° towards basement and a vertical displacement of 1.3 cm, and eventually F5 has a dip of 50° and a vertical displacement of 1.6 cm.

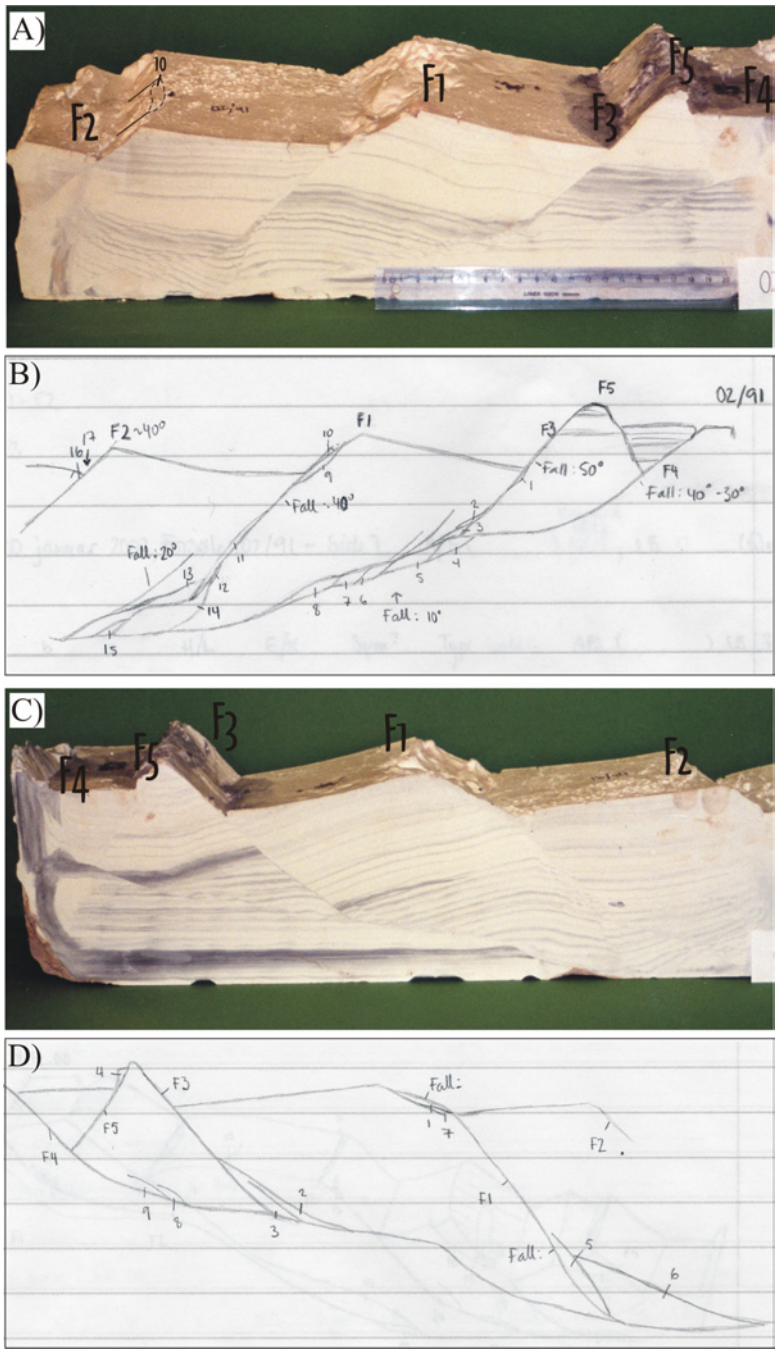

Figure 2.59 Experiment 3 where five faults (F1-F5) are associated with horses. A) Vertical section 1. B) Sketch of the horses measured in the first section C) Vertical section 2. D) Sketch of the horses measured in the second section.

Measures of twenty-seven horses were recorded from this experiment. Similar to the previous experiment, the majority of the horses examined appear along the two vertical sections and can hence be measured along their a- and c-axes. Six of the horses, however, are exposed in three dimensions, such that all of the a-, b- and c-axes could be measured (horse 10, 16, 17, 18 on side 1 and horse 1, 4, 10 on side 2). The horses in this

experiment vary between 1.7 cm and 11.7 cm in the dip dimension (a-axis), between 3 cm and 8.0 cm in the strike dimension (b-axis), and between 0.2 cm and 2.2 cm in thickness (c-axis). Except for horse 1, 2, 3, 11, 12 in the first vertical section and horse 1 in the second vertical section, the horses are interpreted as a result of segment splaying and amalgamation. Some of the horses occur between two faults (e.g. horses 4-8 in section 1 that occur between F3 and F4), whereas the common horse occurs in the hanging wall of one of the faults. The horses are generally left-stepping in section 1 (e.g. horses 4-8), and right-stepping in section 2 (e.g. horses 8 and 9), hence stepping the same way as the relative movement.

The plot of the a-axes (dip dimensions) versus the c-axes (thickness) of the horses is displayed in figure 2.60. An R^2-value of 0.44 implies that the data points are satisfactory constrained to the regression line and the linear relation between the dip dimension and thickness for the horses is good. The data points representing the horses in the plot of the b- versus the c-axes for the horses (figure 2.61), on the other hand, are less constrained to the regression line. An R^2-value of 0 implies that there is no linear relationship between the b- and c-axes for these horses.

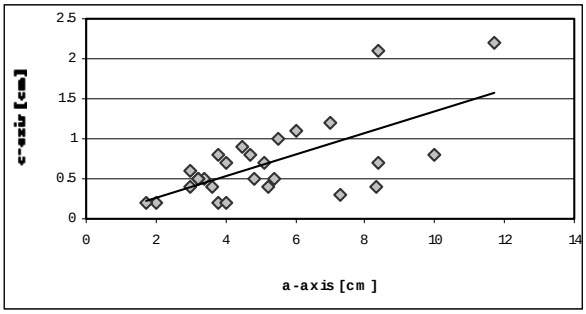

Figure 2.60 Plot of the a-axes versus the c-axes for the horses measured in experiment 3. N = 27 and R^2 = 0.44.

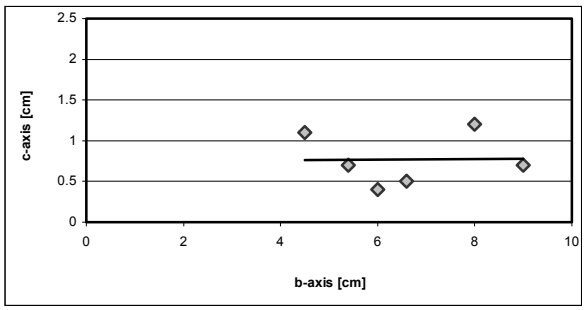

Figure 2.61 Plot of the b- versus the c-axes for the horses that occur within experiment 3. N = 6 and R^2 = 0.

2.7.4 Experiment 4

Four synthetic faults (F1-F4) and two antithetic (F5 and F6) faults appear in experiment 4 (figure 2.62). F1, F2 andF3 are associated with horses. Fault 1 has a gentler slope as compared to the other two, dipping averagely 20°. Fault two and three dip 45° and 60°, respectively.

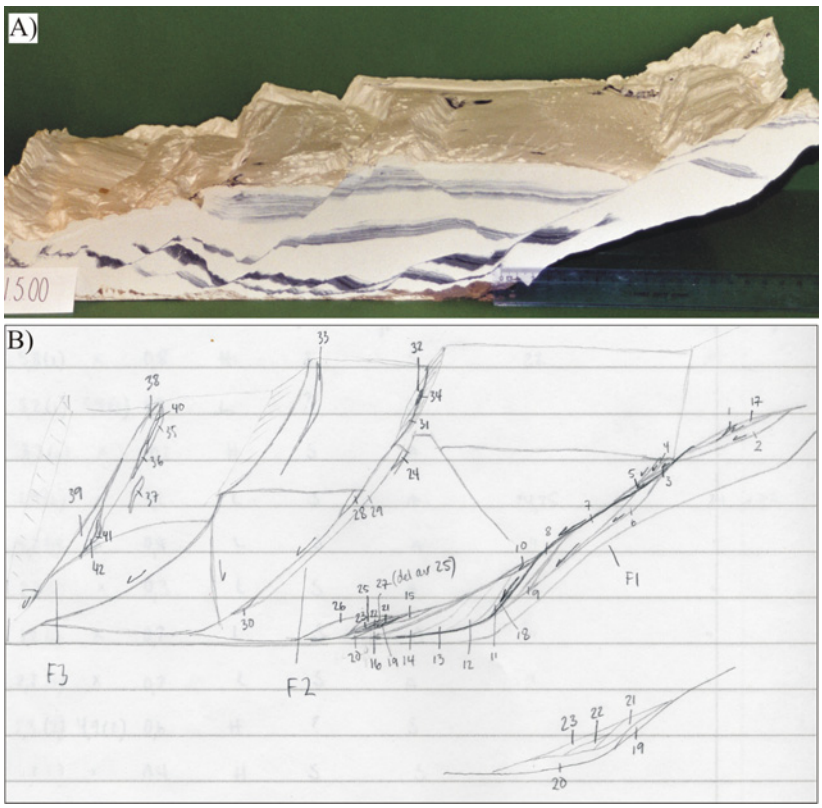

Figure 2.62 A) Experiment 4. Three faults are associated with horses (F1-F3). B) Sketch of the horses.

The experiment host forty-two horses, which is the highest amount of horses observed within the same experiment in this study. The majority of the horses appear in the vertical section, hence exposing their dip dimension and thickness. Eleven horses (e.g. horses 1-4 in the upper part of F 1) can be measured in all the three dimensions, whereas nine horses (e.g. horses 38-42 in F3) are exposed in the strike dimension in addition to thickness. The horses vary between 1.2 cm and 11.1 cm in the dip dimension, between 2.5 cm and 18 cm in the strike dimension, and between 0.2 cm and 2.7 cm in thickness. Ten horses (e.g. horses 1, 2 and 17 in the upper part of F1) are interpreted as asperity bifurcation horses, whereas the majority of the horses that occur in this experiment seem to have generated due to segment splaying and amalgamation

(e.g. horses 6-9 in the middle part of F1). It is not possible to identify any fault core within the experiment with certainty, and the majority of the horses occur in the hanging wall or the footwall of the faults. The horses are generally left-stepping (e.g. horses 11-16 in the lower part of F1), hence stepping the same way as the relative movement.

The plot of the a-axes versus the c-axes is displayed in figure 2.63, whereas the plot of the b- versus the c-axes is displayed in figure 2.64. Satisfactory R^2-values in both of the plots implies that there is a strong linear relation between a- and c-axes and between b- and c-axes for the horses.

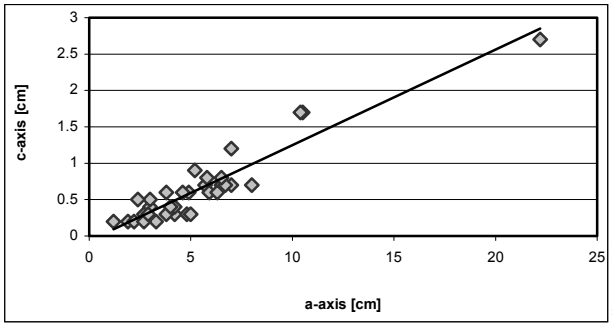

Figure 2.63 Plot of the a- versus the c-axes for the horses measured in experiment 4. N = 33 and R^2 = 0.88.

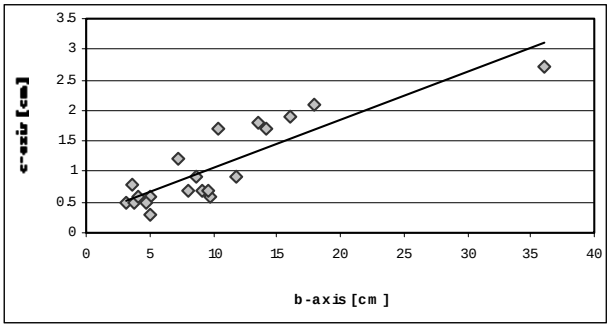

Figure 2.64 Plot of the b- versus the c-axes for the horses that occur within experiment 4. N = 20 and R^2 = 0.76.

2.7.5 Experiment 5

Similar to experiment 3, horses were examined on both of the vertical sections of experiment 5 (figure 2.65). Six faults are generated, and horses occur within four of these (F1-F4). The dips of the faults vary between 40^o and 65^o, and the vertical displacements between 2.8 cm and 4.8 cm.

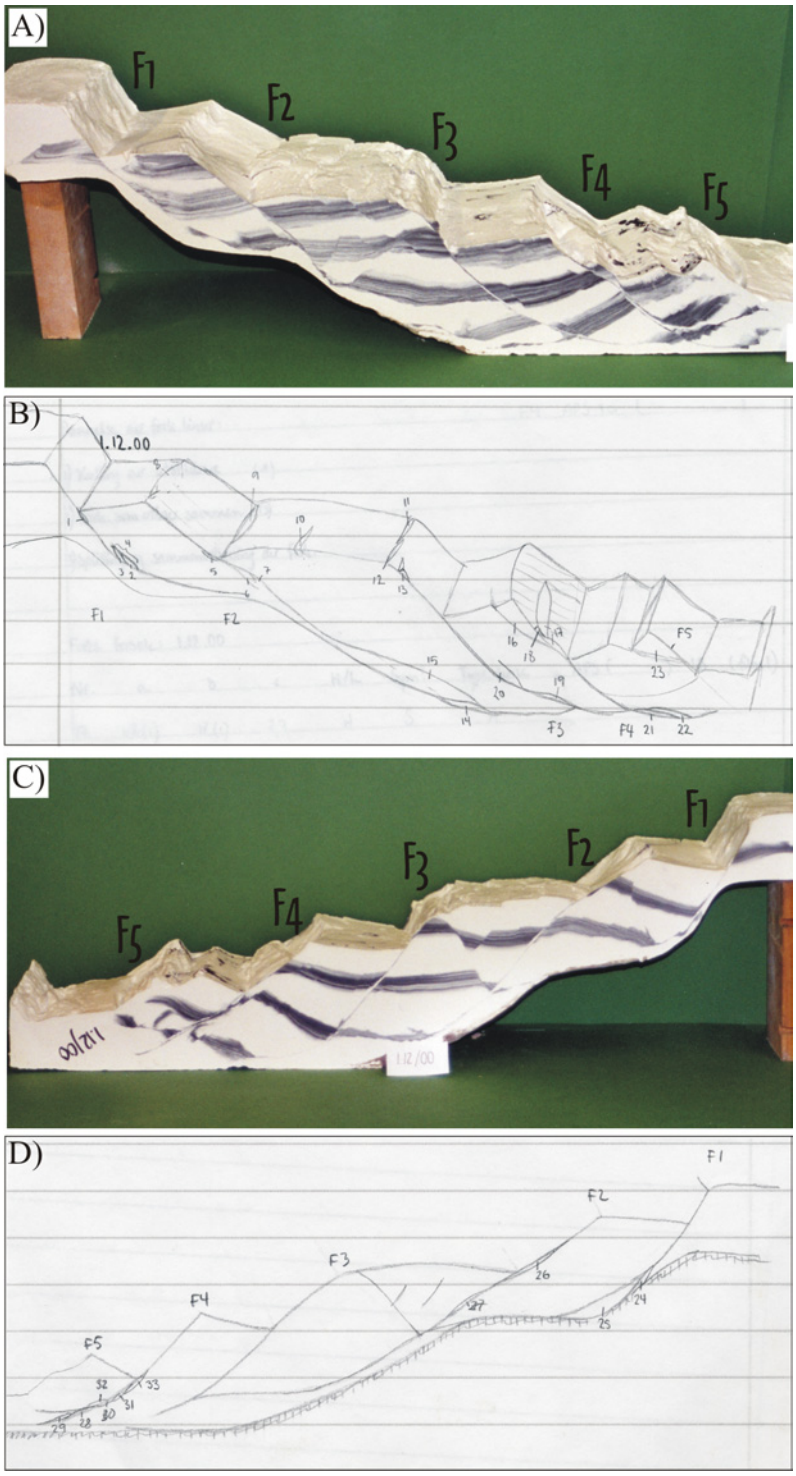

Figure 2.65 Experiment 5. Six faults appear, of which four are associated with horses. A) Vertical section 1. B) Sketch of the first section. C) Vertical section 2. D) Sketch of the second section.

Together 33 horses were measured in this experiment, dominantly along their a- and c-axes. The exceptions are horse 8, 12, 13, 16, 17, 18 and 23 that were measured along all of the three axes, and horse 9, 10 and 11 that were measured along the b- and c-axes. The horses vary between 1.2 cm and 9.6 cm in the dip dimension (a-axis), between 2 cm

and 12 cm in the strike dimension (b-axis) and between 0.2 cm and 2.7 cm in thickness (c-axis). Half of the horses (e.g. horses 1, 2 and 3) are interpreted as asperity bifurcation horses, whereas the other half (e.g. horse 4 and 6) is interpreted as segment splaying or amalgamation horses. About the same amount of horses occurs in the hanging wall as the footwall of the faults. Consistent with the horses in the other experiments, the horses generally step the same way as the relative movement has been, that is left-stepping in vertical section 1 and right-stepping in section 2 (e.g. horses 2, 3, 21 and 22).

The plot of the a- versus the c-axes for the horses in this experiment is displayed in figure 2.66. An R^2-value of 0.49 implies that the data points representing the horses are well constrained to the regression line, and thus that the linear relation between the two axes is satisfactory. Also the data prints representing the b- versus the c-axes of the horses (figure 2.67) are satisfactory constrained to the regression line. Thus, there is a strong relationship also between the b- and c-axes of the horses in this experiment.

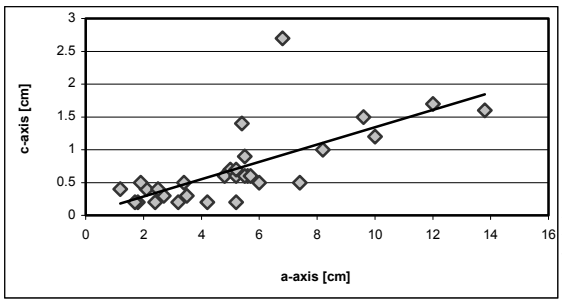

Figure 2.66 Plot of the a- versus the c-axes for the horses that occur within the fifth examined experiment. N = 33 and R^2 = 0.49.

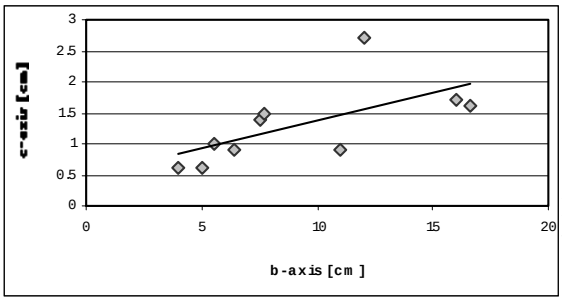

Figure 2.67 Plot of the b- versus the c-axes for the horses measured in plaster of Paris experiment 5. N = 10 and R^2 = 0.41.

Chapter 3

RESULTS

In this chapter the results of the regression analyses of the horses in the three field areas, together with the horses examined in the plaster of Paris experiments, are presented. The data taken from the horses are presented in xy-diagrams. Because of limited exposure in three dimensions it has not been possible to measure in full both the dip dimension (a-axis) and the strike dimension (b-axis) of all of the horses. The thickness (c-axis), on the other hand, has always been measured. However, this implies that a full dataset of a-, b- and c-axes is not available for all of the studied horses. Nevertheless, the c-axis and one of the other axes (a or b) are commonly seen. Hence, the measured dimensions are separated such that the a versus c relation, and the b versus c relation are displayed separately.

To utilize the full potential of the geometrical relations, the data of the horses are represented in three datasets. Initially, the measured length of the horses is projected parallel to both the dip and the strike dimension and most of the horses are plotted both in a-c diagrams and in b-c diagrams. Secondly, the horses exposed in sections that are closer to one of the dimensions are only projected parallel to this dimension, and hence plotted in only one of the diagrams. Finally, the horses are not projected to any of the dimensions, but the length of the horses, as it was measured at the locality, is plotted versus the thickness.

In each subchapter the results of the plotting of the horses examined on Frøya are presented first, then follows the presentation of the results from the plot of the horses in Kilve and on Bornholm. Finally, the results from the plot of the horses in the plaster of Paris experiments are presented.

3.1 Regression analysis

Regression line

Regression analyses are used to examine the relation between to variables, x and y. The regression line is determined by *the least square method*, and is a linear curve that best fits the scattered data points in a diagram. The line is given by:

$$y = \alpha x + \beta$$

The coefficient α denotes the slope of the regression line, whereas the coefficient β gives the intersection with the y-axis, i.e. for $x = 0$. Both α and β are determined for the condition that the sum of the square residuals is at a minimum value.

The gradient of the regression line

The coefficient α gives the gradient for the regression line. In the case of the horses, that is by which amount the thickness (y) increases by an increase of the x-value (dip or strike dimension, or the measured length). The coefficient can be both positive and negative, in which a negative value would imply a negative slope. If the coefficient α is zero, the regression line has no slope and the y-value (thickness) will be constant, independent of the value of x (dip or strike dimension). A low value of α reflects a gentle slope of the regression line, and a high value of α reflects a steep slope.

In this study all of the regression lines have a positive slope, reflecting that the thickness of all of the horses increase by an increase in the dip or strike dimension, or in the measured length, and hence the α coefficients are positive in this study. A gentle slope of the regression line indicates a minor increase in thickness by an increase in the dip or strike dimension, whereas a steep slope indicates a considerable increase in thickness by an increase in one of the other two dimensions (figure 3.1). An α-coefficient of zero would on the other hand be consistent with a constant thickness for every horse, independent of the dip or strike dimension, or the measured length. If the coefficient β

is zero and the coefficient α is 1, this would imply that relation between the thickness of the horses and the dip or strike dimensions is constant.

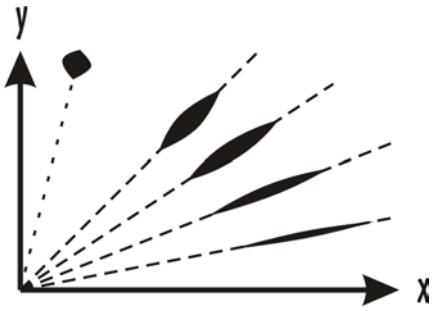

Figure 3.1 Sketch of how the different slopes of a regression line reflect the amount of increase in thickness by an increase in the dip or strike dimension. The steepest regression line in the sketch has an α coefficient of 1, reflecting a horse of which the thickness is equal the dip or strike dimension.

The intersection of the regression line with the y-axis

The coefficient β reflects the intersection with the y-axis when x in the formula above is zero. The coefficient can be positive or negative. Figure 3.2 shows an example of three regression lines, where two of the lines have the same gradients (α-value) but different intersections with the y-axis (β-value). The third regression line is steeper and the y-values along this line are equal the x-values. Two of the regression lines are intersecting the y-axis at zero, whereas the third regression line is intersecting this axis at a positive value.

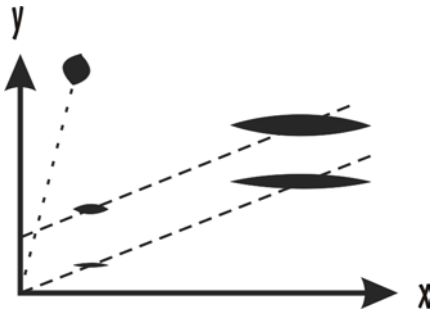

Figure 3.2 Sketch showing two regression lines that have the same gradients, but that intersect the y-axis at different values. The third regression line has a steeper slope, and represents horses of which the thickness is equal to the dip or strike dimension. The axes in this diagram do not have the same values.

At any x-value (dip or strike dimension, or measured length) the upper regression line (figure 3.2) represents horses that have higher y-values (thickness), than the lower regression line as long as the gradients of both of the regressions lines are equal. However, both the gradients and the intersection of the regression line with the y-axes vary in each plot. Due to this, a comparison between all the regression lines would be beyond the intension of this thesis.

R^2-value

R is the *sample correlation coefficient*, or *Pearson's product moment correlation coefficient*, and is a numerical of in which degree the points scatter around a straight line, in this case the regression line. Per definition R must be between -1 and 1. The value R = 1 is consistent with a situation where all the data points lie perfectly on a straight line with a positive slope; R = -1 is also a perfect linear relation in which the line has a negative slope. A value of R close to either of these extremes corresponds to a tight clustering of data points around a straight line, constituting a strong linear relation. With lesser amounts of cluster about a straight line, R assumes smaller numerical values, and R = 0 is interpreted as an absence of linear relation. R^2 represents the proportion of variability in the y values that can be explained by the linear relation.

A satisfactory value of R^2 is dependent upon the number of data points, N. Because the number varies between the plots, also the value of R^2 considered satisfactory differs between each plot. However, an R^2-value of 0.3 is usually considered satisfactory. If N = 30, the level of confidence is then 95%. The estimate of a satisfactory value of R^2 is based on the student-t test, which is given by the formula:

$$t = |R| (N - 2)^{1/2} / (1 - R^2)^{1/2}$$

Average a:c, b:c and l:c ratios

The average a:c, b:c and l:c ratios are estimated from the datasets of the horses. Hence, the ratios are not related to the regression analyses. The ratio specifies how long the horses are in the dip or strike dimension as compared to the thickness. A low ratio will reflect relatively thick horses, whereas a high ratio will reflect relatively slim horses.

Confidence interval

In some diagrams a confidence interval is included. The intervals are estimated by use of the formula:

$$L = t_{1/2\alpha} * S_z * (R_i)^{1/2}$$

where $R_i = 1 + 1/N + (X_i - \mathbf{x})^2 / (N - 1) * S_x^2$

x is the average of x, which is equal to the lengths of the horses in this study,
$t_{1/2\alpha}$ is found in a table of critical values, and
S_z and S_x are standard deviation of z and x, respectively.

The intervals are estimated by a confidence coefficient of 90%. This implies that 90% of the horses in the diagram are within this interval.

3.2 Least reliable dataset

In the localities some of the horses are exposed in sections that are either parallel to the dip or the strike dimension of the fault. However, the majority of the horses are exposed in sections that are between the dip and strike dimension. In such cases the measured length of the horses are projected parallel to both the dip and strike dimension in this chapter. On the other hand, it has always been possible to measure the thickness of the horses directly in the field.

In this chapter the horses exposed in sections between the dip and strike dimension have their dip and strike dimensions estimated (chapter 1.5), and are presented both in a-c and b-c diagrams. The horses that are exposed in sections that are parallel to one of the dimensions are only represented in diagrams where the thickness is plotted versus this dimension. Sections of the horses that are less than 15^o to one of the dimensions are treated as parallel to the dimension.

All the values obtained in the analyses of the data from this dataset are summarized in the end of this chapter (table 3.1). A comparison of the plots of the horses from this dataset is given in chapter 4.1.

3.2.1 Frøya

Horses examined in both the locality at Flatval (locality 1) and at the locality at Skardsvåg (locality 2) contribute to the dataset from Frøya. The lithology in both of the localities consists of migmatitic gneisses intruded by pegmatite (chapter 2.2). The fault in the locality at Flatval is interpreted as a strike-slip fault which may have undergone some normal movement. At Skardsvåg fault surfaces show evidence of oblique slip.

In the locality at Flatval all of the examined horses are located within the fault core. The horses are classified as first order horses, and they are thought to be the result of asperity bifurcation faulting (see chapter 5).

The horses in the locality at Flatval are exposed in a section parallel to the dip dimension, and the data taken from these horses are represented in a-c diagrams (figure 3.3 and figure 3.4). The exception is two horses which could be measured in the strike dimension. These to horses are included in the first of the b-c diagrams (figure 3.5).

The horses examined at Skardsvåg are located within the damage zone in both the hanging wall and footwall, as well as within the fault core. A few larger horses, which are classified as first and second order structures, are found in the damage zone, whereas the majority of the horses, classified as third and fourth order horses, are located within the fault core. Due to the fact that only a part of the dip dimensions of the largest first and second order horses are exposed in the locality, it is not possible to interpret the generation of these horses. The smaller third and fourth order horses are, in accordance to the horses in the locality at Flatval, interpreted as asperity bifurcation horses.

The horses in the locality at Skardsvåg are, however, exposed in a section that is between the dip and strike dimension. In this chapter the measured length of these horses are projected to both the dip and strike dimension, and the horses are represented in both a-c diagrams (figure 3.3 and 3.4) and in b-c diagrams (figure 3.5 and 3.6).

Relation between the a- and c-axes

The relation between the a- and c-axes are presented in figure 3.3 and includes all of the horses examined in the two localities on Frøya. The a-axes vary between 13 cm and 1000 cm, and the c-axes between 3 cm and 250 cm. The regression line has a gradient of 0.26 and intersects the y-axis at –5.5. The R^2- value is 0.92, reflecting a strong linear relation between the variables. It should be noted, however, that the regression line heavily relies on only two points representing larger horses. Also, the spread when it comes to the three middle-sized horses is considerable. Together there are five data points that fall in the range of a > 400 cm. Average ratio between a and c is 6:1.

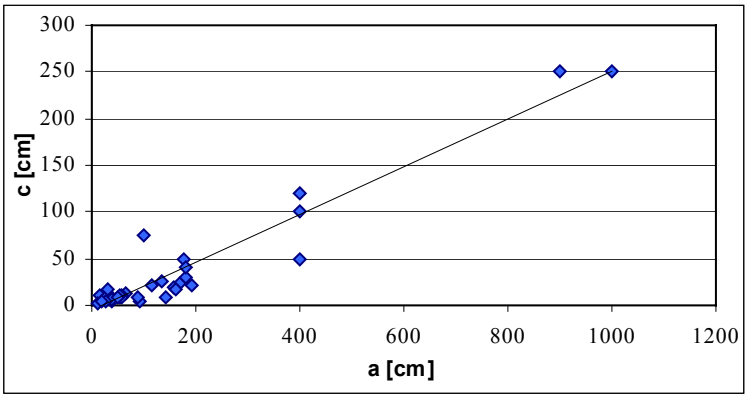

Figure 3.3 Plot of the a- versus the c-axes for the horses in locality 1 and 2 on Frøya. The regression line is given by y = 0.26x – 5.5. R^2 = 0.92, N = 34, and average a:c ratio is 6:1.

Because the regression line strongly depends on the mentioned five points to the right in the diagram, and to study the spread in the dimensions of the smaller horses, the a- and c-axes are re-plotted (figure 3.4), with these five points omitted from the dataset. Thus the plot presents a dataset more homogeneous than the previous. The horses in this diagram have a-axes (dip dimensions) between 13 cm and 200 cm, and c-axes (thickness) between 3 cm and 22 cm. The regression line has a gradient of 0.14, and it intersects the y-axis at +2.4. The R^2-value is 0.60, and linear relation between the axes is satisfactory. The average a:c ratio of the horses is 7:1, indicating that the horses in the more homogeneous dataset are slimmer relative to length than the horses in the entire dataset.

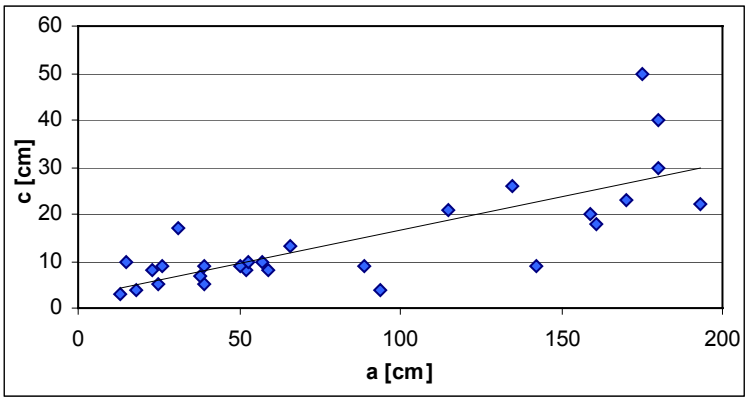

Figure 3.4 Plot of the a- versus the c-axes of the same dataset as in figure 3.3, but where the five data points with the highest a-values are omitted. The regression line is given by y = 0.14x + 2.4. R^2 = 0.60, N = 28, and average a:c ratio is 7:1.

Relation between the b- and c-axes

The plot of the b-axes versus the c-axes in figure 3.5 includes the data from both localities on Frøya. The horses vary between 4 cm and 230 cm in the strike dimension, and between 3 cm and 50 cm in thickness. The regression line has a gradient of 0.08 and it intersects the y-axis at +9.1. The R^2-value is 0.18 for this plot, indicating only a weak linear relation between the dimensions. Average ratio between b and c is 6:1, which is the same as the average a:c ratio when the entire dataset is considered.

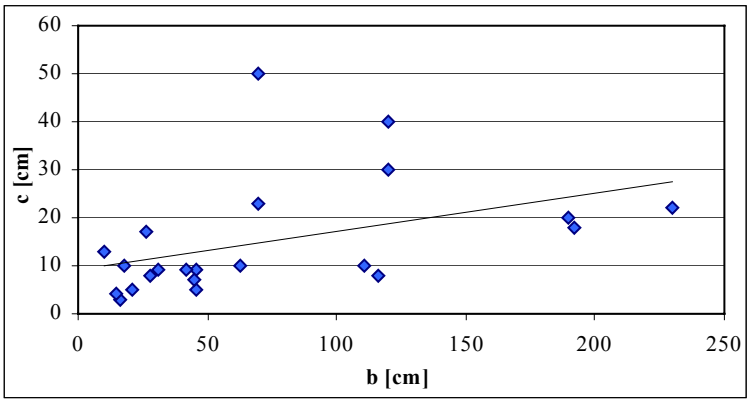

Figure 3.5 Plot of the b- versus the c-axes for the horses in locality 1 and 2 on Frøya. The regression line is given by y = 0.08x + 9.1. R^2 = 0.18, N = 22, and average b:c ratio is 6:1.

The weak linear relation between the strike dimension and thickness for these horses may have several reasons. First, the stress systems in the two localities may have been different. Secondly, the faults may have undergone different amount of displacement. Thirdly, more than one order structures from locality 2 are represented in the diagram. The horses in the two localities are also exposed in different sections. The horses in the locality at Flatval are exposed in a section that is parallel to the dip dimension, whereas

the horses in the locality at Skardsvåg are exposed in a section that is between the two dimensions.

In fact, six of the data points have large y-values (thickness) compared to the affiliated x-values (strike dimensions). Two of these six points represent horses only partly exposed in locality 1, and hence less reliable as compared to the others. Three of the points that deviate from the majority in the diagram represent the only third order structures in the locality at Skardsvåg. The horses therefore deviate from the majority of the horses in the diagram due to their large sizes. The sixth point that deviates from the rest in the diagram represent a horse in the locality at Skardsvåg that is only partly exposed.

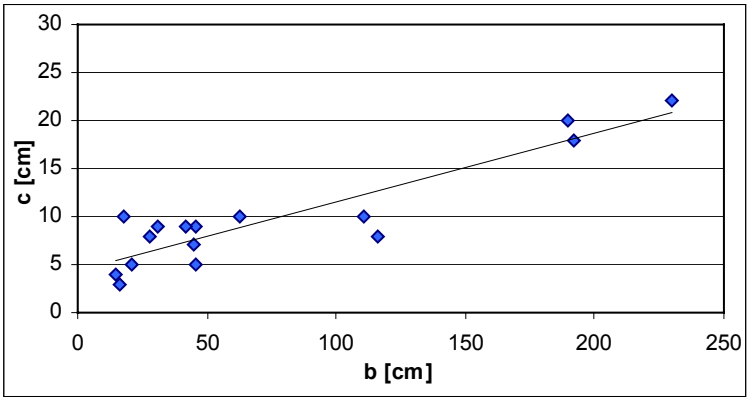

Figure 3.6 Plot of the b- and c-axes for the same dataset as in figure 3.5, but where six points with high c-values compared to the affiliated b-values are omitted. Regression line is given by y = 0.07x + 4.4. R^2 = 0.82, N = 16, and average b:c ratio is 7:1.

Six of the horses plotted in figure 3.5 have very high c-values (thickness) compared to the affiliated b-values. The b- and c-axes are re-plotted with these six horses omitted from the dataset (figure 3.6). The strike dimensions (b-axes) vary between 15 cm and 230 cm, whereas the thickness varies between 3 cm and 23 cm. The regression line for this relatively homogeneous dataset has a gradient of 0.07, and it intersects the y-axis at +4.4. The R^2-value is 0.82, reflecting that the points are well-constrained to the regression line. As for the average a:c ratio in the more homogeneous dataset of the a- and c-axes, the average b:c ratio is 7:1. Based on the ratios the dip dimension of the average horse on Frøya is equal the strike dimension, when the homogeneous datasets of the two dimensions are considered. Besides that, the average horse in the homogeneous dataset is slimmer than the average horse in the entire dataset.

All of the data points in the re-plot only represent horses from locality 2. The horses are therefore generated within the same stress system and the same amount of fault intensity. They are also exposed in the same section. Besides that, all of the horses are fourth order structures. To summarize, the data points representing the selected horses are well constrained to the regression line, reflecting a strong linear relation between the strike dimensions and thickness for these horses.

3.2.2 Kilve

Three localities in Kilve are contributing to the dataset from this field area. The localities are named locality 1, 2 and 3, and all of them are located on the Kilve Beach.

As mentioned in the description of the localities in Kilve (chapter 2.4) the lithology hosting the horses consists of organic-rich shales interbedded with argillaceous limestone. All of the faults are normal faults. The vertical displacement of the fault in locality 1 is 4-5 m, whereas the normal displacement of the fault in locality 2 is 6.5 m. The displacement of the fault in locality 3 is unknown.

Even though three of the horses in locality 1 are located in the fault core, the majority of the horses at this locality are to be found in the damage zone of both the hanging wall and footwall. Two orders of horses are recognized in this locality. The fault core horses are interpreted as asperity bifurcation horses, whereas the horses in the damage zone are interpreted as the result of segment splaying and coalescence (chapter 2.4.2).

In accordance to locality 1, horses in locality 2 are found both within the hanging wall, the footwall and in the fault core of the fault. Similar to locality 1, two orders of horses are recognized in locality 2. The fault core horses in the locality are interpreted as asperity bifurcation horses, whereas the horses in the damage zones are most likely generated by segment splaying and coalescence, in compliance to the horses in locality 1 (chapter 2.4.2).

In locality 3, however, all of the horses examined are fault core horses. The horses are classified as first order horses. As for the fault core horses in localities 1 and 2, the fault core horses in this locality are interpreted as asperity bifurcation horses (chapter 2.4.6).

The horses in locality 1 are exposed in a section between the dip and strike dimensions. The measured lengths of the horses examined in this locality are projected parallel to both of these dimensions. Hence, the horses are plotted in a-c diagrams (figure 3.7 and 3.8) and b-c diagrams (figure 3.9 and 3.10).

The horses in the damage zones of the fault in locality 2 are also exposed in a section between the dip and strike dimensions, and the measured lengths of the horses has been projected parallel to both of these dimensions. Thus, the damage zone horses are represented in a-c diagrams (figure 3.7 and 3.8) as well as in b-c diagrams (figure 3.9, and 3.10). The horses in the fault core in the locality are, on the other hand, exposed in a section parallel to the strike dimension, and these horses are only represented in the b-c diagrams (figure 3.9 and 3.10).

Similar to the fault core horses in locality 2, the fault core horses in locality 3 are exposed in a section parallel to the strike dimension. Hence, the horses in this locality are represented in b-c diagrams only (figure 3.9 and 3.10).

Relation between the a- and c-axes

Figure 3.7 shows the plot of the a-axes versus the c-axes for the horses in localities 1 and 2 in Kilve. The horses vary between 13 cm and 836 cm in the dip dimension (a-axis), and between 0.4 cm and 210 cm in thickness (c-axis). The regression line has a gradient of 0.17 and intersects the y-axis at –4.5. The R^2-value is 0.68, and reflects a satisfactory linear relation between the variables. Average ratio between a and c is 10:1. The majority of the horses are clustered within the lower left part of the diagram, representing relatively small horses.

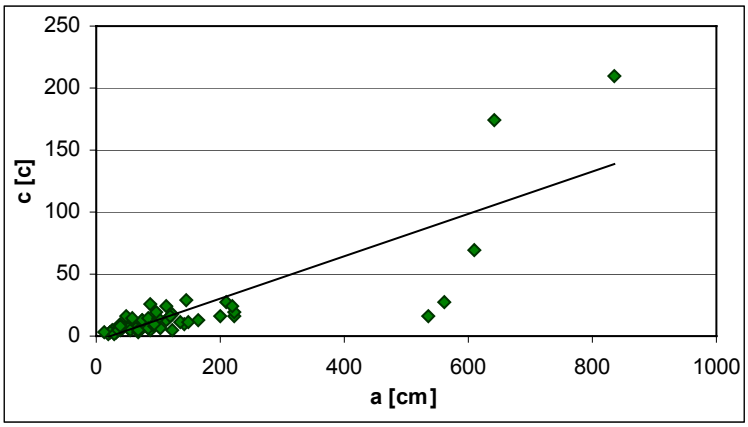

Figure 3.7 Plot of the a- versus the c-axes of the studied horses in locality 1 and 2 in Kilve. The regression line is given by y = 0.17x - 4.5. R^2 = 0.68, N = 61, and average ratio between a and c is 10:1.

Five points deviate from the majority. These points represent larger horses with a-values > 500 cm. Three of these points represent the three horses in locality 2 classified as first order structures (chapter 1). The second two points represent first order horses found in locality 1. Though it should be noted that the majority of the horses measured at this locality are first order horses that plot within the cluster of relatively small horses. Nevertheless, the five points are thought to strongly influence the regression line.

To study the spread in the dimensions of the smaller horses, the a- and c-axes are re-plotted (figure 3.8), with the five points with the highest values of the a-axes omitted from the dataset. The dataset in figure 3.8 is more homogeneous as compared to the dataset in the previous plot (figure 3.7). The horses are less than 230 cm in the dip dimension (a-axis), and the thickness is less than 29 cm. The regression line has a gradient of 0.09 and the intersection of the line with the y-axis is at +3. An R^2- value of 0.50 reflects a satisfactory reliability of the regression line. The average ratio between a and c is 9:1. Thus, the average horse in the more homogeneous dataset is thicker relative to length in the dip dimension as compared to the entire dataset.

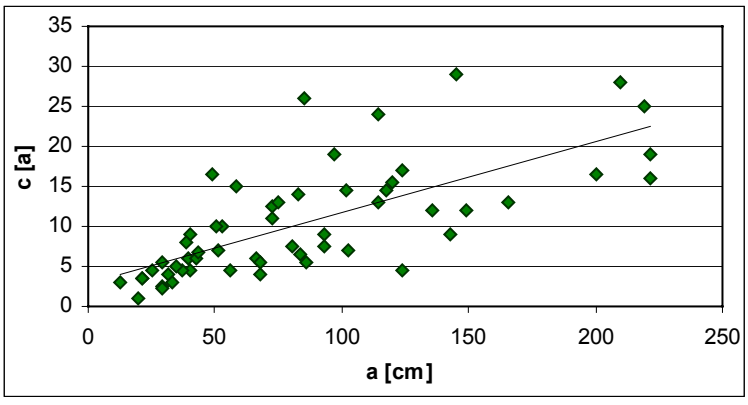

Figure 3.8 Plot of the a- and c-axes of the same dataset as in figure 3.7, but where five points with high a-values compared to the affiliated c-values are omitted. The regression line is given by y = 0.09x + 3. R^2 = 0.50, N = 56, and average a:c ratio is 9:1.

Relation between the b- and c-axes

The thickness of the horses has also been plotted versus the strike dimension for the horses in Kilve (figure 3.9). The plot represents the horses found in localities 2 and 3. The strike dimension of the horses varies between 8 cm and 996 cm, and the thickness of the horses varies between 0.4 cm and 210 cm. The gradient of the regression line is 0.18 and the line intersects the y-axis at –5.3. The R^2-value is 0.86, which reflects a strong linear relation between the axes. Average ratio between b and c is 12:1. Compared to the a:c relation for the entire dataset (figure 3.7), the average horse is longer in the strike dimension as compared to the dip dimension.

Three points represent the larger horses, with b-values > 600 cm, and they strongly influence the regression line. The data points represent three second order horses that occur in locality 2.

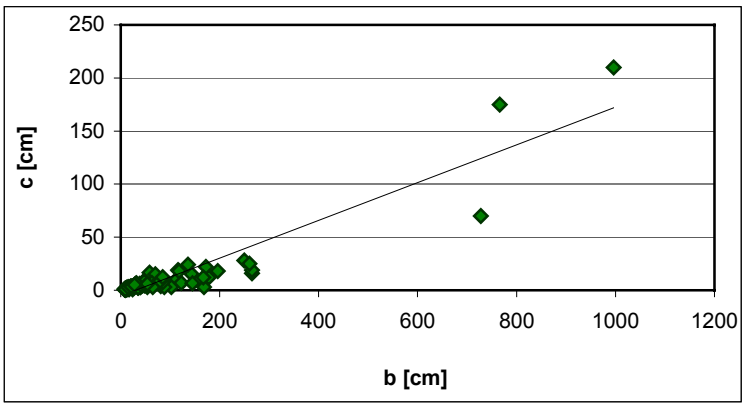

Figure 3.9 Plot of the b-axes versus the c-axes for the horses in locality 2 and 3 in Kilve. The regression line is given by y = 0.18x – 5.3. R^2 = 0.86, N = 73, and average b:c ratio is 12:1.

The b- and c-axes of the horses from localities 2 and 3 are re-plotted in a new diagram (figure 3.10), with the three mentioned points representing the larger horses omitted from the dataset. Hence, the plot represents a more homogeneous dataset of the horses than the previous.

The horses vary between 8 cm and 272 cm in the strike dimension, and between 0.4 cm and 29 cm in thickness. The regression line has a gradient of 0.08, and the intersection with the y-axis is at +1.3. The R^2-value is 0.66, and the linear relation between the dimensions is thus satisfactory. The average b:c ratio is 12:1, which is same as the average ratio b:c for the entire dataset (figure 3.9). Hence, the average horse in both the

entire dataset and in the more homogeneous dataset is equally slim in the strike dimension.

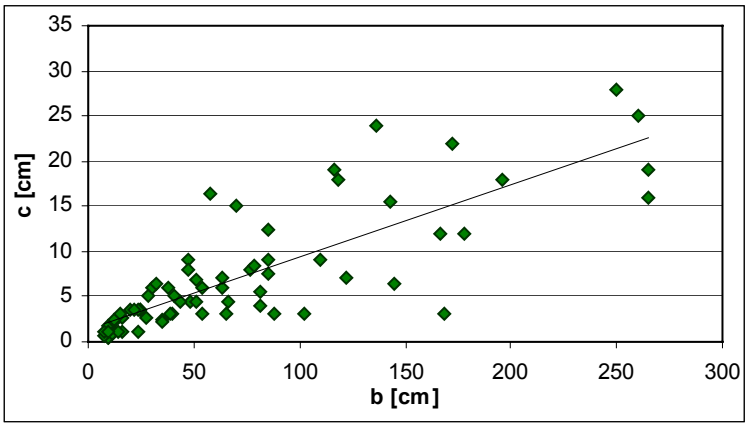

Figure 3.10 Plot of the b- versus the c-axes for the same dataset as in figure 3.9, but with the three largest horses omitted from the dataset. The regression line is given by y = 0.08x + 1.3. R^2 = 0.66, N = 70, and average b:c ratio is 12:1.

3.2.3 Bornholm

Two localities on Bornholm contribute to the dataset of the horses from this field area. One of the localities is in A. Stenders Kvartsgrav, and the other is in the Galgeløkken cliff section (chapter 2.6). In the first locality the horses are found within four faults, namely fault A, C, E, and F. Also in the second locality there are four faults, these being fault 1, 2, 3, and 4.

The horses on Bornholm are hosted by unconsolidated sand interbedded by various amounts of clay. Both the fault system in A. Stenders Kvartsgrav and the faults in the Galgeløkken cliff section are normal faults. The vertical displacement of the fault system in A. Stenders Kvartsgrav is at least 13 m, reflecting an intensive deformation during the generation of the horses. The vertical displacement of the faults in the Galgeløkken cliff section, on the other hand, is less than 5 cm and reflects a low intensity deformation.

Common for the horses in A. Stenders Kvartsgrav is that they are all found within a well-developed fault core, and they seem to be generated by asperity bifurcation (see chapter 2.6.2 for further description).

The four faults examined in the Galgeløkken Cliff section, on the other hand, have no fault core. The horses in this locality are located in the hanging wall and footwall, in addition to between linking fault segments. The horses in the locality are interpreted as the result of segment splaying and coalescence, in addition to segment linkage (more detailed description is given in chapter 2.6.4).

The horses in fault A in A. Stenders Kvartsgrav are exposed in a section between the dip and strike dimensions of the fault, and the measured lengths of these horses are projected parallel to both the dip and strike dimensions. In addition, three of the horses in this fault could be measured directly both in the dip and in the strike dimension. In this chapter the horses in fault A are represented in both an a-c diagram (figure 3.11) and in a b-c diagram (figure 3.12).

The horses examined in fault C could be measured directly both in the dip and in the strike dimension. The horses within this fault are represented in the same diagrams as the horses within fault A (see above).

Contrary to the horses in fault A and C, the horses examined in fault E were exposed in a section parallel to the strike dimension. The horses within this fault are only represented in the b-c diagram (figure 3.12).

Even if some of the horses in fault F are exposed parallel to the strike dimension, the majority of the horses in this fault are exposed in a section that is between the dip and strike dimensions. The horses in fault F are represented in the same a-c and b-c diagrams as the horses in fault A and C (figure 3.11 and 3.12).

The horses examined in fault 1-4 in the Galgeløkken cliff section are exposed in a section that is between the dip and strike dimensions, and they are projected parallel to both of these dimensions. The horses are represented in an a-c diagram (figure 3.11) and in a b-c diagram (figure 3.12).

Relation between the a- and c-axes

The diagram in figure 3.11 displays the plot of the a-axes versus the c-axes for the studied horses on Bornholm. The plot is based on the horses found within fault A, C and F in locality 1 and within fault 1-4 in locality 2. The horses found within fault E are not included in this dataset because these horses are exposed in a section parallel to the strike dimension (b-axis). The thickness (c-axis) of the horses varies between 0.3 cm and 25 cm, and dip dimensions (a-axes) vary between 0.8 cm and 103 cm. The regression line has a gradient of 0.17 and it intersects the y-axis at +0.9. The R^2-value for the regression line is 0.58, and reflects a satisfactory reliability of the regression line. The average ratio between a and c for the horses on Bornholm, when the entire dataset is considered, is 6:1.

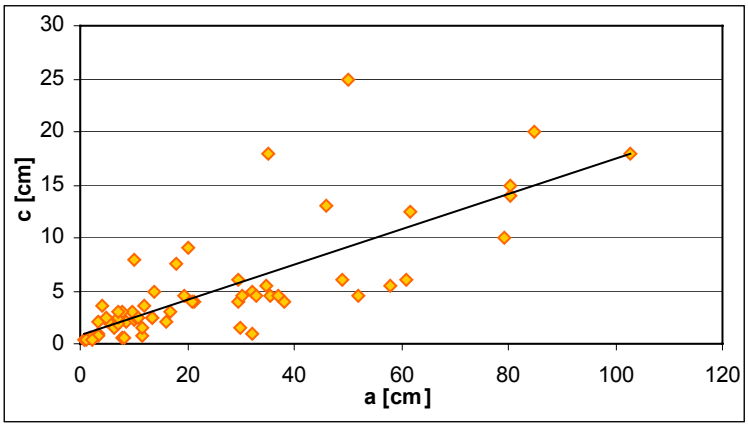

Figure 3.11 Plot of the a-axes versus the c-axes for all the studied horses in locality 1 and 2 on Bornholm, except fault E. The regression line is given by y = 0.17x + 0.9. R^2 = 0.58, N = 61, and a:c = 6:1.

Two of the data points deviate from the rest of the points by having very high c-values (thickness) compared to the affiliated a-values (dip dimensions). The two points represent two horses found within fault F in A. Stenders Kvartsgrav.

Relation between the b- and c-axes

The diagram in figure 3.12 shows the plot of the b-axes versus the c-axes for the horses on Bornholm. The dataset includes the horses found in both of the localities. The strike dimensions (b-axes) of the horses vary between 0.5 cm and 180 cm, and the thickness (c-axis) between 0.3 cm and 18 cm. The gradient of the regression line is 0.08, and the line intersects the y-axis at +1.4. The R^2-value is given by 0.70, which reflects a satisfactory relation between the axes. The average ratio between b and c is 9:1. This

ratio is considerably larger than the average ratio between a and c, which is 6:1. The average horse examined on Bornholm is thus slimmer in the strike dimension than in the dip dimension.

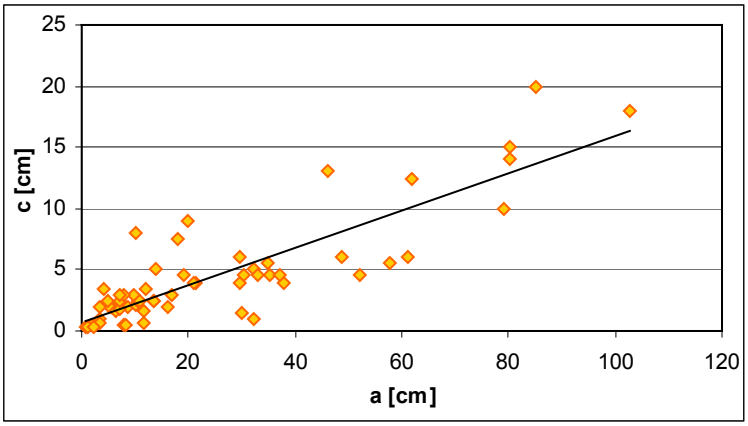

Figure 3.12 Plot of the b- versus the c-axes for the horses in locality 1 and 2 on Bornholm. The regression line is given by y = 0.08x + 1.4. R^2 = 0.70, N = 77, and b:c = 9:1.

3.2.4 Plaster of Paris

The horses examined in the plaster of Paris experiments are found within four different experiments (chapter 2.7).

The horses in the experiments have been developed before lithification of the plaster, and they are all developed in an extensional regime (chapter 2.7). The vertical displacements of the four faults are between 1.3 cm and 4.8 cm.

The majority of the horses examined in the plaster of Paris experiments are situated in the damage zone of the faults, primarily in the hanging wall, but also in the damage zone of the footwall. The majority of the horses are classified as first order structures. The generation of the horses seems to have been dominated by segment splaying and coalescence, together with asperity bifurcation.

The horses examined in the plaster of Paris experiments are exposed in sections that are either parallel to the dip or the strike dimension. The majority of the horses can be measured in only one of the dimensions, though a few can be measured in both of the dimensions. The horses exposed in sections parallel to the dip dimension are

represented in an a-c diagram (figure 3.13), whereas the horses exposed in sections parallel to the strike dimension are represented in a b-c diagram (figure 3.14 and 3.15).

Relation between the a- and c-axes

Figure 3.13 shows the plot of the a-axes versus the c-axes for the horses examined in the plaster of Paris experiments. The thickness of the horses varies between 0.2 cm and 3.5 cm, whereas the dip dimensions (a-axes) vary between 1.2 cm and 22.2 cm. The regression line has a gradient of 0.14 and intersects the y-axis at –0.1. The R^2-value is 0.59, reflecting a satisfactory linear relation between the axes. The average a:c ratio for the horses is 9:1.

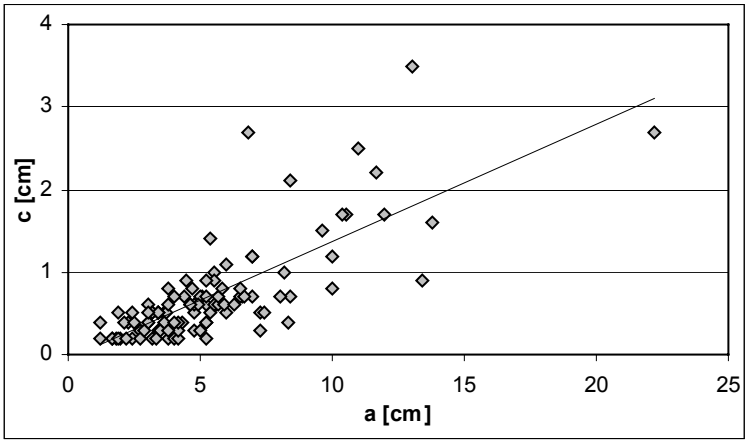

Figure 3.13 Plot of the a-axes versus the c-axes for the horses examined in the plaster of Paris. The regression line is given by y = 0.14x – 0.1. R^2 = 0.59, N = 104, and average ratio a:c = 9:1.

Relation between the b- and c-axes

The relations between the b- and c-axes for the horses examined in the plaster of Paris experiments are plotted in figure 3.14. The thickness (c-axis) of the horses varies between 0.3 cm and 3.5 cm. The strike dimensions of the horses vary between 3.2 cm and 36 cm. The regression line has a gradient of 0.09 and it intersects the y-axis at 0.4. The R^2-value is given by 0.53, which reflects a satisfactory linear relation between the axes. The average ratio between the b- and c-axes is 9:1, which is the same as the average a:c ratio.

However, one data point deviates from the rest by representing a horse having a b-axis (strike dimension) in excess of 20 cm.

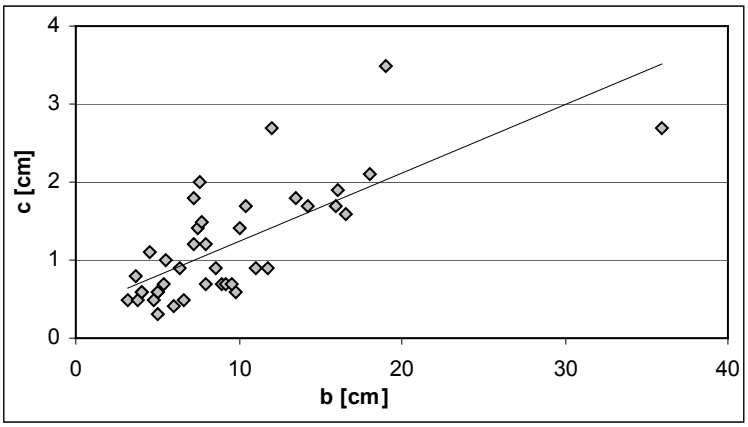

Figure 3.14 Plot of the b-axes versus the c-axes for the horses examined in the plaster of Paris. The regression line is given by y = 0.09x + 0.4. R^2 = 0.53, N = 40, and average ratio b:c = 9:1.

Because the regression line in the plot of the b- versus the c-axes is thought to heavily rely on the one mentioned point that deviates from the other, the b- and c-axes are re-plotted with this point omitted from the dataset (figure 3.15). The maximum strike dimension of the horses is then 19 cm, whereas the thickness variations are the same as previously. The regression line has a gradient of 0.12 and it intersects the y-axis at +0.1. The R^2-value is 0.55, reflecting that the points are better constrained to this regression line. However, the average b:c ratio is still 9:1.

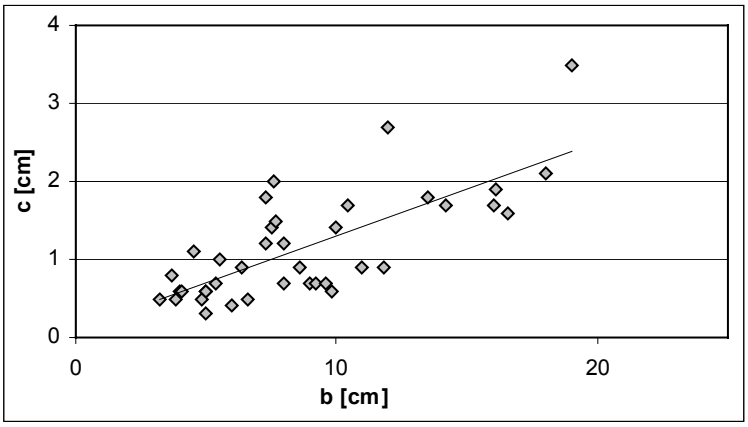

Figure 3.15 Plot of the b-versus the c-axes for the same dataset as in figure 3.14, but where one point with high b-value compared to the affiliated c-value is omitted from the dataset. The regression line is given by y = 0.12x + 0.1. R^2 = 0.55, N = 39, and average b:c ratio is 9:1.

Table 3.1 Overview of values obtained in the plots of the least reliable dataset.

LEAST RELIABLE DATASET						
Figure	**Plot**	**Dataset**	**Regression line**	**R^2-value**	**N**	**Ratio**
3.3	a-c	Frøya, entire	y = 0.26x - 5.5	0.92	34	6:1
3.4	a-c	Frøya, specified	y = 0.14x + 2.4	0.66	28	7:1
3.5	b-c	Frøya, entire	y = 0.08x + 9.1	0.18	22	6:1
3.6	b-c	Frøya, specified	y = 0.07x + 4.4	0.82	16	7:1
3.7	a-c	Kilve, loc. 1 and 2	y = 0.17x – 4.5	0.68	61	10:1
3.8	a-c	Kilve, loc. 1 and 2, specified	y = 0.09x + 3	0.50	56	9:1
3.9	b-c	Kilve, loc. 2 and 3	y = 0.18x – 5.3	0.86	73	12:1
3.10	b-c	Kilve, loc. 2 and 3, specified	y = 0.08x + 1.3	0.66	70	12:1
3.11	a-c	Bornholm, entire	y = 0.17x + 0.9	0.58	61	6:1
3.12	b-c	Bornholm, entire	y = 0.08x + 1.4	0.70	77	9:1
3.13	a-c	Plaster of Paris, entire	y = 0.14x – 0.1	0.59	104	9:1
3.14	b-c	Plaster of Paris, entire	y = 0.09x + 0.4	0.53	40	9:1
3.15	b-c	Plaster of Paris, specified	y = 0.12x + 0.1	0.55	39	9:1

3.3 Second most reliable dataset

In the previous chapter the horses exposed in sections between the dip and the strike dimensions are projected parallel to both of these dimensions. In this dataset the measured length of the horses is projected parallel to only the dimension that is closest to the exposed section of the horses. Hence, the measured length of the horses exposed in sections between 15^o and 45^o to the dip dimension, are only projected parallel to the dip dimension. Likewise, the measured length of the horses exposed in sections between 15^o and 45^o to the strike dimension are only projected parallel to the strike dimension. Horses exposed in sections that are less then 15^o to one of the dimensions are, in accordance to the dataset in the previous chapter, considered parallel to this dimension.

Since the measured length of the horses is not projected parallel to a dimension that has an angle of more than 45^o to the exposed section, the dataset in this chapter is more reliable than the dataset in the previous chapter. However, by only projecting the measured length of the horses to one of the dimensions the majority of the horses are plotted in either a-c diagrams or b-c diagrams. This implies that the majority of the

horses only are studied in one of the dip and strike dimensions. Horses exposed in all the three dimensions are, however, represented in both a-c and b-c diagrams.

As for the previous dataset, the values obtained from the analyses of this dataset are summarized at the end of the chapter (table 3.2). Further, a comparison of the plots of the horses displayed in this chapter is given in chapter 4.2.

3.3.1 Frøya

The horses in the locality at Flatval are, as already mentioned earlier in this chapter, exposed in a section that is parallel to the dip dimension. The horses in this locality are thus represented in an a-c diagram (figure 3.16). Two of the horses in the locality could, however, be measured in the strike dimension as well, but the two horses are considerable thick in relation to the dip dimension, and are omitted from the dataset. The two mentioned horses were also omitted in the re-plot of the horses in the previous section (figure 3.6) for the same reason.

In the locality at Skardsvåg the horses are exposed in a section between the two dimensions. However, the section of the exposed horses is closer to the strike dimension than the dip dimension, and the measured length of the horses in this locality are only projected parallel to the strike dimension. This implies that the horses from the locality are only represented in the b-c diagram in this chapter (figure 3.17).

Relation between the a- and c-axes

The data plotted in figure 3.16 represent the horses examined in the locality at Flatval on Frøya. The diagram shows the a-axes (dip dimensions) of the horses plotted versus the c-axes (thickness). The horses in the locality at Skardsvåg are not represented because they are not exposed satisfactorily in the dip dimension. The thickness of the horses in the locality at Flatval varies between 4 cm and 26 cm, whereas the dip dimensions vary between 52 cm and 170 cm. The gradient of the regression line is 0.12, and the line intersects the y-axis at +0.9. The R^2-value for the plot is 0.36, which reflects a satisfactorily linear relation between the axes. The average a:c ratio is 10:1.

The low R^2-value for the regression line may be explained by the small dataset from this locality.

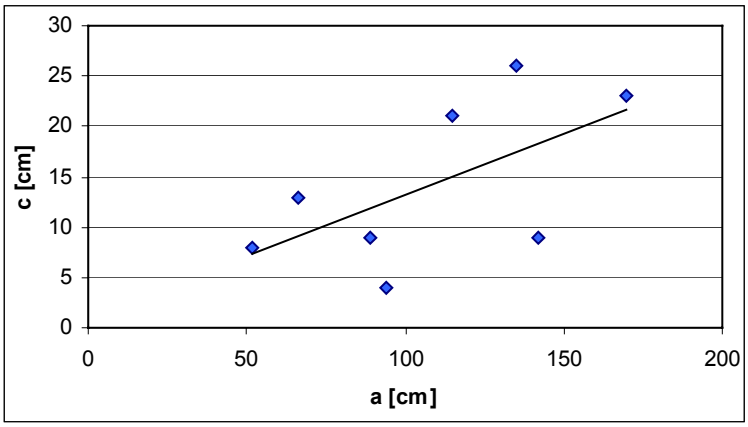

Figure 3.16 Plot of the a-versus the c-axes for the horses in the locality at Flatval on Frøya. The regression line is given by y = 0.12x + 0.9. R^2 = 0.36, N = 8, and average ratio between a and c is 10:1.

Relation between the b- and c-axes

The diagram in figure 3.17 presents the second plot of the horses on Frøya. Here, the thickness (c-axis) is plotted versus the strike dimensions (b-axes) of the horses, and only the horses from the locality at Skardsvåg are included in the dataset. The plot is equal to the plot shown in figure 3.6. Hence, the average horse on Frøya is longer in the dip dimension as compared to the strike dimension.

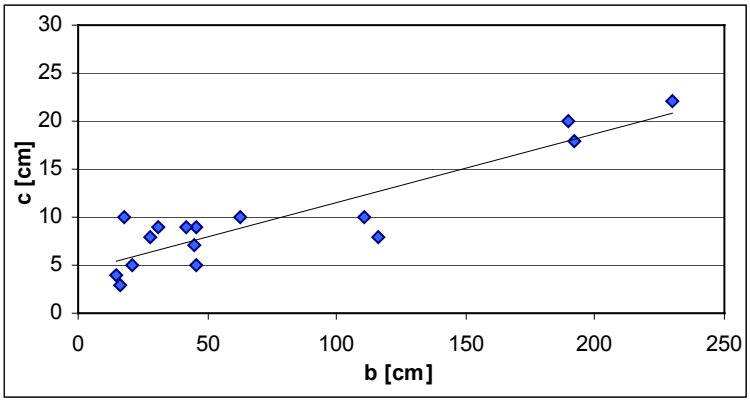

Figure 3.17 Plot of the b-versus the c-axes for the horses in the locality at Skardsvåg on Frøya. The regression line is given by y = 0.07x + 4.4. R^2 = 0.82, N = 16, and average ratio between b and c is 7:1.

3.3.2 Kilve

The horses in locality 1 in Kilve are exposed in a section between the dip and strike dimensions, but nevertheless closest the dip dimension. The length of the horses

measured in the field has therefore only been projected parallel to the dip dimension in this chapter. For this reason, the horses in this locality are only represented in a-c diagrams (figure 3.18 and 3.19).

The horses in the damage zone in locality 2 are, similar to the horses in locality 1, exposed in a section between the dip and strike dimensions. However, contrary to locality 1 the section in this locality is closer to the strike dimension than the dip dimension. Hence, the measured length of the horses is only projected parallel to the strike dimension in this chapter. The horses examined within the fault core are, on the other hand, exposed in a section parallel to the strike dimension, and no corrections of the measured lengths have been done. Thus, the horses in locality 2 are represented only in a b-c diagram (figure 3.20) in this section.

As mentioned earlier in this chapter the fault core horses in locality 3 are, similar to the fault core horses within locality 2, exposed in a section parallel to the strike dimension. Thus, no corrections of the measured length of the horses in this locality have been made, and the horses are represented in the b-c diagram (figure 3.20).

Relation between the a- and c-axes

Of the three localities studied at the Kilve Beach, locality 1 is the only locality that satisfactorily exposes the horses in the dip dimension. For this reason, only the horses examined in this locality are represented in the a-c diagram (figure 3.18). The thickness of these horses varies between 4 cm and 29 cm, whereas the dip dimensions vary between 29 cm and 201 cm. The regression line has a gradient of 0.07, and it intersects the y-axis at +4.3. The R^2-value is only 0.27, which reflects a weak and unsatisfactory linear relation. The average a:c ratio is 9:1.

The low reliability of the regression line may be due to two points with high c-values (thickness) compared to the affiliated a-values (dip dimensions). Both points represent first order structures found within locality 1. However, the majority of the horses found in this locality, and which are represented in the diagram, are of the same order.

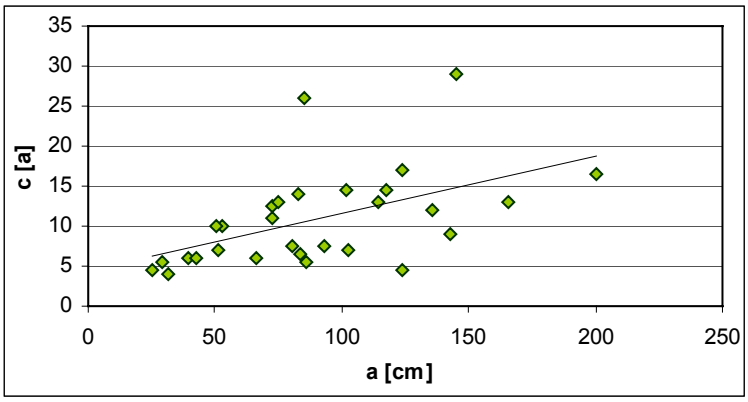

Figure 3.18 Plot of the a-versus the c-axes for the horses in locality 1 in Kilve. The regression line is given by y = 0.07x + 4.3. R^2 = 0.27, N = 29, and average ratio between a and c is 9:1.

Two of the horses have very high c-values compared to the affiliated a-values, and they deviate from the rest of the points. The data of the horses examined in locality 2 are re-plotted with these two horses omitted from the dataset (figure 3.19). The thickness of the horses varies between 4 cm and 17 cm, and the dip dimensions between 29 cm and 201 cm. The regression line has a gradient of 0.06, and the intersection of the line with the y-axes is at +4.6. An R^2-value of 0.37 reflects that the linear relation between the axes is now satisfactory. The average a:c ratio is 10:1, indicating that the horses are slimmer relative to length as compared to the previous plot.

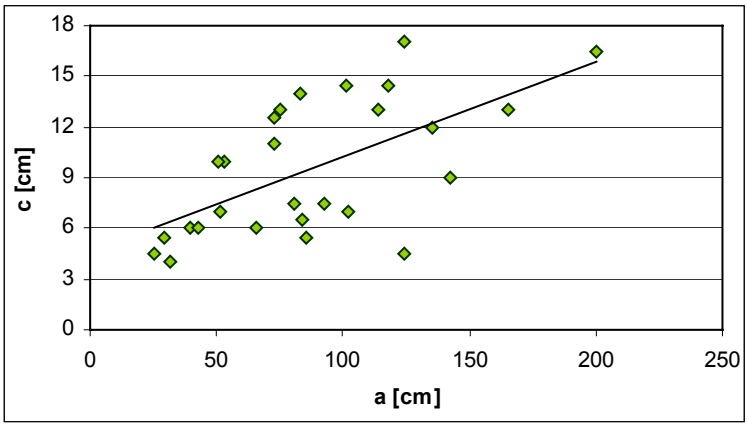

Figure 3.19 Plot of the a-versus the c-axes for the same dataset as in figure 3.18, but where the two data points with the highest c-values compared to the affiliated a-values are omitted. The regression line is given by y = 0.06x + 4.6. R^2 = 0.37, N = 27, and the average ratio a:c = 10:1.

Relation between the b- and c-axes

The plot of the b-axes versus the c-axes for the horses on the Kilve Beach is based on the horses examined in localities 2 and 3, and includes the horses found within the damage zone of the hanging wall and footwall, as well as the horses within the fault core (figure 3.20). The horses vary between 8 cm and 265 cm in the strike dimension and between 0.4 cm and 28 cm in thickness. The regression line has a gradient of 0.1,

and it intersects the y-axis at +1.3. The R^2-value is 0.66, which reflects a satisfactory linear relation between the axes. The average b:c ratio between of the horses is 12:1. Compared to the average a:c ratio for the horses in Kilve, the average horse seems to be slimmer relative to length in the strike dimension as compared to the dip dimension.

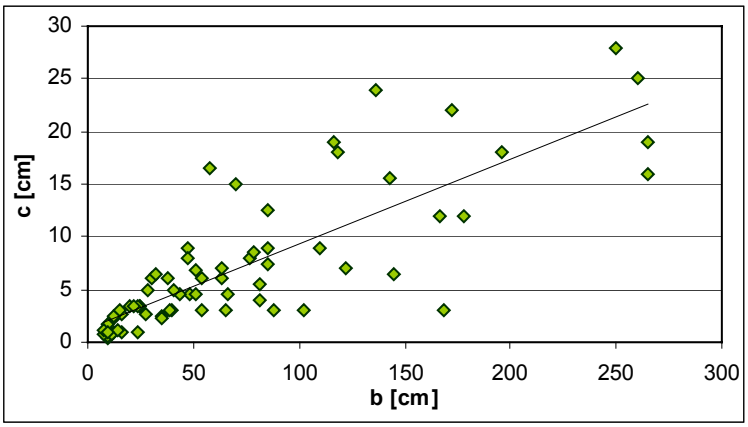

Figure 3.20 Plot of the b-versus the c-axes for the horses in locality 2 and 3 in Kilve, including the examined horses within the fault core. The regression line is given by y = 0.08x + 1.3. R^2 = 0.66, N = 70, and average ratio between b and c is 12:1.

3.3.3 Bornholm

The horses in A. Stenders Kvartsgrav are found in four different faults, which are exposed in different sections. The horses in fault A are exposed in a section that is closer to the strike dimension than the dip dimension. In addition, three of the horses in fault A were exposed in the both dip and strike dimensions. The three horses are plotted both in an a-c diagram (figure 3.21) and in a b-c diagram (3.22), whereas the rest of the horses in this fault are plotted only in the b-c diagram (figure 3.22).

In accordance to the three horses in fault A, the horses within fault C are exposed in sections parallel to both the dip and strike dimension. They are therefore represented in the same diagrams as the three mentioned horses in fault A (figure 3.21 and 3.22). The horses in fault E, however, were exposed in a horizontal section, and therefore parallel to the strike dimension. The horses examined in this fault are represented only in the b-c diagram (figure 3.22). The majority of the horses found within fault F are exposed in a section closer the dip dimension than the strike dimension. Hence, the data taken from these horses are only projected parallel to the dip dimension, and thus only represented in the a-c diagram (figure 3.21). Nevertheless, some horses are exposed in both the dip

and strike dimensions. These horses are represented in both the a-c diagram (figure 3.21) and in the b-c diagram (figure 3.22).

The horses examined in the four faults in the Galgeløkken cliff section are all exposed in the same section, which is between the strike and dip dimensions. Nevertheless, the orientation of the section rotates slightly across the locality, such that the sections that expose the horses in fault 1, 2 and 3 are closest the strike dimension, whereas the section that exposes the horses in fault 4 are closest the dip dimension. Consequently, the horses in fault 1, 2 and 3 are projected parallel to the dip dimension, and therefore represented in the a-c diagram (figure 3.21), whereas the data of the horses in fault 4 are projected parallel to the strike dimension, and represented in the b-c diagram (figure 3.22).

Relation between the a- and c-axes

The plot of the dip dimension (a-axis) versus the thickness (c-axis) for the horses on Bornholm is based on the horses found within fault F, C, and some of the horses within fault A in A. Stenders Kvartsgrav, and the horses found within fault 4 in the Galgeløkken cliff section (figure 3.21). The thickness of these horses varies between 0.3 cm and 20 cm, whereas the dip dimensions vary between 1.2 cm and 85 cm. The regression line for the plot has a gradient of 0.2, and it intersects the y-axis at +1.2. The R^2-value is 0.58, which reflects a satisfactory linear relation between the axes. The average a:c ratio is 5:1.

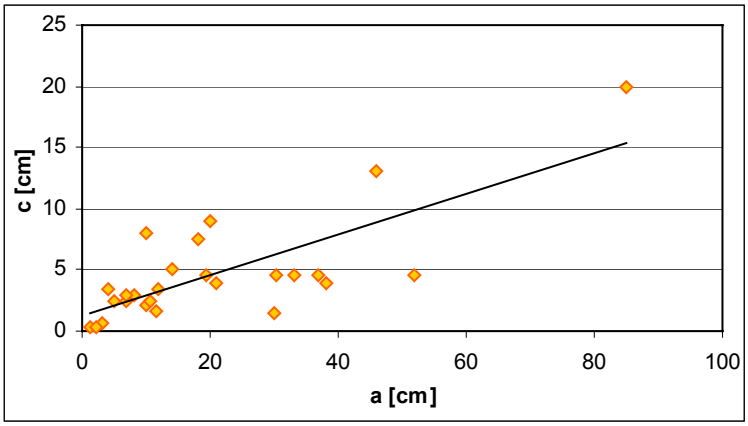

Figure 3.21 Plot of the a- versus the c-axes for the horses within fault F, C, and some of the horses within fault A in A. Stenders Kvartsgrav, and the horses within fault 4 in the Galgeløkken cliff section on Bornholm. The regression line is given by y = 0.17x + 1.2. R^2 = 0.58, N = 25, and average ratio between a and c is 5:1.

Relation between the b- and c-axes

Nevertheless, the majority of the horses examined on Bornholm are best exposed in the strike dimension. The plot of the strike dimensions versus the thickness (figure 3.22) is based on the horses found within fault A, C, E and some of the horses in fault F in A. Stenders Kvartsgrav, and fault 1, 2 and 3 in the Galgeløkken cliff section. The thickness of the horses varies between 0.3 cm and 18 cm, and the strike dimensions between 1.6 cm and 180 cm. The regression line has a gradient of 0.08, and the intersection of the y-axis is at +1.3. The R^2-value for the regression line is 0.69, which reflect a satisfactory linear relation between the axes. The average b:c ratio is 10:1. A comparison of this ratio with the a:c ratio shows that the average horse on Bornholm is relatively slimmer in the strike dimension than in the dip dimension.

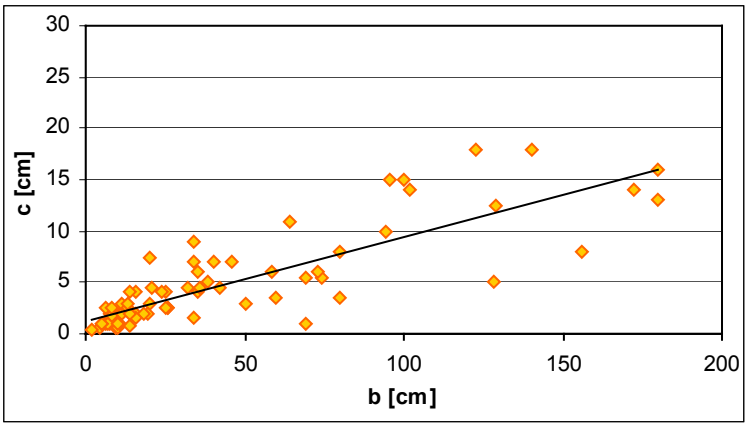

Figure 3.22 Plot of the b-versus the c-axes for the horses in fault A, C and E in A. Stenders Kvartsgrav and fault 1, 2 and 3 in the Galgeløkken cliff section on Bornholm. The regression line is given by y = 0.08x + 1.3. R^2 = 0.69, N = 70, and average ratio between b and c is 10:1.

3.3.4 Plaster of Paris

The horses in the plaster of Paris experiments are exposed in sections that are either parallel to the dip dimension or parallel to the strike dimension. This implies that the horses cannot be plotted in more than one way. For the majority of the studied horses, that is in either an a-c diagram or a b-c diagram. A few of the horses are, nevertheless, exposed in both the dip and strike dimension, and are represented in both of the diagrams. The plots of the horses are shown previously in this chapter (figure 3.13, 3.14 and 3.15).

Table 3.2. Summary of the values obtained in the plots of the second most reliable dataset.

SECOND MOST RELIABLE DATASET						
Figure	**Plot**	**Dataset**	**Regression line**	**R^2-value**	**N**	**Ratio**
3.16	a-c	Frøya, loc. 1	y = 0.12x + 0.9	0.36	8	10:1
3.17	b-c	Frøya, loc. 2	y = 0.07x + 4.4	0.82	16	7:1
3.18	a-c	Kilve, loc. 1	y = 0.07x + 4.3	0.27	29	9:1
3.19	a-c	Kilve, loc. 1, specific	y = 0.06x + 4.6	0.37	27	10:1
3.20	b-c	Kilve, loc. 2 and 3	y = 0.08x + 1.3	0.66	70	12:1
3.21	a-c	Bornholm, fault A, C, F and 3	y = 0.17x + 1.2	0.58	25	5:1
3.22	b-c	Bornholm, fault A, C, E, 1-3	y = 0.08x + 1.3	0.69	70	10:1

3.4 Most reliable dataset

In this chapter the horses are presented in diagrams where the measured length of the horses is plotted versus the thickness. The horses are therefore presented as they appear at the localities. Because no corrections have been made, this dataset is considered the most reliable. In accordance to the previous chapter, only the more homogeneous datasets from the different localities are represented in this chapter.

The values obtained from the plots of the horses are summarized at the end of the chapter (table 3.3). Further, a comparison of the datasets is given in chapter 4.3.

3.4.1 Frøya

The diagram in figure 3.23 includes both the horses examined in the locality at Flatval and in the locality at Skardsvåg. The largest horses in the locality at Skardsvåg, which exceed 350 cm in length and 30 cm in thickness, are omitted from the dataset. The length of the horses in the diagram varies between 21 cm and 300 cm, and the thickness between 3 cm and 26 cm. The regression line intersects the y-axis at +5.6, and has a gradient of 0.06. The R^2-value for the regression line is 0.47, indicating a satisfactory linear relation between the dimensions. The average ratio between the length and the thickness is 9:1. The stippled lines in the diagram bound the estimated interval in which 90% of the horses plot.

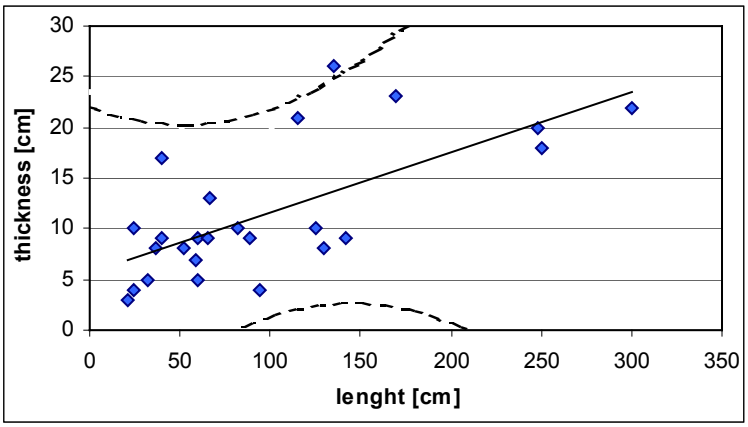

Figure 3.23 Plot of the thickness versus the measured length of the horses on Frøya. Both horses from the locality at Flatval and Skardsvåg are included in the dataset. The regression line is given by y = 0.06x + 5.6. R^2 = 0.47, N = 25, and average ratio between length and thickness is 9:1.

However, the main stress systems in the two localities may not have been the same. Secondly, the faults may have undergone different amount of displacement. Thirdly, two orders of horses (third and fourth order) from locality 2 are represented in the diagram, whereas first order horses are represented from locality 1. Finally the horses in the two localities are exposed in different sections. The horses in the locality at Flatval are exposed parallel to the dip dimension, whereas the horses in the locality at Skardsvåg are exposed in a section between the dip and strike dimensions, though closer to the strike dimension.

Due to the differences between the localities, the data taken from the horses in the localities are plotted in each diagram (figure 3.24 and 3.25).

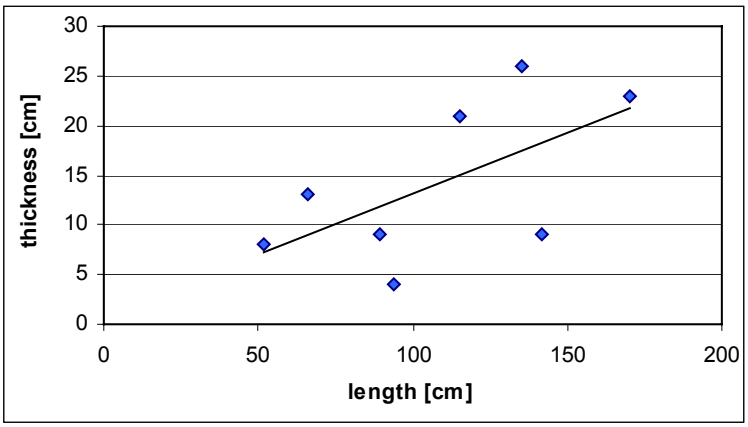

Figure 3.24 Plot of the length versus the thickness for the horses examined in the locality at Flatval on Frøya. The regression line is given by y = 0.12x + 0.9. R^2 = 0.36, N = 8, and average ratio between length and thickness is 10:1.

The diagram in figure 3.24 is the same plot as in figure 3.16. The R^2-value for the regression line is 0.36, reflecting that the points are less constrained here as compared to the plot of all the horses (figure 3.23).

The diagram shown in figure 3.25 presents only the horses examined in the locality at Skardsvåg. In accordance to the diagram of all of the horses (figure 3.23), the largest horses are omitted from the dataset. The length of the horses varies between 21 cm and 300 cm, whereas the thickness varies between 3 cm and 22 cm. The data points that represent the horses in the locality generate a regression line that intersects the y-axis at +5.3, and that has a gradient of 0.05. Both the intersection and the gradient of this line are similar to the intersection and gradient of the regression line generated by the plot of all of the horses on Frøya. The dataset from these horses therefore probably control the plot of all of the horses (figure 3.23) to a large extent. The R^2-value is 0.67, which reflects a satisfactory linear relation between the dimensions. The average ratio between the length and the thickness of the horses is 8:1. Hence, the average horse in the locality at Skardsvåg is thicker relative to length as compared to the average horse in the entire dataset. The points representing horses from only the locality at Skardsvåg are better constrained to the regression line in this diagram, confirmed by the R^2-value.

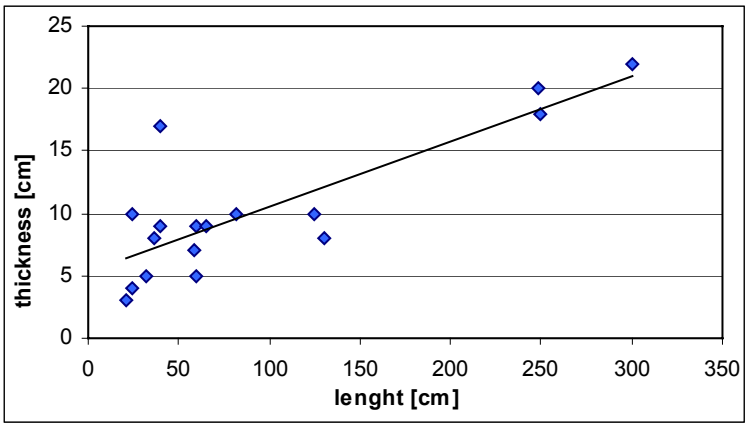

Figure 3.25 Plot of the length versus the thickness for the horses examined in the locality at Skardsvåg on Frøya. The regression line is given by y = 0.05x + 5.3. R^2 = 0.67, N = 17, and average ratio between length and thickness is 8:1.

3.4.2 Kilve

The data points in figure 3.26 represent the horses examined in localities 1, 2, and 3 in Kilve. The horses with lengths in excess of 400 cm and thickness in excess of 30 cm are omitted from the dataset. The variation in length of the horses is between 8 cm and 346 cm, and the variation in thickness between 0.4 cm and 28 cm. The regression line for the data points intersects the y-axis at +2.4, and has a gradient of 0.07. The R^2-value is 0.56, which reflects a satisfactory linear relation. The average ratio between the length

and thickness is 12:1. As for the plot of the entire dataset from Frøya (figure 3.23), the stippled lines in this diagram bounds the interval in which 90% of the horses plot.

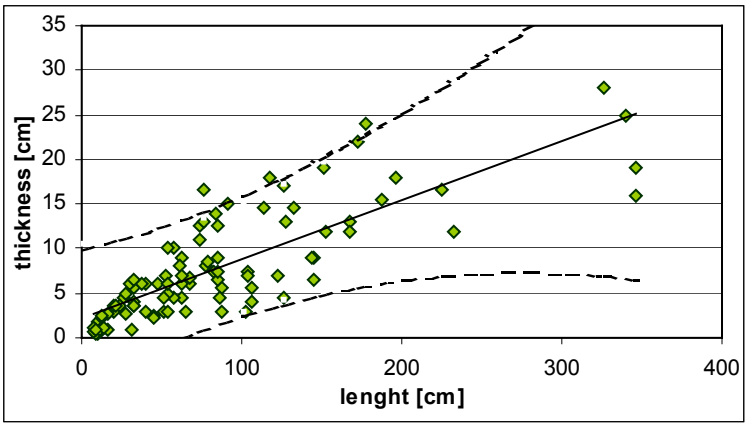

Figure 3.26 Plot of the thickness versus the length exposed in field for the horses within localities 1, 2, and 3 in Kilve. The regression line is given by y = 0.07x + 2.4. R^2 = 0.56, N = 99, and average ratio between the length and thickness is 12:1.

The horses examined in Kilve occur in three different faults, and each fault exposes different sections of the horses. The horses in locality 1 are nearly exposed in the dip dimension, the horses in locality 3 are in the strike dimension, whereas the horses in locality 2 are exposed in a section between the strike and dip dimensions. To examine the differences or similarities between the horses in the three localities the horses in each fault are plotted in their own diagram (figure 3.27, 3.28, 3.29 and 3.30).

The regression line generated by the data points representing the horses in locality 1 (figure 3.27) has a gradient of 0.07 and it intersects the y-axis at +4.4. Thus the gradient is the same as the gradient in the plot of all of the horses in Kilve, whereas the intersection with the y-axis is at a higher value. The reliability of the regression line, denoted by an R^2-value of 0.27, is unsatisfactory. The average ratio between the length and thickness of the horses in locality 1 is 10:1, and the average horse in the locality is therefore thicker than the average horse in the entire dataset.

The R^2-value is less than 0.3, and reflects that the data points in this diagram are weak linear relation between the axes. However, removing the two points that deviate the most lead to an acceptable R^2-value (equal to the plots in figure 3.18 and 3.19, respectively).

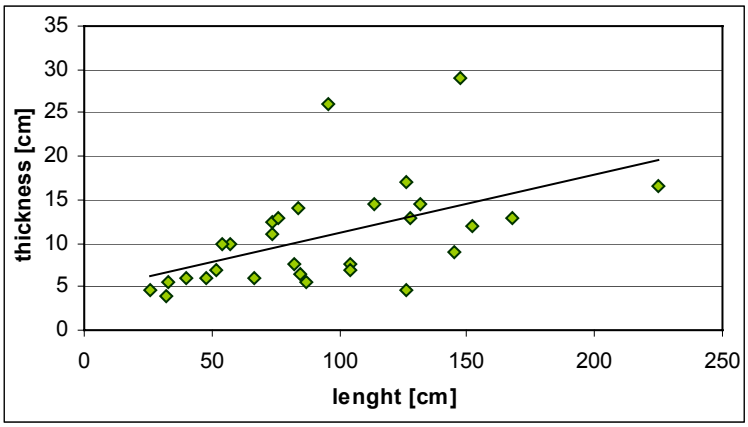

Figure 3.27 Plot of the thickness versus the length exposed in field for the horses within locality 1 in Kilve. The regression line is given by y = 0.07x + 4.4. R^2 = 0.27, N = 29, and the average ratio between the length and thickness is 10:1.

In the plot of the horses in locality 2 (figure 3.28) the horses vary between 8 cm and 346 cm in length, and between 0.4 cm and 28 cm in thickness. Both the thickness and the length variations are equal to the equivalent variations in the plot of all of the horses in Kilve (figure 3.26). The regression line has a gradient of 0.06, and it intersects the y-axis at +1.4. The R^2-value is 0.72, and the linear relation is strong. The average ratio between the length and the thickness of the horses in locality 2 is 13:1. The average horse in the locality is thus slimmer than the average horse in the entire dataset.

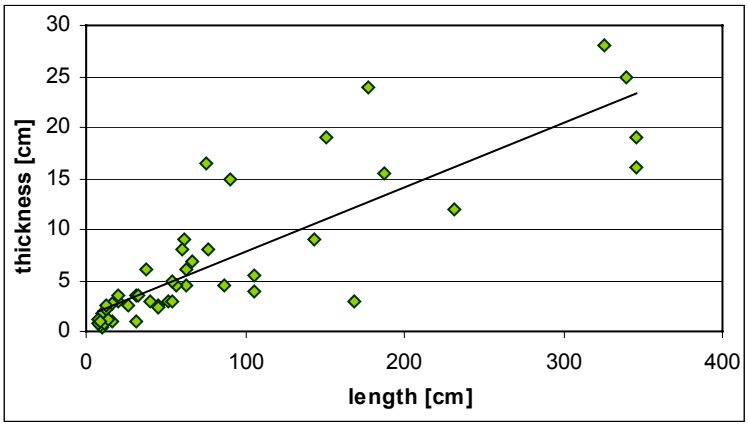

Figure 3.28 Plot of the length versus the thickness for the horses in locality 2. The regression line is given by y = 0.06x + 1.4. R^2 = 0.72, N = 49, and average ratio between length and thickness is 13:1.

Some of the horses in locality 2 are found within the damage zone, whereas other horses are found within the fault core. To study the differences or similarities between the horses, the damage zone horses are plotted in a diagram (figure 3.29), and the fault core horses in another (figure 3.30).

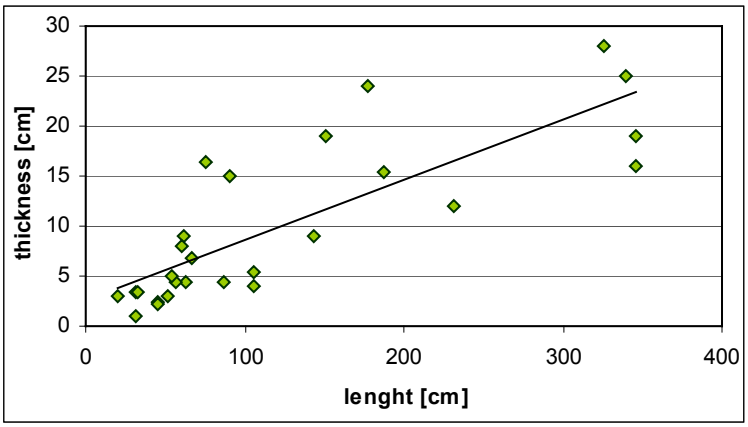

Figure 3.29 Plot of the length versus the thickness for only the damage zone horses in locality 2. The regression line is given by y = 0.06x + 2.5. R^2 = 0.66, N = 27, and average ratio between length and thickness is 14:1.

The data points in figure 3.29 represents only the damage zone horses in the hanging wall and footwall in locality 2. When just these horses are considered, the length of the horses varies between 20 cm and 346 cm, and the thickness between 1 cm and 28 cm. The data points generate a regression line that has a gradient of 0.06, and that intersects the y-axis at +2.5. The gradient is not distinguishable from the gradient in the plot of all of the horses in the locality (figure 3.26). The R^2-value is 0.66, which reflects a satisfactory linear relation. The average ratio between the length and the thickness is 14:1, which means that the average horse in the damage zone in the locality is considerable slimmer than the average horse in the entire dataset.

In the plot of only the fault core horses found in locality 2 (figure 3.30), the length of the horses varies between 8 cm and 168 cm, and the thickness between 0.4 cm and 8 cm. The regression line has a gradient of 0.03, and it intersects the y-axis at +1.6. The R^2-value is 0.28, which is not a satisfactory value. The value reflects an unsatisfactory linear relation between the axes. The average ratio between the length and thickness of the fault core horses is estimated to 13:1.

One of the data points in the diagram is highly deviating from the rest of the points, and the weakness of the linear relation may be due to this point. The point represents a horse of which the strike dimension is not fully exposed in the locality.

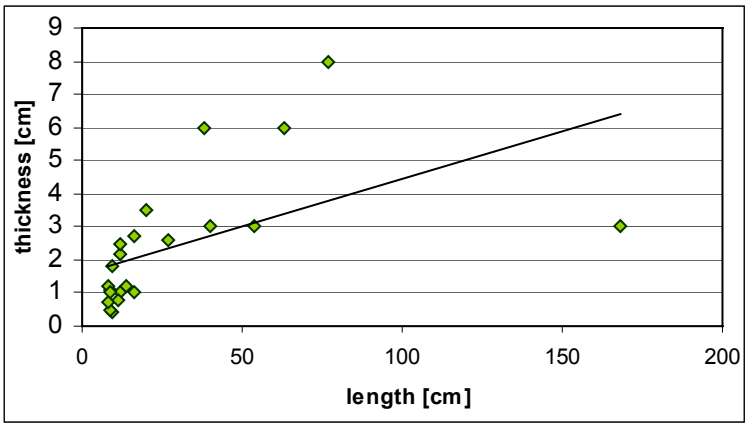

Figure 3.30 Plot of the length versus the thickness for the fault core horses in locality 2 in Kilve. The regression line is given by y = 0.03x + 1.6. R^2 = 0.28, N = 22, and average ratio between length and thickness is 13:1.

The diagram in figure 3.31 is a re-plot of the fault core horses examined in locality 2 in Kilve, but where the mentioned data point is omitted from the dataset. The lengths of the horses vary between 8 cm and 77 cm, and the thickness between 0.4 cm and 8 cm. The regression line generated by the points has a gradient of 0.09, and it intersects the y-axis at +0.4. Contrary to the previous plot, the reliability of the regression line is satisfactory, denoted by an R^2-value of 0.78. Hence, the linear relation between the axes is now satisfactory. When it comes to the average ratio between the length and the thickness, this ratio is 11:1. This ratio is lower than the equivalent ratio in the previous plot of the fault core horses in the locality (figure 3.30). The average fault core horse is thicker than both the average horse in the entire dataset (figure 3.28) from this locality and than the average damage zone horse (figure 3.29).

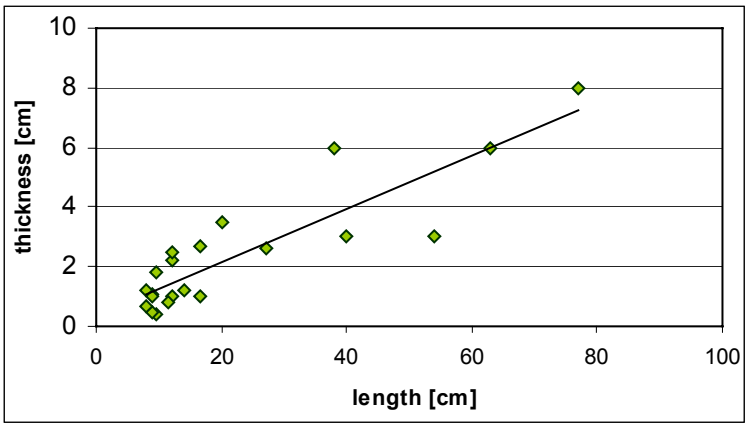

Figure 3.31 Plot of the length versus thickness for the same dataset as in figure 3.30, except for one large horse that highly deviates from the rest of the horses. The regression line is given by y = 0.09x + 0.4. R^2 = 0.78, N = 21, and average ratio between length and thickness is 11:1.

The diagram in figure 3.32 shows the plot of the length versus the thickness for the horses found in locality 3 in Kilve. All of the horses are fault core horses. The length of the horses varies between 21.5 cm and 196 cm and the thickness between 3 cm and 22

cm. The regression line generated for this plot has a gradient of 0.08 and it intersects the y-axis at +1.7. The R^2-value for the regression line in the diagram is 0.51, which reflects a satisfactory linear relation. The average ratio between the length and the thickness of the horses is 12:1, implying that the average horse in this locality is slimmer than the average fault core horse in locality 2.

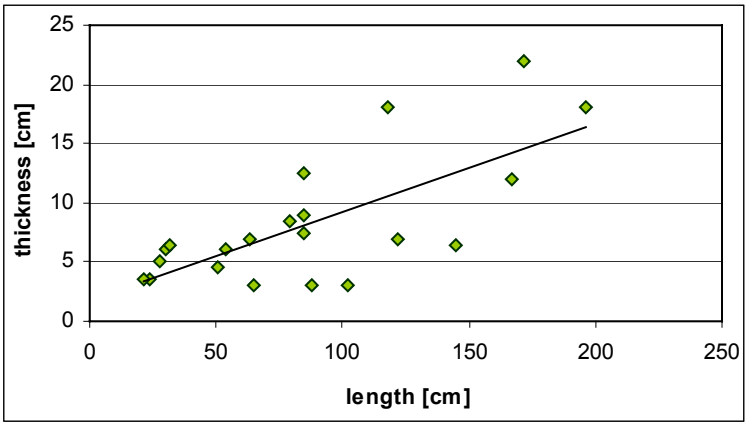

Figure 3.32 Plot of the length versus the thickness for the fault core horses found within locality 3 in Kilve. The regression line is given by y = 0.08x + 1.7. R^2 = 0.51, N = 21, and the average ratio between the length and thickness is 12:1.

3.4.3 Bornholm

All of the horses examined on Bornholm in A. Stenders Kvartsgrav and the Galgeløkken cliff section are included in the diagram shown in figure 3.33. The length of the horses in this plot varies between 1.3 cm and 190 cm, and the thickness between 0.3 cm and 25 cm. The data points produce a regression line that has a gradient of 0.09, and that intersects the y-axis at +1.5. The R^2-value is 0.59, and the linear relation between the axes is hence satisfactory. In compliance with the Frøya horses, the average ratio between the length and the thickness of the Bornholm horses is 9:1. The stippled lines in the diagram bounds the estimated interval in which 90% of the horses plot.

However, the horses examined on Bornholm are found in two localities, and the fault characteristics in the two localities are very different (chapter 2.2). The horses from the two localities are therefore re-plotted in their own diagram (figure 3.34 and 3.35).

The data points in the diagram in figure 3.34 represent only the horses examined in the A. Stenders Kvartsgrav. When only the horses in this locality are included, the length varies between 5 cm and 180 cm and the thickness varies between 1 cm and 25 cm. The

regression line has a gradient of 0.09, and it intersects the y-axis at +2.2. The R^2-value is 0.51, which reflects a satisfactory reliability of the regression line. The average ratio between the length and the thickness for the horses is 8:1, and the average horse in the locality is therefore thicker than the average horse in the entire dataset.

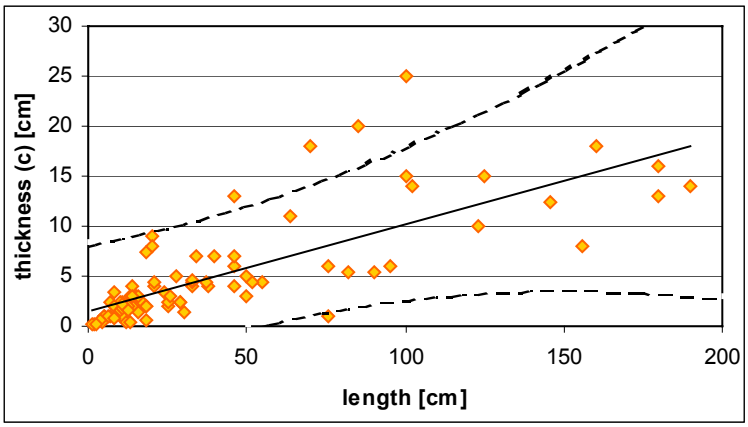

Figure 3.33 Plot of the thickness versus the length for the horses in A. Stenders Kvartsgrav and in the Galgeløkken cliff section. The regression line is given by y = 0.09x + 1.5. R^2 = 0.59, N = 83, and the average ratio between the length and thickness is 9:1.

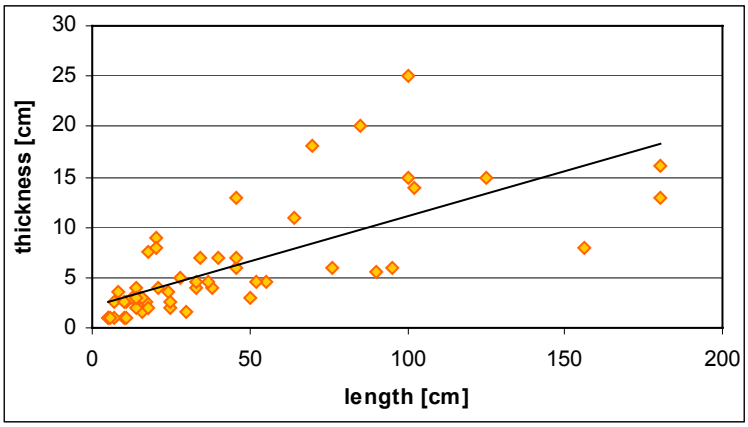

Figure 3.34 Plot of the length versus the thickness of the horses in the A. Stenders Kvartsgrav on Bornholm. The regression line is given by y = 0.09x + 2.2. R^2 = 0.51, N = 53, and the average ratio between the length and thickness is 8:1.

The diagram in figure 3.35 shows the plot of the horses examined in the Galgeløkken cliff section. The length of the horses in this locality varies between 1.3 cm and 190 cm, and the thickness between 0.3 cm and 18 cm. The plot of the horses generates a regression line that intersects the y-axis at +0.4, and that has a gradient of 0.08. The R^2-value is 0.87, which indicates a strong linear relation between the dimensions. The average ratio between the length and the thickness is 12:1, and the average horse in the Galgeløkken cliff section is slimmer than the average horse in A. Stenders Kvartsgrav.

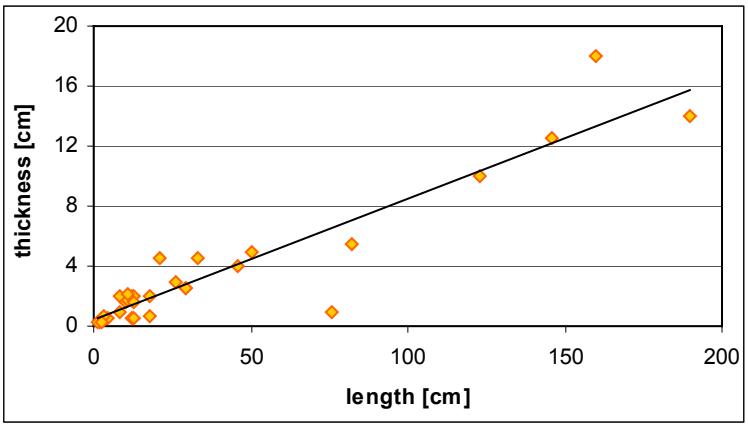

Figure 3.35 Plot of the length versus the thickness for the horses in the Galgeløkken cliff section on Bornholm. The regression line is given by y = 0.08x + 0.4. R^2 = 0.87, N = 30, and the average ratio between length and thickness is 12:1.

All of the horses in the Galgeløkken cliff section are exposed in the same section. The horses in A. Stenders Kvartsgrav are, on the other hand, exposed in different sections. The horses in the fault termed fault E are exposed horizontally, and therefore in the strike dimension. The horses in fault A are better exposed in the strike dimension than in the dip dimension, except for a few of the horses that were able to measure both in the dip and in the strike dimension. The horses examined in fault F, however, are exposed in the dip dimension. Because the horses are exposed in such different section they are re-plotted. The horses in fault F, C and the horses in fault A that are better exposed in the dip dimension than the strike dimension is plotted in an own diagram (figure 3.36), and the horses in fault E together with the rest of the horses in fault A that are better exposed in the strike dimension are plotted in an own diagram (figure 3.37). Additionally, there seem to be two trends in the diagram of all of the horses in the locality, and the two trends may be caused by the differences in the sections that expose the horses.

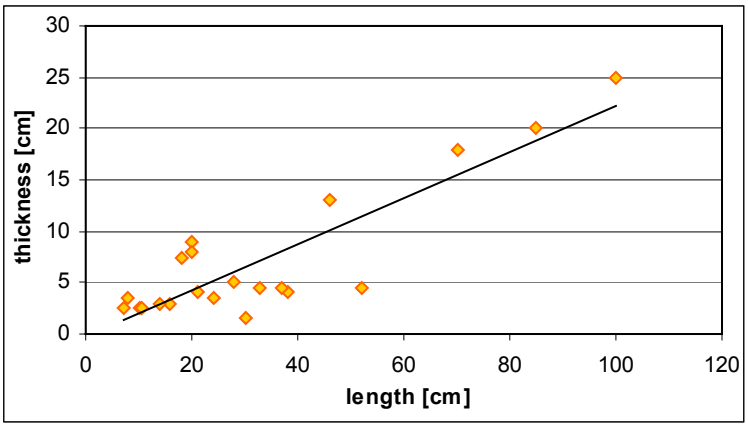

Figure 3.36 Plot of the length versus the thickness for the horses in fault C, F, and some of the horses in fault A in A. Stenders Kvartsgrav on Bornholm. The regression line is given by y = 0.22x – 0.2. R^2 = 0.77, N = 21, and average ratio between the length and thickness is 6:1.

The diagram in figure 3.36 shows the plot of the horses examined in fault C and F, and also some of the horses in fault A. Common for these horses is that they are better exposed in the dip dimension than in the strike dimension. The length of the horses in this diagram varies between 7 cm and 100 cm, and the thickness between 1.5 cm and 25 cm. The regression line has a gradient of 0.22, and it intersects the y-axis at –0.2. The linear relation between the dimensions is satisfactory, denoted by an R^2-value of 0.77. Compared to plot of all of the horses in this locality (figure 3.32) the data points are better clustered to the regression line in this diagram. The average ratio between the length and thickness of the horses in this plot is 6:1, which is considerably lower than the ratio of the horses in the locality. The average horse in this dataset, which consists of the horses that are better exposed in the strike dimension than in the dip dimension, are therefore slimmer than the average horse in the diagram of all of the horses.

The majority of the horses within fault A are better exposed in the strike dimension than in the dip dimension, and together with the horses in fault E they are plotted in an own diagram (figure 3.37). The length of the horses varies between 5 cm and 180 cm, and the thickness between 1 cm and 16 cm. The regression line has a gradient of 0.08, and it intersects the y-axis at +1.6. The R^2-value is 0.73, which indicates a satisfactory linear relation between the dimensions. As in the plot of the horses within fault E and the majority of the horses within fault A, the data points in this diagram are better constrained to the regression line than in the diagram of all of the horses in the locality. The average ratio between the length and the thickness is 9:1. The average horse in this diagram is therefore slimmer than the average horse in the plot of all of the horses (figure 3.34), and than the average horse in the dataset of the horses found within fault E, C, and the majority of the horses found within fault A (figure 3.36).

The reliability of the regression line in the two previous plots is better than in plot of all of the horses in the locality. It is also noticeable that the two datasets are causing the two trends that appear in the diagram of all of the horses in A. Stenders Kvartsgrav.

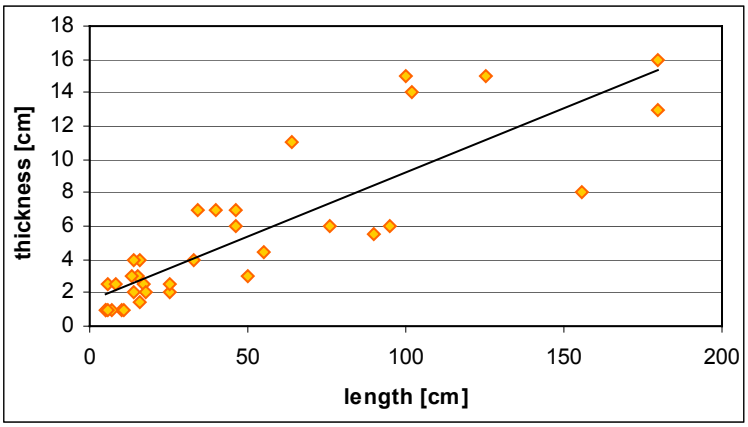

Figure 3.37 Plot of the length versus the thickness for the horses in fault E, and the majority of the horses in fault A, in A. Stenders Kvartsgrav on Bornholm. The regression line is given by y = 0.08x + 1.6. R^2 = 0.73, N = 35, and average ratio between the length and the thickness is 9:1.

3.4.4 Plaster of Paris

The plot of the length versus thickness for the horses located in the plaster of Paris is displayed in figure 3.38. The lengths of these horses vary between 1.2 cm and 22.2 cm, whereas the thickness varies between 0.2 cm and 3.5 cm. The regression line has a gradient of 0.13 and the line intersects the y-axis at 0. An R^2-value of 0.59 implies a satisfactory linear relation between the length and thickness for these horses. The average l:c ratio for the horses is 9:1. The stippled lines in the diagram bounds the interval of which 90% of the horses plot.

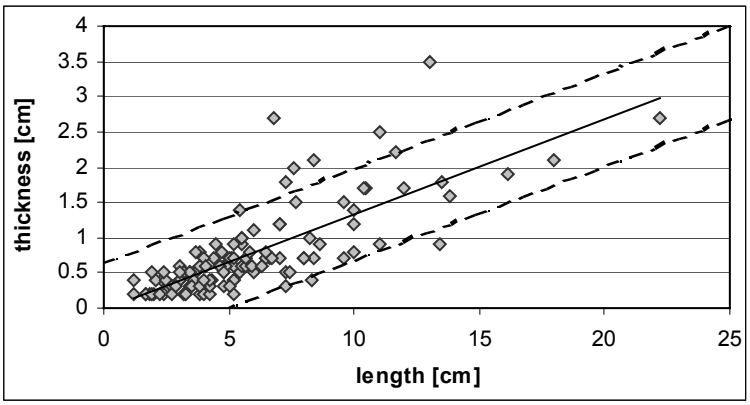

Figure 3.38 Plot of the length versus the thickness for the horses found in the plaster of Paris. Regression line is given by y = 0.13x. R^2 = 0.59, N = 119 and l:c = 9:1.

3.4.5 Plot of the entire dataset

The plot of the lengths and thicknesses for all the horses in the most reliable dataset (N = 323) is displayed in figure 3.39. The stippled curves in the diagram are drawn by hand, and show the maximum and minimum curves for the dataset, respectively. When

all the horses are considered, the lengths of the horses vary between 1.2 cm and 346 cm, whereas the thickness varies between 0.2 cm and 28 cm. The regression line has a gradient of 0.08, and the line intersects with the y-axis at +1.3. An R^2-value of 0.71 reflects a strong linear relation between the axes. The average ratio between length and thickness for the horses in this dataset is 10:1.

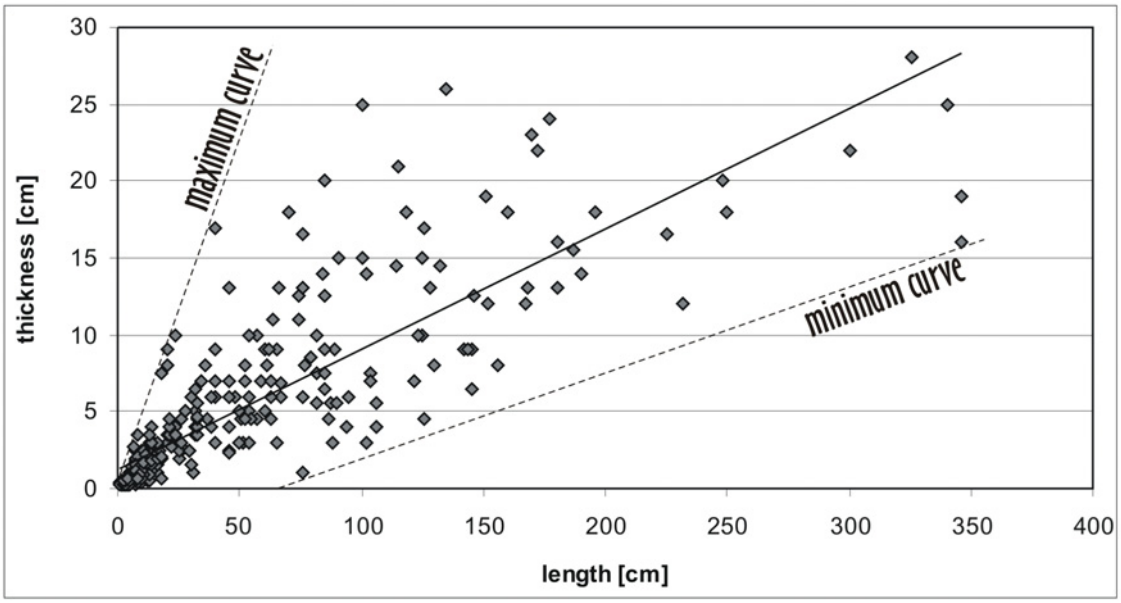

Figure 3.39 Plot of the length versus the thickness for all the horses in the most reliable dataset. The regression line is given by y = 0.08x + 1.3. R^2 = 0.71, N = 323, and average l:c ratio is 10:1.

Table 3.3 Overview of the values obtained by plots of the most reliable dataset.

MOST RELIABLE DATASET						
Figure	**Plot**	**Dataset**	**Regression line**	**R^2-value**	**N**	**Ratio**
3.23	I:c	Frøya, entire	y = 0.06x + 5.6	0.47	25	9:1
3.24	I:c	Frøya, loc. 1	y = 0.12x + 0.9	0.36	8	10:1
3.25	I:c	Frøya, loc. 2	y = 0.05x + 5.3	0.67	17	8:1
3.26	I:c	Kilve, entire	y = 0.07x + 2.4	0.56	99	12:1
3.27	I:c	Kilve, loc. 1	y = 0.07x + 4.4	0.27	29	10:1
3.28	I:c	Kilve, loc. 2	y = 0.06x + 1.4	0.72	49	13:1
3.29	I:c	Kilve loc. 2, damage zone	y = 0.06x + 2.5	0.66	27	14:1
3.30	I:c	Kilve, loc. 2, fault core	y = 0.03x + 1.6	0.28	22	13:1
3.31	I:c	Kilve, loc. 2, fault core, spec.	y = 0.09x + 0.4	0.78	21	11:1
3.32	I:c	Kilve, loc. 3	y = 0.08x + 1.7	0.51	21	12:1
3.33	I:c	Bornholm, entire	y = 0.09x + 1.5	0.59	83	9:1
3.34	I:c	Bornholm, loc. 1	y = 0.09x + 2.2	0.51	53	8:1
3.35	I:c	Bornholm, loc. 2	y = 0.08x + 0.4	0.87	30	12:1
3.36	I:c	Bornholm, fault C, F and A	y = 0.22x – 0.2	0.77	21	6:1
3.37	I:c	Bornholm, fault E and A	y = 0.08x + 1.6	0.73	35	9:1
3.38	I:c	Plaster of Paris	y = 0.13x	0.59	119	9:1
3.39	I:c	Most reliable dataset, entire	y = 0.08x + 1.3	0.71	323	10:1

Chapter 4

COMPARATIVE ANALYSES

In this chapter I will compare the results obtained from the three different study areas and the Plaster of Paris experiments. I will first compare the results obtained from the least reliable dataset, then the second most reliable dataset and eventually the results obtained from the most reliable dataset. In the end, I will compare the three different datasets. A description of the parameters used in the comparisons is given in chapter 3.

4.1 Comparison of the results obtained from the least reliable dataset

Here a comparison of the results obtained from the least reliable dataset (chapter 3.2) is given. The comparison is based on the most homogeneous datasets from the three field areas and the plaster of Paris experiments. This implies that horses represented by data points that highly deviate from the major trends in each diagram are omitted.

It is the same horses as displayed in figure 3.4 and 3.6 that represent the horses examined on Frøya in this comparison. Likewise, it is the same horses as displayed in figure 3.8 and 3.10 that represent the horses examined in Kilve, and the same horses as displayed in figure 3.11 and 3.12 that represent the horses on Bornholm. The horses studied in the plaster of Paris experiments represented here are also displayed in figure 3.13 and 3.15.

To more easily study the similarities and/or differences between the four datasets, all the data of the horses are displayed in the same diagrams. Hence, the a- versus c- relation for the four datasets is displayed in one diagram (figure 4.1), and the b- versus c- relations in another (figure 4.2).

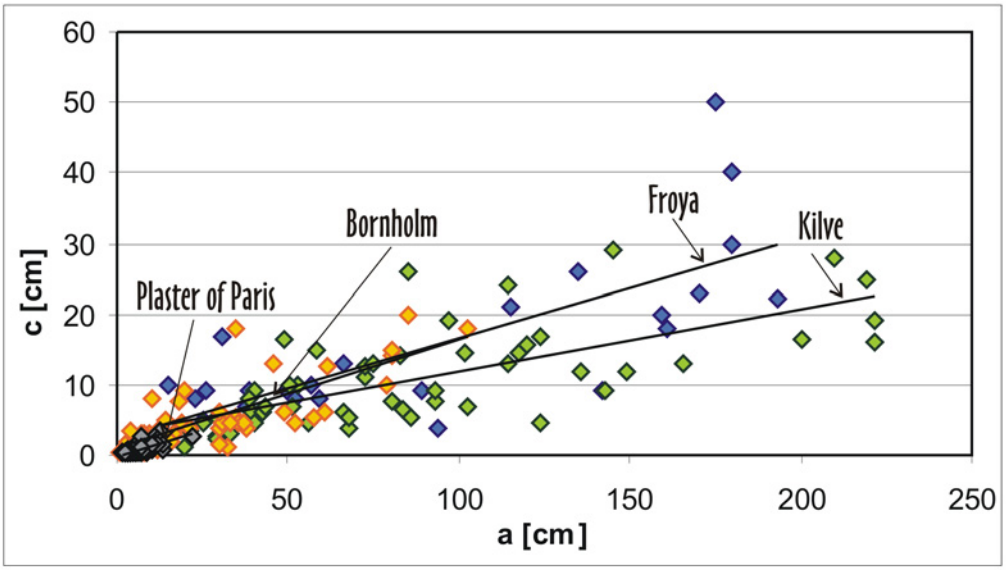

Figure 4.1 Plot of the a- versus c-axes for the horses examined in the three field areas and in the plaster of Paris experiments. Blue points represent horses from Frøya, green points represent horses from Kilve, yellow points represent horses from Bornholm, and grey points represent horses from the plaster of Paris experiments.

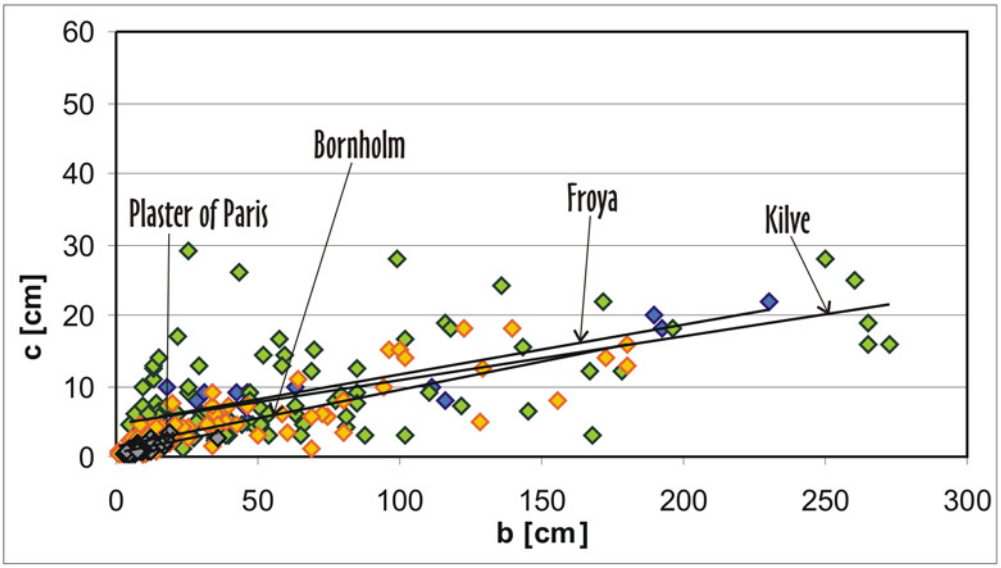

Figure 4.2 Plot of the b- versus the c-axes for the horses examined in the three field areas and in the plaster of Paris experiments. The horses are represented by the same colors as in figure 4.1.

Location of the data points in the diagrams

The points representing horses measured on Frøya are largely spread in both diagrams. The dip dimensions vary between 13 cm and 193 cm, and the strike dimensions between

15 cm and 230 cm. The thickness varies between 3 cm and 50 cm in the diagram of the a- versus c-axes, and between 3 cm and 23 cm in the diagram of the b- versus c-axes.

The data points representing the horses measured in Kilve has a spread similar to the horses on Frøya. The dip dimension varies between 13 cm and 230 cm, whereas the strike dimensions vary between 4 cm and 272 cm. The spread in the strike dimensions is larger than the spread in the dip dimensions. The thickness variations are between 0.4 cm and 29 cm in both diagrams. Hence, the spread of the data points in the diagrams are similar to the spread of the points representing horses from Frøya.

The data points representing the horses on Bornholm are less spread in the diagram as compared to the Frøya and Kilve horses. The dip dimensions vary between 0.8 cm and 103 cm, and the strike dimensions between 0.5 cm and 180 cm. Similar to the Kilve horses these are more spread in the strike dimension than in the dip dimension. The thickness of the horses varies between 0.3 cm and 20 cm in the diagram of the a- versus c-axes and between 0.3 cm and 18 cm in the diagram of the b- versus c-axes. Thus, the thickness variations for the horses on Bornholm are similar to the horses on Frøya and in Kilve. Nevertheless, horses with smaller dip and strike dimensions than horses from Frøya and Kilve are represented in both diagrams.

The horses measured in plaster of Paris have the smallest spread in both diagrams. The dip dimensions for these horses vary between 1.2 cm and 22.2 cm and the strike dimensions between 3.2 cm and 36 cm. The thickness varies between 0.2 cm and 3.5 cm in the diagram of the a- versus c-axes, and between 0.3 cm and 3.5 cm in the diagram of the b- versus c-axes. Similar to the Bornholm horses, some points representing the plaster of Paris have smaller dip and strike dimensions as compared to horses from Frøya and Kilve.

Intersections of the regression lines with the y-axes

The regression lines for the horses from Frøya intersect the y-axes at relatively high values. In the diagram of the a- versus c-axes (figure 4.1) the intersection is at +2.4, and in the diagram of the b- versus c-axes (figure 4.2) the intersection is at +4.4.

Also the regression lines generated by the horses from Kilve intersect the y-axes at relatively high values. In the diagram of the a- versus c-axes (figure 4.1) the intersection is at +3, whereas the intersection is at +4.4 in the diagram of the b- versus c-axes (figure 4.2).

The data points representing horses from Bornholm generate a regression line that intersects the y-axis at +0.8 in the diagram of the a- versus c-axes and at +1.4 in diagram of the b- versus c-axes. Hence, both intersections are at lower values as compared to the regression lines for the horses from Frøya and Kilve.

The lowest intersections are, however, the intersections of the regression lines for the plaster of Paris horses. In the diagram of the a- versus c-axes the intersection is at –0.1, whereas the intersection is at +0.4 in the plot of the b- versus c-axes.

Gradients of the regression lines

In the plot of the a- versus c-axes (figure 4.1) the gradients of the regression lines generated by points representing horses from Frøya and the plaster of Paris experiments are both 0.14 (table 4.1). The gradient of the regression line generated by the horses on Bornholm is 0.15, which is nearly the same. The horses in Kilve, on the other hand, generate a regression line that deviates from the others by having a gradient of 0.09. Hence, this line has a gentler slope as compared to the others.

The four regression lines in the plot of the b- versus c-axes (figure 4.2) are concurrent. The gradients of these lines vary between 0.06 and 0.09, where the regression line generated by the horses in Kilve has the gentlest slope and the line generated by the horses in the plaster of Paris has the steepest slope (table 4.2).

The R^2-values

The R^2-values for the four regression lines vary between 0.50 and 0.73 in the plot of the a- versus c-axes (table 4.1). The lowest value is given for the points representing horses from Kilve, whereas the highest value is given for the points representing horses from

Bornholm. However, these are all values indicative of strong linear relations between the axes, which represent the dip dimensions and thickness of the horses.

There is a larger spread between the R^2-values given for the regression lines in the plot of the b- versus c-axes (table 4.2) as compared to the values given in the plot of the a- versus c-axes. Here, the R^2-values for the plot of the horses from Frøya, Bornholm and the plaster of Paris experiments vary between 0.53 and 0.82. The lowest of these values is given for the plot of the horses found in the plaster of Paris, whereas the highest value is given for the plot of the horses found on Frøya. These values do all reflect a strong linear relation between the b- and c-axes, which represent the strike dimensions and the thickness. However, the lowest value, which is 0.33, is given for the plot of the horses from Kilve. Hence, the linear relation between the b- and c-axes for the horses measured in Kilve is weaker, though satisfactory, as compared to the relations for the other horses.

The average a:c and b:c ratios

Both the average a:c and b:c ratios for the horses examined on Frøya are 7:1. Thus, based on this dataset these horses are equally shaped in the dip and strike dimensions. Further, both dimensions for an average horse are seven times the thickness.

The same ratios for both the horses from Kilve and the plaster of Paris are both 9:1 (table 4.2). Hence, both are equally shaped in both dip and strike dimensions, similar to the horses from Frøya. However, these ratios are higher, implying that these horses are slimmer relative to length as compared to the horses from Frøya. Consequently, both the dip and strike dimensions for an average horse measured in Kilve, or in the plaster of Paris, is nine times the thickness.

Table 4.1 Values obtained in the plots of the a- versus c-axes for the horses in the least reliable dataset (figure 4.1).

Lithology/ material	Spread in diagram	Intersection	Gradient	R^2-value	Average a:c ratio
Frøya	Large spread a: 13 cm – 193 cm c: 3 cm – 50 cm	+2.4	0.14	0.60	7:1
Kilve	Large spread a: 13 cm – 230 cm c: 0.4 cm – 29 cm	+3	0.09	0.50	9:1
Bornholm	Medium spread a: 0.8 cm – 103 cm c: 0.3 cm – 20 cm	+0.8	0.15	0.73	6:1
Plaster of Paris	Small spread a: 1.2 cm – 22.2 cm c: 0.2 cm – 3.5 cm	-0.1	0.14	0.59	9:1

Table 4.2 Values obtained in the plots of the b- versus c-axes for the horses in the least reliable dataset (figure 4.2).

Lithology/ material	Spread in diagram	Intersection	Gradient	R^2-value	Average b:c ratio
Frøya	Large spread b: 15 cm – 230 cm c: 3 cm – 23 cm	+4.4	0.07	0.82	7:1
Kilve	Large spread b: 3 cm – 272 cm c: 0.4 cm – 29 cm	+4.9	0.06	0.33	9:1
Bornholm	Medium spread b: 0.5 cm – 180 cm c: 0.3 cm – 18 cm	+1.4	0.08	0.70	9:1
Plaster of Paris	Small spread b: 3.2 cm – 36 cm c: 0.3 cm – 3.5 cm	+0.4	0.09	0.53	9:1

The horses from Bornholm are the only horses that have different a:c and b:c ratios in this dataset. The a:c ratio is only 6:1, whereas the b:c ratio is 9:1. Hence, the horses are relatively thicker in the dip dimensions than in the strike dimensions based on these

ratios. Compared to the horses from Frøya, these horses are thicker in the dip dimension but slimmer in the strike dimension relative to length. Compared to the horses in Kilve and the plaster of Paris experiments they are equally slim in the strike dimension but thicker in the dip dimension.

4.2 Comparison of the results obtained from the second most reliable dataset

The comparison of the horses in this section is based on the results obtained from the second most reliable dataset (chapter 3.3). Similar to the comparison of the results obtained from the least reliable dataset, the comparison here is based on the most homogeneous datasets from each of the field areas and the plaster of Paris experiments.

It is the same horses as displayed in figure 3.16 and 3.17 that represent the horses from Frøya in this comparison. Likewise, it is the same horses as displayed in figure 3.19 and 3.20 that represent the horses from Kilve, and the same horses as displayed in figure 3.21 and 3.22 that represent the horses from Bornholm. The horses from the plaster of Paris experiments represented here are the same as in the comparison of the least reliable dataset, namely the same as displayed in figure 3.14 and 3.15.

Similar to the comparison of the least reliable dataset, the horses from the three field areas and the plaster of Paris experiments are displayed in the same diagrams to more easily study the similarities and/or differences. Hence, the diagram in figure 4.3 presents the a- versus c-relation of the horses, whereas the diagram in figure 4.4 presents the b-versus c-relation.

Location of the data points in the diagrams

The data points representing the horses from Frøya are largely spread in both diagrams (figure 4.3 and 4.4). The dip dimensions vary between 52 cm and 170 cm, whereas the strike dimensions vary between 15 cm and 230 (table 4.3 and 4.4). Hence, the spread of the strike dimensions is larger than the spread of the dip dimensions. The thickness

varies between 4 cm and 26 cm in the diagram of the a- versus c-axes, and between 3 cm and 22 cm in the diagram of the b-versus c-axes.

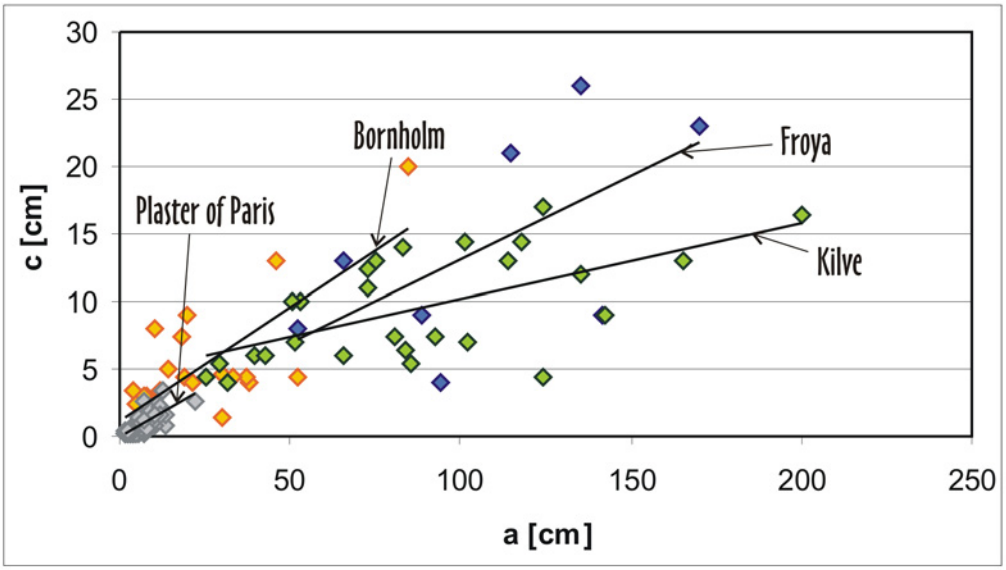

Figure 4.3 Plot of the a-axes versus the c-axes for the data in the second most reliable dataset. The horses are represented by the same colors as in figure 4.1.

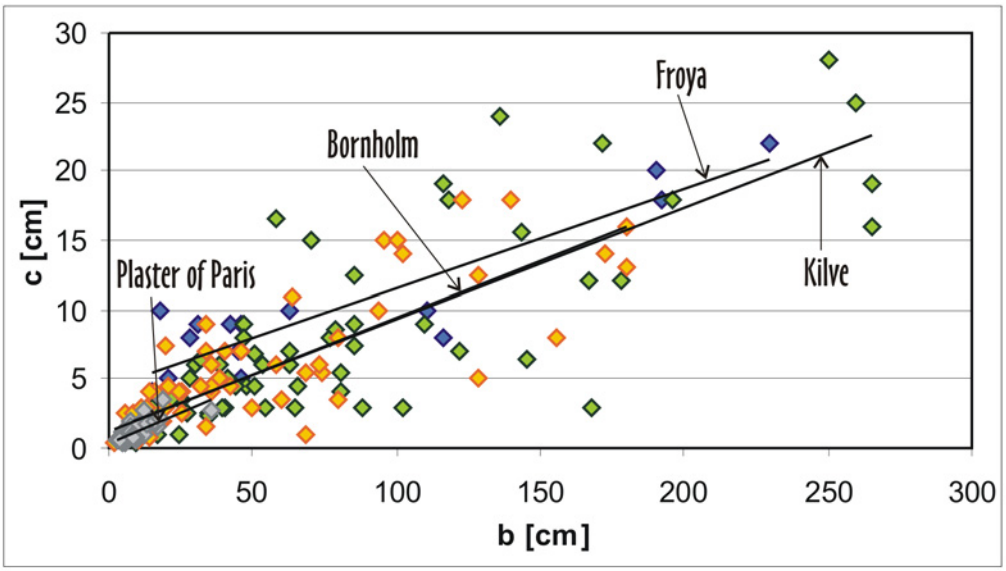

Figure 4.4 Plot of the b-axes versus the c-axes for the horses examined in the four datasets. The horses are represented by the same colors as in figure 4.1.

Similar to the points representing horses from Frøya, the points representing the horses from Kilve have a large spread in both diagrams (figure 4.3 and 4.4). These horses vary between 25.6 cm and 200.5 cm in the dip dimension (table 4.3), and between 15 cm and 265 cm in the strike dimension (table 4.4). Thus, the spread in the strike dimensions is larger than the spread in the dip dimensions. The thickness of these horses varies

between 4 cm and 17 cm in the diagram of the a- versus c-axes, and between 0.4 cm and 28 cm in the diagram of the b- versus c-axes.

The points representing the horses from Bornholm have a medium spread in the diagrams (figure 4.3 and 4.4). Their dip dimensions vary between 1.2 cm and 85 cm (table 4.3), and their strike dimensions between 1.6 cm and 180 cm (table 4.4). The thickness of these horses varies between 0.3 cm and 20 cm in the plot of the a- versus c-relation, and between 0.3 cm and 18 cm in the plot of the b- versus c-relation. Hence, horses with smaller dip and strike dimensions and thickness as compared to the points representing horses from Frøya and Kilve are present in the diagrams.

Nevertheless, the data points representing the plaster of Paris horses have the smallest spread of the four datasets in both diagrams. These horses vary between 1.2 cm and 22.2 cm in the dip dimension, and between 3.2 cm and 36 cm in the strike dimension. The variation in thickness is between 0.2 cm and 3.5 cm in the plot of the a- versus c-axes, and between 0.3 cm and 3.5 cm in the plot of the b- versus c-axes.

Intersections of the regression lines with the y-axes

The regression lines given in the plots of the horses on Frøya intersect the y-axes at very different values in the two diagrams (table 4.3 an 4.4). The lowest intersection is in the plot of the a- versus c-relation (figure 4.3), where the intersection is at +0.9. The highest intersection, on the other hand, is in the plot of the b- versus c-relation, where the intersection is at +4.4 (figure 4.4).

As for the plot of the horses on Frøya, the regression lines given in the plots of the horses found in Kilve intersect the y-axes at very different values. In the plot of the a-versus c-relation the intersection is at +4.6, whereas the intersection is at +1.3 in the plot of the b- versus c-relation (table 4.3 and 4.4). Hence, the highest intersection is in the diagram displaying the a- versus c-relation, whereas the lowest intersection is in the diagram displaying the b- versus c-relation. This is opposite of the intersections for the regression lines generated by the horses on Frøya.

Unlike the regression lines for points representing the horses from Frøya and Kilve, the two regression lines for the horses on Bornholm intersect the y-axes at almost the same values in both diagrams (figure 4.3 and 4.4). The intersection in the a-c diagram is at +1.2, and the intersection in the b-c diagram is at +1.3. Hence, the regression line intersects the y-axis at the same value as the regression line for the horses in Kilve in the diagram displaying the a- versus c-relation.

The plots of the plaster of Paris horses are the same as described in the comparison of the least reliable dataset. Thus these horses have already been described (chapter 4.1). In accordance to the horses on Bornholm, the horses in the plaster of Paris generate regression lines in the two diagrams that intersect the y-axes at more similar values than the horses from Frøya and Kilve. In the diagram of the a- versus c-axes the intersection is at –0.1, whereas the intersection is at +0.4 diagram of the b- versus c-axes. The regression lines for the plaster of Paris intersect the y-axes at the lowest values as compared to the regression lines for the horses found in the three field areas.

Gradients of the regression lines

In the plot of the a- versus c-axes (figure 4.3), the majority of the regression lines for the horses on Frøya, on Bornholm and the horses in the plaster of Paris experiments have similar gradients. The gradient of the regression lines for these horses vary between 0.12 and 0.17 (figure 4.3). The regression line with the steepest slope of these, is the one generated for the horses on Frøya, whereas the gentlest slope is given for the regression line generated for the horses on Bornholm (table 4.3). The regression line generated for the horses in Kilve deviates the most from the others, by having a gradient of only 0.06 in this diagram.

In the plot of the b- versus c-axes, on the other hand, the gradients of the four regression lines are more congruent (figure 4.4). Here, the gradients vary between 0.07 and 0.09. The steepest regression line is the line generated for the horses found in the plaster of Paris, whereas the regression line with the gentlest slope the line generated for the horses on Frøya (table 4.4).

The R^2-values

The highest R^2-values in the plot of the a- versus c-axes are 0.58 and 0.59, which are given for the horses on Bornholm and in the plaster of Paris, respectively (table 4.3). Thus, there is a strong relation between the dip dimensions and thickness for these horses. The values for the horses on Frøya and in Kilve are 0.36 and 0.37, respectively, indicating weaker relations between the dimensions. Nevertheless, these linear relations are considered satisfactory in this study.

The points in the diagram displaying the b- versus c-relation (figure 4.4) are better constrained to the regression lines, as compared to the plot of the a- versus c-axes. The highest value is 0.82, given for the horses on Frøya (table 4.4). The lowest value is 0.53, given for the horses in the plaster of Paris experiments. This implies that there is a strong linear relation between the strike dimension and thickness for the horses in all the four datasets.

The average a:c and b:c ratios

The average a:c ratio for the horses examined on Frøya is 10:1, whereas the average b:c ratio for these horses is 7:1. Based on these ratios, the horses measured on Frøya are relatively slimmer in the dip dimension than in the strike dimension.

When it comes to the horses in Kilve the average a:c and b:c ratios are 10:1 and 12:1, respectively. Based on these ratios the horses are relatively slimmer in the strike dimension than in the dip dimension, which is opposite of the horses on Frøya. The a:c ratios for the horses on Frøya and in Kilve are equal, whereas the b:c ratio for the horses in Kilve is higher as compared to the horses on Frøya. This latter implies that the horses in Kilve are relatively slimmer in the strike dimensions than the horses on Frøya.

The average a:c ratio for the horses examined on Bornholm is not more than 5:1, which is the lowest ratio in this comparison. The average b:c ratio, on the other hand, is 10:1. Hence, the horses on Bornholm are averagely twice as long in the strike dimensions as compared to the dip dimensions based on this dataset. The horses are equally slim in the

strike dimensions as compared to the horses on Frøya and in Kilve, but thicker in the dip dimensions than these horses.

Table 4.3 Values obtained from in the plots of the a- versus c-axes for the horses in the second most reliable dataset (figure 4.3).

Lithology/ material	Spread in diagram	Intersection	Gradient	R^2-value	Average a:c ratio
Frøya	Large spread a: 52 cm – 170 cm c: 4 cm – 26 cm	+0.9	0.12	0.36	10:1
Kilve	Large spread a: 26 cm – 201 cm c: 4cm – 17 cm	+4.6	0.06	0.37	10:1
Bornholm	Medium spread a: 1.2 cm – 85 cm c: 0.3 cm – 20 cm	+1.2	0.17	0.58	5:1
Plaster of Paris	Small spread a: 1.2 cm – 22.2 cm c: 0.2 cm – 3.5 cm	-0.1	0.14	0.59	9:1

Table 4.4 Values obtained from the plot of the b- versus c-axes for the horses in the second most reliable dataset (figure 4.4).

Lithology/ material	Spread in diagram	Intersection	Gradient	R^2-value	Average b:c ratio
Frøya	Large spread b: 15 cm – 230 cm c: 3 cm – 22 cm	+4.4	0.07	0.82	7:1
Kilve	Large spread b: 15 cm – 265 cm c: 0.4cm – 28 cm	+1.3	0.08	0.66	12:1
Bornholm	Medium spread b: 1.6 cm – 180 cm c: 0.3 cm – 18 cm	+1.3	0.08	0.69	10:1
Plaster of Paris	Small spread b: 3.2 cm – 36 cm c: 0.3 cm – 3.5 cm	+0.4	0.09	0.53	9:1

Both average a:c and b:c ratios for the horses in the plaster of Paris are 9:1. Hence, the horses in the plaster of Paris are equally shaped in both dimensions. Furthermore, the

horses in the plaster of Paris are relatively thicker in the dip dimensions as compared to the horses on Frøya and Kilve, whereas they are relatively slimmer than the horses on Bornholm in this dimension. Except the horses on Frøya, the horses are also relatively thicker in the strike dimension than the other horses based on this dataset.

4.3 Comparison of the results obtained from the most reliable dataset

This section presents a comparison of the results obtained from the most reliable dataset (chapter 3.4). The comparison based on the most homogeneous dataset of the horses from the four datasets, similar to the comparisons of the least reliable dataset and the second most reliable dataset.

It is the same horses as displayed in figure 3.23 that represent the horses on Frøya, and the same data as displayed in figure 3.26 and 3.33 that represent the horses in Kilve and on Bornholm, respectively. The horses in the plaster of Paris experiments are also displayed in figure 3.38.

The horses in the diagrams mentioned above are displayed in the same diagram (figure 4.5) to more easily study the similarities and/or differences between the datasets.

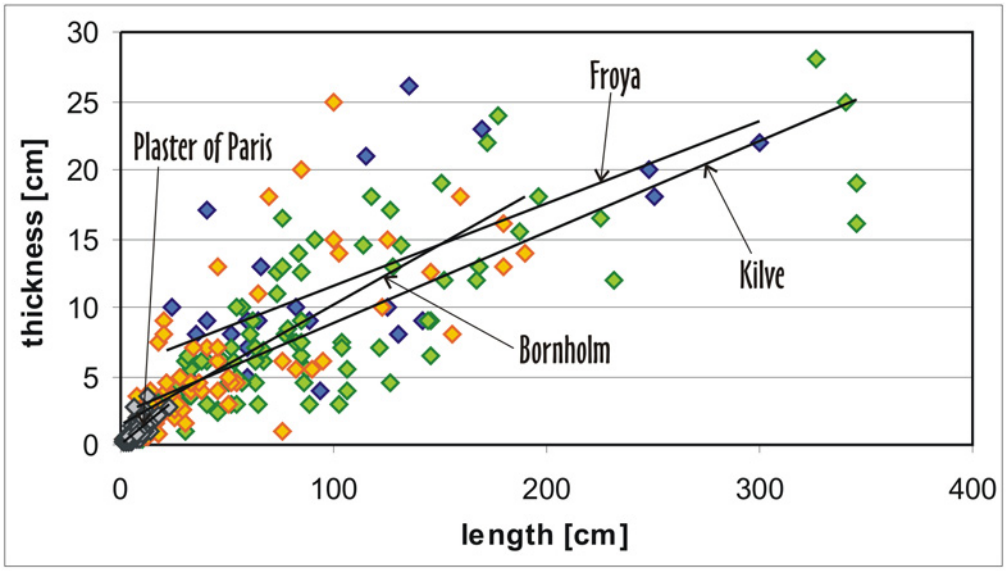

Figure 4.5 Plot of the measured length versus the thickness for horses in the four most reliable datasets. The horses are represented by the same colors as in figure 4.1.

Location of the data points in the diagram

The data points representing the horses examined on Frøya are few and they have a medium spread in the diagram (figure 4.5). The length of the horses varies between 21 cm and 300 cm, and the thickness between 3 cm and 26 cm (table 4.5). Hence, there are no horses with small lengths represented in the diagram.

Compared to the other horses, the data points representing the horses in Kilve have the largest spread in the diagram. The lengths of these horses vary between 8 cm and 346 cm, and the thickness between 0.4 cm and 28 cm. Thus, both horses with smaller and larger lengths, as compared to the horses on Frøya, are represented in the diagram.

The points representing the horses on Bornholm have a medium spread in the diagram. The lengths of the horses vary between 1.3 cm and 190 cm, whereas the thickness varies between 0.3 cm and 25 cm. Thus, the maximum lengths of the horses on Bornholm are roughly half the length of the horses on Frøya and in Kilve. However, horses with smaller lengths as compared to the horses on Frøya and in Kilve are represented in the diagram.

The data points representing the horses found in the plaster of Paris have the smallest spread in the diagram of the four datasets. The lengths of these horses vary between 1.2 cm and 22.2 cm, and the thickness between 0.2 cm and 3.5 cm.

Intersections of the regression lines with the y-axis

The regression line generated by the data points representing the horses on Frøya intersects the y-axis at +5.6. This is the highest intersection of the four regression lines in this comparison (table 4.5).

The data points representing the horses examined in Kilve, on the other hand, generate a regression line that intersects the y-axis at +2.4. Hence, the line intersects the y-axis at a lower than the regression line for the horses on Frøya.

The intersection of the regression line generated by the data points representing the horses examined on Bornholm with the y-axis is at +1.5. Consequently, the intersection is lower than the intersection of the regression lines for both the horses on Frøya and in Kilve.

However, the lowest intersection with the y-axis, which is at origin, is for the regression line generated by the horses in the plaster of Paris.

Gradients of the regression lines

The gradient of the regression line generated by the horses on Frøya, in Kilve and on Bornholm are concurrent, having gradients between 0.06 and 0.09 (table 4.5). The regression line generated by the horses in the plaster of Paris has a gradient of 0.13. Hence, this latter regression line has the steepest slope as compared to the others.

The R^2-values

The R^2-values given for the regression lines vary between 0.47 and 0.59. The highest value is for the plot of the horses in the plaster of Paris, whereas the lowest value is for the plot of the horses on Frøya. Nevertheless, all the values indicates that the points in each dataset are well constrained to the regression lines. Furthermore, the values indicate that there is a strong relation between the length and thickness for the horses in all four datasets.

Average l:c ratios

The average ratio between the length and thickness for the horses examined on Frøya is 9:1, implying that the length of the average horse on Frøya is nine times the thickness (table 4.5).

The equivalent ratio for the horses examined in Kilve is 12:1, which indicates that the lengths of these horses are twelve times the thickness. Hence, the horses in Kilve are slimmer as compared to the horses on Frøya based on the most reliable dataset.

The average ratio between the length and the thickness for the horses on Bornholm is 9:1, which is equal to the ratio for the horses on Frøya. Thus, based on the ratios the horses on Bornholm and on Frøya are equally slim, whereas the horses on Bornholm are relatively thicker than the horses in Kilve.

In accordance to the horses on Frøya and Bornholm, the horses in the plaster of Paris have an average l:c ratio of 9:1. The horses in these three datasets are equally slim, whereas they are not as relatively thicker as compared to the horses in Kilve.

Table 4.5 Values obtained in the plot of the length versus thickness for the horses in the most reliable dataset (figure 4.5).

Lithology/ material	Spread in diagram	Intersection	Gradient	R^2-value	Average l:c ratio
Frøya	Medium spread length: 21 cm – 300 cm thickness: 3 cm – 26 cm	+5.6	0.06	0.47	9:1
Kilve	Large spread length: 8 cm – 346 cm thickness 0.4 cm – 28 cm	+2.4	0.07	0.56	12:1
Bornholm	Medium spread length: 1.3 cm – 190 cm thickness: 0.3 cm – 25 cm	+1.5	0.09	0.59	9:1
Plaster of Paris	Small spread length: 0.2 cm – 22.2 cm thickness: 0.2 cm – 3.5 cm	0	0.13	0.59	9:1

4.4 Comparison of the three datasets

I will now present a comparison between the three datasets. It should be noted that when the a- or b-axis of a horse is estimated from the measured length, the estimation is always less than the measured length (chapter 1.4). In the second most reliable dataset the horses poorly exposed in the dip dimensions are omitted from the plots a- versus c-axes. Similarly, the horses poorly exposed in the strike dimensions are omitted from the plots of the b- versus c-axes in this dataset. For this reason, the a:c and b:c ratios in the

second most reliable dataset are expected to be higher as compared to the least reliable dataset. However, because no estimations have been made in the most reliable dataset, the l:c ratios are expected to be the absolutely highest. In this comparison the least reliable dataset is also referred to as the first dataset, the second most reliable dataset is also referred to as the second dataset, and the most reliable dataset is also referred to as the third dataset.

4.4.1 Comparison of the horses measured on Frøya

The horses measured on Frøya vary by having a medium or large spread in the diagrams (figure 4.1 - 4.5). The intersections of the regression lines with the y-axes vary between +0.9 and +5.6, where the lowest intersection is in the plot of the a- versus c-relation in the second dataset (table 4.3) and the highest intersection is in the plot of the lengths versus thickness in the third dataset (table 4.5). The gradients of the regression lines vary between 0.06 and 0.14 in the three diagrams. The R^2-values vary between 0.36 and 0.82. The lowest value is in the plot of the a-axes versus c-axes in the second most reliable dataset (table 4.3), whereas the highest value is in the plot of the b- versus c-axes in the first and second datasets (table 4.2 and 4.4).

As expected, the horses have a larger average a:c ratio in the second dataset than in the first dataset. The plot of the b- versus c-axes for the horses on Frøya in the second dataset is equal the same plot in the first dataset. Hence, the b:c ratios are equal in these two datasets. The plot of the a- versus c-relation in the second dataset is based entirely of horses in the locality at Flatval, whereas the plot of the b- versus c-relation in this dataset is based entirely of the horses in the locality at Skardsvåg.

However, it should be noted that third and fourth order horses are represented from the second locality, whereas first order horses are represented from the first locality. Secondly, the horses in the first locality are exposed in the dip dimension, and for this reason the a-axes for these horses are not estimated. The b-axes in the second locality, on the other hand, are estimated because horses are exposed in a section between the dip and strike dimension. This may explain why the horses on Frøya seem to be relatively slimmer in the dip dimension as compared to the strike dimension.

Nevertheless, the l:c ratio for the horses in the third dataset, in which all of the horses on Frøya are included, is 9:1. This ratio is higher than the b:c ratio in the first and second datasets. However, the l:c ratio is higher than the a:c ratio in the first dataset and lower than the a:c ratio in the second dataset.

4.4.2 Comparison of the horses measured in Kilve

The horses examined in Kilve are largely spread in all diagrams as compared to the rest of the horses. The intersections of the regression lines for these horses vary between +1.3 and +4.9. The lowest intersection is in the plot of the b- versus c-relation in the second dataset (figure 4.4), whereas the highest intersection is in plot of the b- versus c-relation in the first dataset (figure 4.2). The gradients of the regression lines are similar, only varying between 0.06 and 0.09. The lowest R^2-values, which are 0.37 and 0.33, are in the plot of the a- versus c-relation in the second dataset and in the plot of the b-versus c-relation in the first dataset, respectively. The highest R^2-value, which is 0.66, is given in the plot of the b- versus c-relation in the second dataset.

In the first dataset both the a:c and b:c ratios are 9:1. In accordance to the expectations mentioned earlier, both of these ratios are higher in the second dataset. Here, the a:c and b:c ratios are 10:1 and 12:1, respectively. Thus, the horses seem to be slimmer in the strike dimension as compared to the dip dimensions. Nevertheless, it is only horses from locality 1 that are represented in the plot of the a- versus c-relation in the second dataset. These horses are dominantly located in the damage zone. The horses represented in the plot of the b- versus c-relation in this dataset, on the other hand, are from locality 2 and 3. In locality 2 the horses are located both in the damage zone as well as within the fault core, whereas the horses in locality 3 are located exclusively in the fault core. I will return to this in the discussion (chapter 5).

The l:c ratio for the horses in Kilve is 12:1. Hence, the horses in Kilve are relatively slimmer as compared to the horses on Frøya.

4.4.3 Comparison of the horses measured on Bornholm

The horses examined on Bornholm have a medium spread in the diagrams as compared to the horses in the other datasets. The regression lines for these horses intersect the y-axes between +0.8 and +1.5. The lowest intersection is in the plot of the a- versus c-relation of the first dataset (figure 4.1), whereas the highest intersection is in the plot of the lengths versus thickness in the third dataset (figure 4.5). The steepest regression line for these horses is given by a gradient of 0.17, and is in the plot of the a- versus c-relation in the second dataset. The gentlest slope, on the other hand is given by a gradient of 0.08, and is in the plot of the b- versus c-relation in both the first and second datasets. The R^2-values vary between 0.58 and 0.73, reflecting strong linear relations between the variables in all diagrams.

As expected, the b:c ratio in the first dataset is less than the ratio in the second dataset. However, the a:c ratio in the second dataset is less than the ratio in the first dataset, which is the opposite of what is expected. In the first dataset horses from both localities are present. In the second dataset, on the other hand, only horses within fault 4 are present from the Galgeløkken cliff section. Thus, the majority of the horses in the plot of the a- versus c-axes in the second dataset are horses found in A. Stenders Kvartsgrav. The majority of the horses in the Galgeløkken section are located in the damage zone, whereas the horses in A. Stenders Kvartsgrav are located in the fault core. Also the vertical displacement of the faults in which the horses are located varies greatly between the localities (chapter 2.6). The difference in the location of the horses may cause the a:c ratio in the second dataset to be less than in the first dataset. I will return to this in the discussion (chapter 5). However, an interesting aspect is the large differences between the a:c and b:c ratios in both the first and the second dataset (table 4.1 - 4.4). This may imply that the horses are significantly slimmer relative to length in the strike dimension as compared to the dip dimension.

The l:c ratio for all the horses measured on Bornholm is 9:1, which is between a:c and b:c ratios in the second dataset. Hence, this ratio is equal the l:c ratio for the horses on Frøya.

4.4.4 Comparison of the studied plaster of Paris horses

The smallest spread in all diagrams is the spread of the horses examined in the plaster of Paris experiments. These horses were measured in either dip or strike dimension, and appear identically in the first and second dataset (table 4.1 - 4.4). The intersections of the regression lines generated for these horses with the y-axes vary between –0.1 and +0.4. Hence, the regression lines for these horses intersect the y-axes are the lowest values of all the datasets in all diagrams. The gradients of the lines vary between 0.09 and 0.14. The steepest regression line is in the plot of the a- versus c-axes, whereas the gentlest slope is for the regression line in the plot of the b- versus c-axes. The R^2-values are between 0.53 and 0.59, all indicative of strong linear relations between the variables.

Both a:c, b:c and l:c ratios are 9:1 for these horses. For this reason the l:c ratio is equal the l:c ratios for the horses on Frøya and on Bornholm.

Chapter 5

DISCUSSION

This chapter presents a comparative analysis of the main results obtained. Furthermore, the results are discussed in context of the hypothesis that constitutes the basis for this study.

The architecture of faults is important to the fluid communication along and across fault zones, because contacts between units of high or low permeability control the fluid flow (Childs et al. 1997, Knipe 1997, Knipe et al. 1997, Losh et al. 1999). The geometry of faults is generally very complex. Nevertheless, horses and duplexes are dominant intrinsic geometrical features within both the damage zone and, especially, within the fault core (Caine et al. 1996, Gabrielsen & Braathen In press). Due to the importance of the horses and duplexes to the permeability of the fault zones, the dimensions of these features are of particular interest. However, to my knowledge, studies on the dimensions of extensional horses have not previously been presented in the literature.

The main aim in this study has been to find out which parameters influence the shape and dimensions of the horses that often constitutes the main elements of faults, particularly emphasizing the following:

1) The type of tectonic environment.
2) The type of mechanism active in the generation and development of the horses. The type of mechanisms are also related to other aspects that influence the shape of the horses, such as:

- **a)** The "order" of the horse in context of its dynamic development.
- **b)** The position of the horses relative to, and within, the fault core.
- **c)** Strain hardening/strain softening processes.

3) The amount of displacement across the fault.
4) The lithology of the host rock.

To evaluate each of the factors above, a detailed study of horses, and the faults in which they occur, has been carefully carried out. The precise length and thickness of the horses has been measured, and the amount of overlap and their tendency to step towards the right or left has been noted. In addition, the amount of dip, displacement and the width of the faults were noted. Two of the faults are found on Frøya, where the host rocks consist of migmatitic gneiss and pegmatite (chapter 2.2), and three of the faults are found in Kilve (southwestern England), where the host rocks consist of argillaceous limestone and shale (chapter 2.4). On Bornholm, a fault system consisting of several fault branches in addition to four distinctive faults were examined, these occurring in nearly unconsolidated sandstone (chapter 2.6). Eventually, faults occurring within five plaster of Paris experiments were examined (chapter 2.7).

The measurements of the horses constitute the basis for three datasets (chapter 3). However, the comparison and the discussion of the horses are primarily based on the dataset where the measured length and thickness of the horses, as they appear in the outcrops are used in the plots of the horses (chapter 3.3). This is because this dataset is the most reliable of the three, and because a comparison of all of the three datasets would have been too complex and chaotic.

Six parameters are obtained from the measurements of the horses (chapter 4). Not all of the parameters described in the previous chapter are considered here, however, mainly because this would make the comparison/discussion very chaotic. The basic parameter used to enlighten the influence of the factors mentioned above is the average l:c ratio.

I will now discuss the different factors that influence the shape of the horses in the same order as listed above.

5.1 The tectonic environment

One principal factor that influences the shape of the horses is presumably the stress system that was active during faulting. This is because parameters such as the partitioning of slip among faults, or the interaction between fault segments will differ in different tectonic environments (Wojtal 1994). Also the thickness, a parameter which

influences the rates of nucleation and growth of small faults associated with the major faults, will differ between tectonic regimes (Wojtal 1994). In addition, also the mechanisms involved in the generation of the horses differ between environments. For instance, horses within an extensional fault are typically generated by fault segments that either splay or amalgamate to the main fault, and they are often found within faults where a flat and ramp exist in the footwall, forming a duplex (Gibbs 1984, Gabrielsen & Clausen 2001) (figure 5.1). In contractional regimes, on the other hand, horses and duplexes are more typically generated as a result of a progressive collapse of footwall ramps, causing a significant increase in the thickness of the fault zone (Boyer & Elliot 1982) (figure 5.2), and in strike-slip regimes the development of Riedel, anti-Riedel shears and P-shears are the dominating mechanisms involved in the generation of horses (figure 5.3).

Mechanisms dominating in the generation of horses in a tectonic environment may not be constricted to this regime only. The theory of Boyer & Elliot (1982) for developing horses and duplexes in thrust regimes may also apply in strike-slip regimes, for instance in transpressional zones, and in extensional regimes. Also riedel and anti-riedel shearing, which is common in strike-slip regimes, may influence the angle of faulting in other regimes. This may be the case in extensional faulting, where the angle of segment splaying and amalgamation to the main fault may be controlled by the same angles as in Riedel shearing (figure 5.4). However, the shapes of horses that occur in different tectonic environments are presumably different because the mechanisms dominating in their generation differ between the environments.

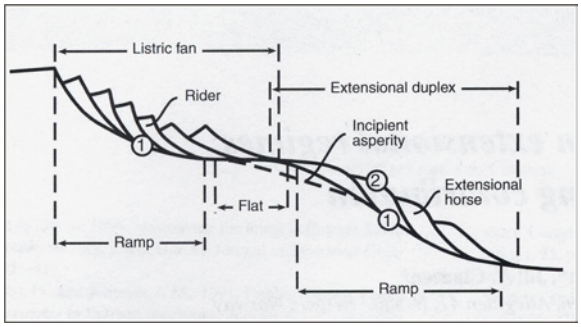

Figure 5.1 Schematic sketch of the ramp-flat-ramp structure, which is typical of extensional faulting, and associated horses. 1 = floor fault, 2 = roof fault. Gabrielsen & Clausen (2001).

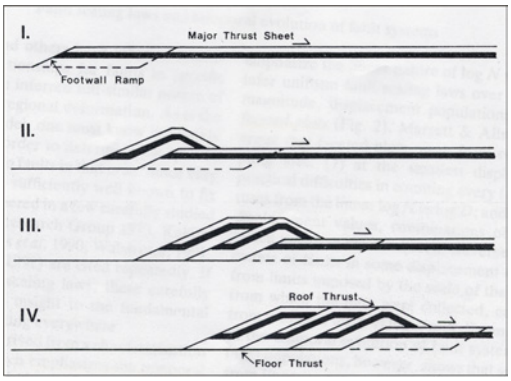

Figure 5.2 Model for development of horses and duplexes. The model is redrawn by Wojtal (1994), and is based on the theory of Boyer & Elliot (1982)

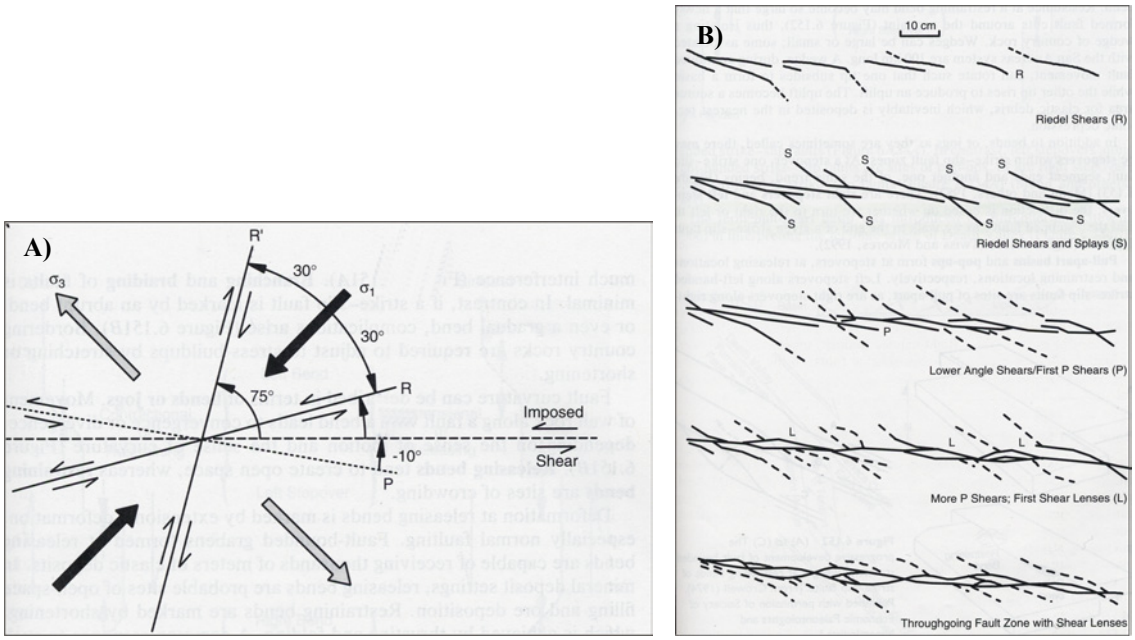

Figure 5.3 A) Sketch showing the Riedel (synthetic), the anti-Riedel (antithetic) and the P shears in a left-handed strike-slip zone. B) Sketch showing the interrelationships of Riedel shears, splays, and P-shears in a right-handed strike-slip zone, and how they combine to produce a braided shear pattern with horses. After Woodcock & Schubert (1994).

Nevertheless, due to limitations of this thesis, only horses within primarily extensional regimes are considered in this study. Hence, horses occurring in faults subjected to different stress conditions have not been compared. The exceptions may be the fault in the locality at Flatval on Frøya (chapter 2.2.1), where it is not possible to establish the relative movement.

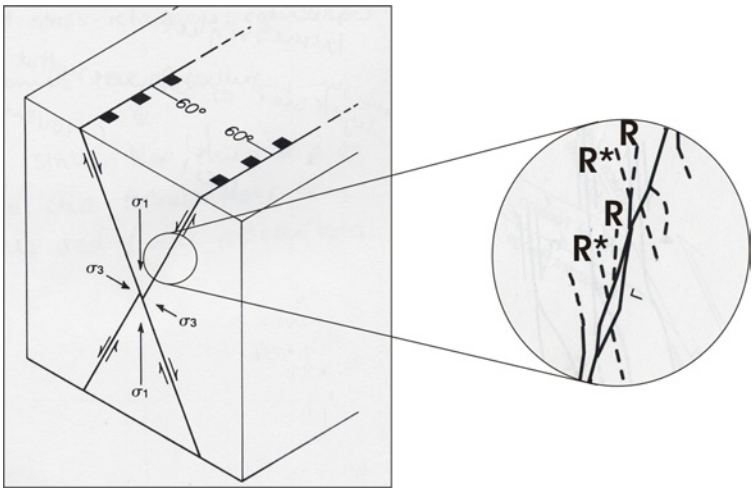

Figure 5.4 Sketch showing how Riedel shearing are assumed to control the angle of segment splaying and amalgamation to the main fault, and which in turn may result in generation of horses. Based on Davis & Reynolds (1996) and Woodcock & Schubert (1994).

5.2 Mechanism active in the initiation and the development of the horses

Another important factor controlling the shape of the horses is the mechanisms active in their development. As already mentioned, different mechanisms are assumed to dominate within different tectonic environments. However, since I have focused on horses generated in extensional regimes in my study, I will also focus on the mechanisms that dominate in these regimes. Studies indicate that several mechanisms may contribute to development of the horses, namely tip-line bifurcation, segment linkage, tip-line bifurcation, asperity bifurcation, segment splaying, and segment amalgamation (Childs et al. 1997, Gabrielsen & Clausen 2001) (figure 5.5). The first three mechanisms are primary processes, which are affiliated with the establishment of the fault plane, whereas the latter three are secondary processes related to the development of the fault zone after a continuous fault plane is established (Gabrielsen & Clausen 2001). Of these, segment linkage, asperity bifurcation, and footwall and hanging wall segment splaying and amalgamation are the most commonly observed in the experiments, and are also believed to be the most common in natural faults (Gabrielsen & Clausen 2001).

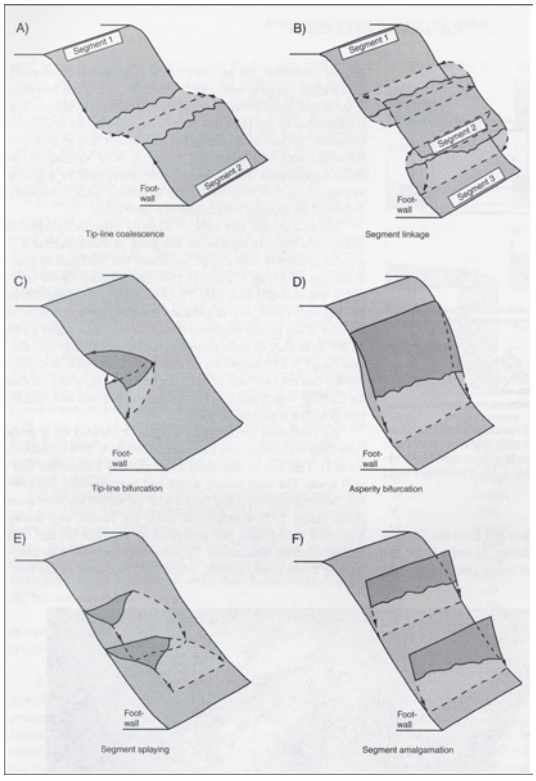

Figure 5.5 Principal sketches of configurations that contribute to development of extensional horses: A) tip-line coalescence, B) segment linkage, C) tip-line bifurcation, D) asperity bifurcation, E) hanging-wall segment splaying, and F) hanging-wall segment amalgamation. Small arrows indicate tip-line growth directions. (Gabrielsen & Clausen 2001).

5.3 The order of the horse in context of its dynamic development

Another factor which influences the shape of the horses, and which is related to the mechanism active in their generation, is the "order" of the horse. After the establishment of a horse, continued deformation may lead to splaying of the original horse into smaller horses due to asperity bifurcation (figure 5.5D). The original horse is termed a first order horse, whereas the smaller horses which the first order horse splits into are termed second or third order horses according to its hierarchical status in the development of the duplex. Horses of different orders are expected to have different shapes, because new horses are initiated by new faults cutting into the pre-existing horse with a typical angle of approximately 30^{o} to the surface of the 'old' horse (Anderson 1951, Wojtal 1994, Peacock & Sanderson 1992; figure 5.6).

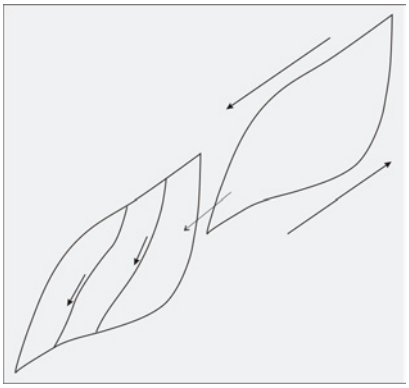

Figure 5.6 Schematic sketch of an original first order horse that is splayed into smaller second order horses.

One of the main topics in this study has been to determine whether or not there are differences in geometry when the large (higher order) and the small (lower order) horses are considered. In this context, it is reasonable to assume that the latter are defined either as part of the higher order horses or that they may be identified where they occur as e.g. arrays of equally shaped, overlapping features (figure 5.7).

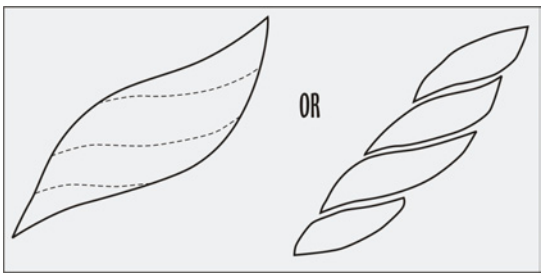

Figure 5.7 Principal sketch showing that small horses may either be a part of a higher order horse, or as arrays of equally shaped, overlapping features.

This may be consistent with that process in which large horses split into smaller horses by a continuous process of shearing. If a first order horse consists of second order horses, the latter cut the first order horse in such a way that faults defining these horses cut into the pre-existing horse with an angle to the surface of the 'old' horse. The second order horses are hence generally thicker relative to their length and width as compared to that of the first order horse. To examine if there is a difference in shape between a higher order horse and associated smaller, lower order horses, the l:c ratios for the hierarchal horses are compared.

Three of the horses in the locality at Skardsvåg on Frøya are third order horses consisting of three fourth order horses (figure 2.11, 5.8). The average l:c ratio for the three third order horses is 13:1, whereas the same ratio for the forth order horses inside the three third order horses is 7:1. This implies that the smaller (lower order) horses are significantly thicker relative to length than the higher order horses defining them.

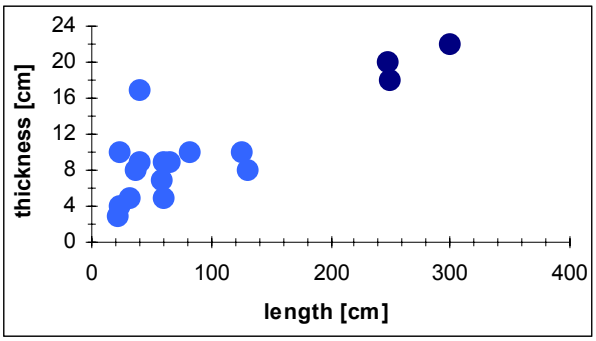

Figure 5.8 Plot of the three third order horses (dark blue, N = 3) and the forth order horses (light blue, N = 14) found in the locality at Skardsvåg on Frøya.

Another set of such horses is found in locality 2 on the Kilve beach, where third order horses are bounded by a second order horse (figure 2.28, 5.9). Here, the second order horse has an l:c ratio of 18:1, whereas the average ratio for the third order horses is 15:1. As for the horses on Frøya, the highest order horse is significant slimmer relative to length than the horses bounded by this.

The last two sets of such horses are found in fault A (figure 2.43, 5.10) and in fault E (figure 2.46, 5.11) in A. Stenders Kvartsgrav on Bornholm. In fault A five second order horses are inside a first order horse. Here, the l:c ratio for the first order horse is 8:1, whereas the average ratio for the second order horses is 11:1. Hence, the highest order horse is significantly thicker relative to length than the second order horses defined by

this. In fault E seven second order horses are found within a first order horse. In this case the first order horse has an average l:c ratio of 6:1, whereas the average ratio for the second order horses is 7:1. In accordance to the horses in fault A, the highest order horse is thicker relative to length than the second order horses inside.

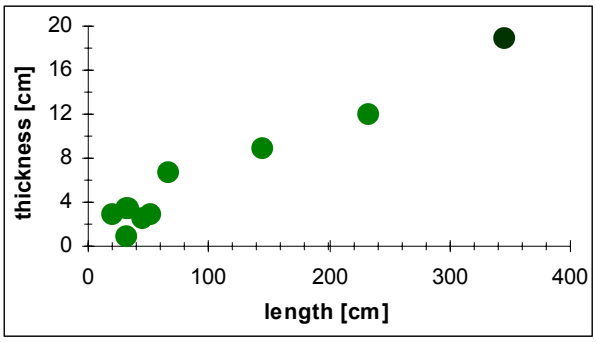

Figure 5.9 Plot of a second order horse (dark green) and the eight third order horses bounded by the third order horse (light green) found within locality 2 in Kilve.

In the case of the examined horses on Frøya and in Kilve, the horses of higher order are slimmer relative to length when compared to the lower order horses inside. In contrast to this, the higher order horses examined on Bornholm are thicker relative to length when compared to the lower order horses inside.

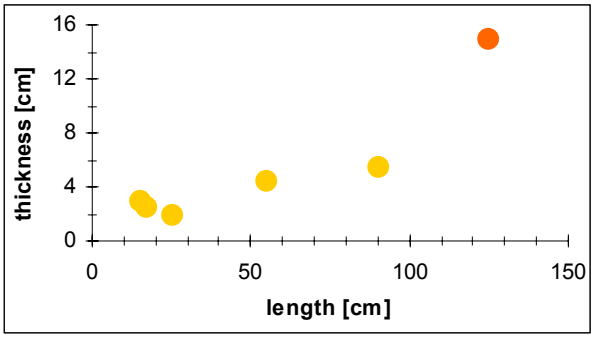

Figure 5.10 Plot of a first order horse (orange) and five second order horses (yellow) bounded by the first order horse that appear within fault A in A. Stenders Kvartsgrav on Bornholm.

The differences between the studied areas may be explained by the lithology of each area. The gneiss on Frøya and the limestone in Kilve are relatively 'strong' rocks compared to the nearly unconsolidated sandstones on Bornholm, which then represent a 'weak' rock in this study. When the examined horses in gneiss or limestone were generated, the higher order horse was sliced into a new set of horses that are thicker relative to length than the original horse. Contrary, when the horses examined in unconsolidated sandstone were generated, the higher order horses were sliced into slimmer horses compared to the original horse. It is thereby concluded that the shape of

the higher order horses differ from the shape of the lower order horses, and that the way they differ changes from one geological setting to another.

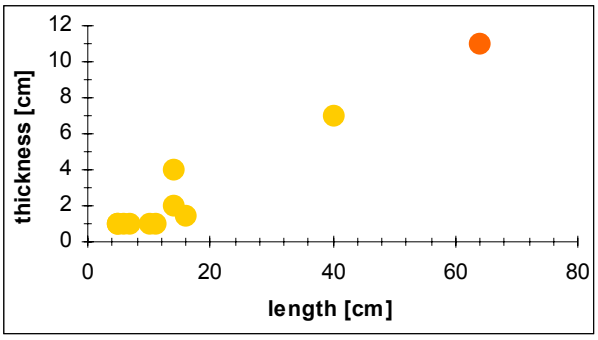

Figure 5.11 Plot of a first order horse (orange) and ten second order horses (yellow) inside which are found within fault E in A. Stenders Kvartsgrav on Bornholm.

Different mechanical properties in rocks have large effect on how horses splay into smaller horses, i.e. by how the new faults cut an original horse to form a new set of horses. Faults splaying into a horse in 'strong' rocks may have a tendency of having high angles to surfaces that surround the horse. In contrary, faults splaying into a horse in 'weak' rocks, may have a tendency to have considerably lower angles to the surrounding surfaces (figure 5.12).

In any case, common for all of the rocks is that there is a difference between the shape of high order horses and the lower order horses that it splays into. This is in accordance to the assumption proposed earlier in this chapter that the shape of a horse is affected by the order of the horse.

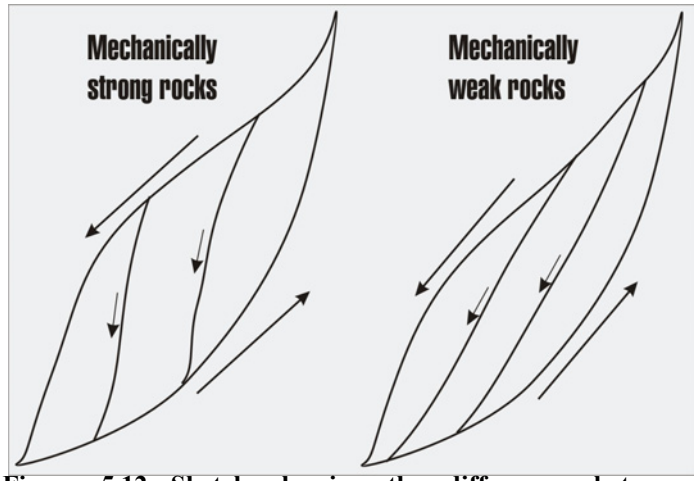

Figure 5.12 Sketch showing the differences between splaying of mechanically strong and weak rocks. The horses within 'strong' rocks have a tendency to splay into thicker horses with continued deformation, whereas the opposite is the case for horses within 'soft' rocks.

5.4 The position of the horses relative to, and within, the fault core

Horses are found within the damage zone as well as within the fault core of a fault zone (figure 5.13). However, because strain may vary greatly between the different parts of the faults, the shape of horses found within the fault core are likely to differ from horses found within the damage zone. Even though fault zones may become thicker during initial slip increments, the most active portion of a fault eventually narrows, some times into a layer dominated by banded cataclasites, pervasively cleaved rocks, or some combination of the two (Wojtal & Mitra 1988, Woodward et al. 1988). The shape of the horses in the fault core and damage zone is also likely to differ because different mechanisms may be dominating within the different parts of the fault zone. Whereas segment splaying and amalgamation are mechanisms that dominate in the damage zone, at least in the initial stages of faulting, asperity faulting probably dominate in the fault core (Gabrielsen & Clausen 2001). So, even if several mechanisms have contributed in the generation of horses, the horses formed in the later stages of faulting are likely to have been initiated by asperity faults, due to the fact that the majority of the movement along faults commonly occur within this part. As a result of this, it may be impossible to identify the mechanism generating the original horses with certainty. Another important factor is that fault rocks may mechanically harden (Wojtal & Mitra 1986), and therefore have different mechanical properties than the rocks in the damage zone. I will return to the effect of different mechanical properties later in this chapter.

Analyses of data from locality 2 in Kilve (chapter 2.4.4), which includes both horses that occur within the damage zone and horses that occur within the fault core, show that the average l:c ratio for the fault core horses is 11:1, whereas the ratio for the damage zone horses is 14:1. This implies that the horses in the fault core are significantly thicker, relative to length, than the horses in the damage zone of the fault.

Based on the two ratios it is concluded that there is a difference between the shapes of horses that occur relative to, and within, the fault core, where the fault core horses seem to be thicker relative to length. It is also worth mentioning that most of the movement across the fault zone has occurred in the fault core. The movement is again related to the

mechanism initiating the horses, and it therefore also seems like asperity bifurcation horses, which is assumed to dominate in the fault core, are thicker than horses initiated by segment splaying and amalgamation.

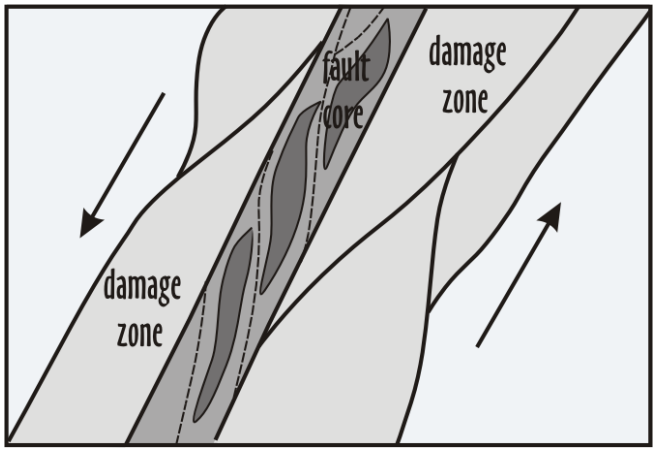

Figure 5.13 Sketch showing how horses may be present in both the fault core and the damage zone.

Another important factor when considering the difference in shape between horses in the fault core and the damage zone, is the differences in lithology as described in the previous chapter. For example, the high content of relatively strong rocks like limestone within the core, as is the case for some sections of the described localities in Kilve, may influence the faulting of the horses, such that increased amount of limestone also increases the angle of faulting relative to an original horse (Peacock & Sanderson 1992) (figure 5.12). Also, fault rocks present in the core may have hardened mechanically due to faulting. These may also represent 'strong' rocks, affecting the generation of new horses in the same manner as above.

5.5 Strain hardening or strain softening process

An additional important factor assumed to influence the shape of the horses is the type of process that has taken place in the zone during deformation. Horses occurring in fault zones subjected to dynamic strain hardening are assumed to obtain different shapes as compared to horses that occur in fault zones characterized by strain softening (figure 5.14).

Continuous deformation in strain-hardening fault zones either results in widening of the fault core, or the establishment of new faults (Wojtal 1994, Shipton & Cowie 2003,

Gabrielsen & Braathen In press). In such zones segment splaying and amalgamation are believed to be the main mechanisms active in the generation of horses in the hanging wall as well as in the footwall (Gabrielsen & Clausen 2001). Continuous deformation along faults in strain-softening fault zones, on the other hand, is more likely to occur along the already established fault planes (Gabrielsen & Braathen In press). In this case irregularities, which occur along such fault planes, are likely to be smoothened by asperity bifurcation faults (Gabrielsen & Clausen 2001). Asperity bifurcation is believed to be the main mechanism active in generating new horses or deforming horses in strain-softening zones.

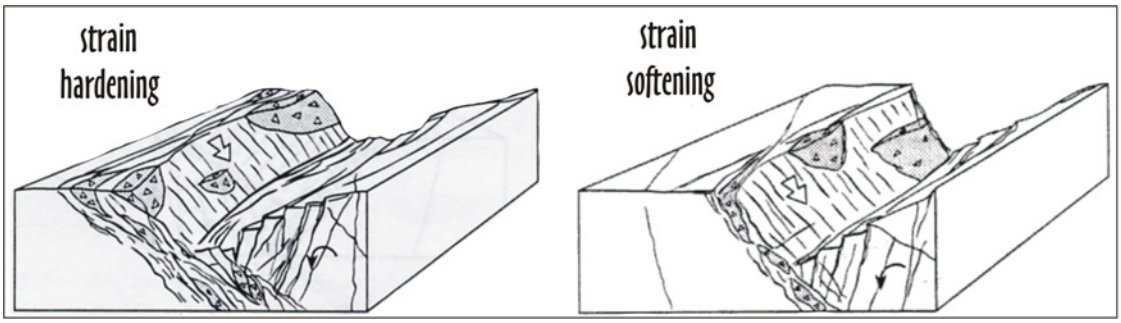

Figure 5.14 Schematic presentation of a strain-hardening fault zone, in which continued faulting lead to a thickening of the zone, and a strain-softening fault zone, in which the fault zone narrows. (Braathen & Gabrielsen 1998).

5.6 The amount of displacement across the fault

The amount of displacement across the fault is also an important factor which may influence the shape of the horses. Hence, it is suggested that the shape of horses occurring in faults with a relatively large vertical displacement will differ from those occurring in faults with less vertical displacement.

Different mechanisms are involved in the generation of horses at different stages of deformation. In early stages of deformation, processes such as tip-line coalescence, segment linkage and tip-line bifurcation are involved in the generation of the horses. These processes are affiliated with the establishment of the fault (Gabrielsen & Clausen 2001). In later stages, processes such as asperity bifurcation and segment splaying and amalgamation are involved in their generation. These are processes that are associated

with the development of the fault zone after a continuous fault plane is established. However, by extreme extension the fault zone may collapse, and the horses are smeared out along the fault plane to constitute a homogeneous mass (Gabrielsen & Clausen 2001).

On Bornholm horses have been examined in A. Stenders Kvartsgrav, a sand pit, and in the Galgeløkken cliff section. Both localities expose horses occurring in nearly unconsolidated sandstone (chapter 2.6). The fault zone in the sand pit has a vertical throw in excess of 13 m, whereas the four faults in the cliff section has vertical throws of less than 5 cm, and the horses examined in two localities are thus compared to study the influence of displacement on the shape of horses. It should be noted, however, that the fault system in the sand pit consists of several fault segments. Nevertheless, each of the segments has still undertaken significantly more displacement as compared to the four distinctive faults in the cliff section. The general size of the horses in the two localities differs greatly, in which the horses in the sand pit provide an average l:c ratio of 8:1 (figure 3.34) and the horses in the cliff section provide an average ratio of than 12:1 (figure 3.35). Based on this observation, the horses are therefore thicker, relative to length, in the faults with the highest vertical displacement.

Based on the horses examined in the two localities it is concluded that the shape of the horses vary significantly with vertical displacement, and it seems like horses occurring in faults with a high vertical displacement are thicker than horses in faults with less vertical displacement. As previously mentioned, asperity bifurcation processes are assumed to dominate in later stages of deformation. It may therefore also be concluded that horses generated by such processes are thicker than horses generated by processes such as for instance tip-line bifurcation and segment linkage. This is in accordance to the observation made previously in this chapter (chapter 5.4).

5.7 The lithology of the host rock

The last factor that may influence the shape of the horses is the lithology of the host rock. It is thus assumed that there is a difference between horses that occur in different lithologies.

The Coulomb theory of failure predicts the orientation of shear failure planes. The law is an equation that describes the height and slope of the linear envelope of failure for rocks in compression:

$$\sigma_c = \sigma_o + \tan \phi \ (\sigma_N), \text{ where}$$

σ_c = critical shear stress required for faulting,
σ_o = cohesive strength,
ϕ = angle of internal friction, and
σ_N = normal stress.

The Coulomb theory of failure predicts shear failure planes at $< 45^o$ (typically about 25^o) to the maximum compressive stress (σ_1), the angle being determined by the coefficient of internal friction ($\tan \phi$). Based on the fact that the internal friction varies with rock type, the rock type will influence the angle of faulting and therefore also the geometry of the horses that may result (Peacock & Sanderson 1992).

However, this is valid only for isotropic and homogeneous material, whereas anisotropies (directional heterogeneity) are present in nearly all crustal rocks. Presence of anisotropies in a rock is important, due to the fact that anisotropies can strongly affect fault orientation (e.g. Anderson 1951, Billings 1954, Donath 1961).

Anisotropies in rocks may be layering (alternations of materials with differing mechanical properties), continuous anisotropy (directional variations in mechanical properties produced by penetrative fabrics), and discrete planes of weakness (planes with reduced cohesion and coefficients of sliding friction) (Peacock & Sanderson 1992).

In addition to the angle of internal friction, the cohesive strength (σ_o) of the rock is also an important factor that may influence the shape of the horses. For instance, if an existing horse is subdued to stress, the strain may be alongside the horse if the horse consists of a ‘strong’ rock, instead of through the horse, which might be the case in a ‘weaker’ rock (figure 5.15).

Based on the Coulomb theory of failure, one should expect that horses occurring in 'strong' rocks are thicker due to the higher angle of friction in stronger rocks.

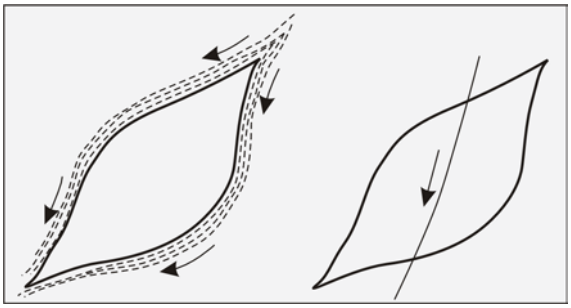

Figure 5.15 The deformation in the fault may either go around the horse or it may cut the horse in half.

The three lithologies in this study is gneiss pervaded by pegmatite (Frøya), argillaceous limestone interbedded with shale (Kilve), and nearly unconsolidated sandstone (Bornholm). The analogue experiments were carried out in plaster of Paris. The gneiss is assumed to be the rock with the strongest mechanical properties in this study, the limestone with the medium mechanical properties, and the nearly unconsolidated sandstone is assumed to be the rock with the weakest mechanical properties. The horses in the plaster of Paris experiments were generated before solidification of the plaster, such that this plaster is assumed to represent the material with the absolutely weakest mechanical properties. Furthermore, there is presumably a relationship between the mechanical properties and the angle of internal friction, ϕ. This implies that it is also likely that faults in the mechanically strongest rocks tend to form at the highest angles to σ_1. The horses examined on Frøya are therefore expected to be the thickest horses, the horses in Kilve are expected to be of medium thickness, the horses examined on Bornholm thinner than the horses in Kilve and, eventually, the horses generated in the plaster of Paris experiments are expected to be the slimmest horses in this study.

When all the horses examined on Frøya are considered, the average l:c ratio is 9:1. This is the same ratio as the ones given for both the horses examined on Bornholm and the horses in the plaster of Paris experiments. Conversely, the horses examined in Kilve have an average ratio of 12:1, which is a significantly larger ratio. The horses examined in Kilve clearly give the highest average l:c ratio, implying that these horses, hosted by argillaceous limestone and shale, are slimmer relative to length than the horses examined in the other lithologies and in the experiments.

Based on the average ratios for these horses, there seem to be no clear relation between the shape of the horses and the lithology of the host rocks. The average l:c ratio for the horses examined in Kilve deviates from the ratios given by the other horses, whereas the other horses has averagely the same l:c ratios, despite the fact that the host rocks on Frøya, on Bornholm and in the plaster of Paris experiments are assumed to have significantly different mechanical properties.

Nevertheless, it should be noted that horses of about 10 m length and 1-2 m thickness are observed in both gneiss and limestone interbedded with shale, whereas the largest horses observed in the nearly unconsolidated sandstone have lengths less than 2 m and thickness of about 30 cm. The largest horses are thereby located in the 'strongest' lithologies.

However, it should be noted that in addition to different lithologies, many of the other factors that influence the shape of the horses are present. The horses on Bornholm and on Frøya, for instance, occur within the fault core, whereas the horses in Kilve occur both within the fault core and the damage zone. Also the amount of vertical displacement varies significantly between the faults, a factor that also influences the shape of the horses. Furthermore, the horses on Bornholm occur within strain-softening fault zones, whereas the horses examined in Kilve and on Frøya occur within strain-hardening zones. These are all factors that should be considered when comparing the shape of the horses.

5.8 General shapes and dimensions of horses

To investigate the general shapes and dimensions of horses, absolutely all horses represented in the most reliable dataset are plotted in the same diagram (figure 3.39). As the diagram shows, the lengths of the horses in this study are between 1.2 cm and 346 cm, whereas the horses are between 0.2 cm and 28 cm in thickness. The absolutely smallest l:c ratio for the horses is recorded to 3:1, which is the ratio for a horse measured in A. Stenders Kvartsgrav on Bornholm. Hence, the thickest horse in this study has a length that is only three times the thickness. The absolutely largest l:c ratio, on the other hand, is recorded to 31:1, which is the ratio for a horse in the fault in

locality 3 in Kilve. The slimmest horse in this study has thereby a length that is thirty-one times the measured thickness. However, the average l:c ratio when all the horses are included is 10:1. Hence, the average horses in this study have lengths that are ten times the measured thicknesses.

Chapter 6

CONCLUSIONS

The data of horses support the proposal that the shapes and dimensions of horses are not completely arbitrary, but dependent of several factors. Based on data from this study shapes and dimensions of horses are influenced by:

- The type of mechanism active in the generation of the horses. Horses examined here are generally interpreted as generated either by asperity bifurcations or by splaying and amalgamation of fault segments. Asperity bifurcation horses seem to be thicker relative to length as compared to horses generated by segment splaying and amalgamation.

- The 'order' of the horse in context of its dynamic development. For horses occurring in gneisses or limestones, higher order horses are relatively slimmer than lower order horses bounded by the higher order horses. In contraire, for horses occurring in sandstone, higher order horses are thicker relative to length than the lower order horses that are bounded by the higher order horses.

- The position of the horses relative to, and within, the fault core. Horses occurring within fault cores seem to be thicker relative to length as compared to horses occurring within damage zones. This may be related to the mechanism active in their generation, as asperity bifurcation probably dominates in the fault core, whereas segment splaying and amalgamation probably dominate in the damage zone.

- The amount of displacement across the fault. Horses in faults with large displacement seem to be thicker relative to length as compared to horses in faults with less displacement. This may again be related to the mechanism active in their generation, as horses generated at late stages of faulting seem to be

asperity bifurcation horses, whereas segment splaying and amalgamation horses dominate at earlier stages.

- Lithology of the host rock. There are no clear evidences of the role of the lithology of the host rock. Nevertheless, large horses in the order of tens of meters in length and 1-2 m in thickness were only observed in gneiss and in limestone. The largest horses observed in nearly unconsolidated sandstone, on the other hand, are less than 2 m long and 25 cm thick.

- The average l:c ratio, when absolutely all the horses measured in this study are considered, is 10:1. The general horse in this study thus has a length that is ten times the thickness. Furthermore, the recorded horses have lengths between 1.2 cm and 346 cm and thicknesses between 0.2 cm and 28 cm.

References

Anderson, E. M. (1951). The dynamics of faulting and dyke formation with application to Britain, *Oliver & Boyd.* p. 209.

Arndorff, L. (1993). Lateral relations of deltaic palaeosols from the Lower Jurassic Rønne Formation on the island of Bornholm, Denmark. *Palaeogeography, Palaeoclimatology, Palaeoecology* 100: 235-250.

Askvik, H. & Rokoengen, K. (1985). Geologisk kart over Norge. Kristiansund 1: 250.000, Norges Geologiske Undersøkelse.

Bering, D. H., Boyd, R., Grønlie, A., Solli, A., Atakan, K., Bryhni, I., Gautneb, H., Krill, A., Lynum, R., Olesen, O. & Rindstad, B. I. (1986). Berggrunnsgeologisk rekognosering av fire områder på kysten av Møre og Trøndelag. *Norges Geologiske Undersøkelse Rapport* 86.182 p. 127.

Billings, M. P. (1954). Structural geology (2nd edition), *Prentice Hall, Englewood Cliffs, New Jersey* p. 514.

Bixler, W. G., Elmore, R. D. & Engel, M. H. (1998). The origin of magnetization and geochemical alteration in a fault zone, Kilve, England. *Geological Journal* 33: 89-105.

Blystad, P., Brekke, H., Færseth, R. B., Larsen, B. T., Skogseid, J. & Tørudbakken, B. (1995). Structural elements of the Norwegian continental shelf. Part II: The Norwegian Sea Region. *Norwegian Petroleum Directorate Bulletin* 8: p. 45.

Boyer, S. E. & Elliot, D. (1982). Thrust systems. *American Association of Petroleum Geologist Bulletin* 66 (9): 1196-1230.

Braathen, A. (1996). Bruddsoner på Frøya og Nord-Hitra. *Norges Geologiske Undersøkelse Rapport* 96.023 (23) p. 15.

Braathen, A. & Gabrielsen, R. H. (1998). Lineament architecture and fracture distribution in metamorphic and sedimentary rocks, with applicance to Norway. *Norges Geologiske Undersøkelse* p. 53.

Brekke, H. & Riis, F. (1987). Tectonics and basin evolution of the Norwegian shelf between 62^{o} and 72^{o}N. *Norsk Geologisk Tidsskrift* 67: 295-322.

Bukovics, C., Shaw, N. D., Cartier, E. G. & Ziegler, P. A. (1984). Structure and development of the Mid-Norway continental margin. In: *Petroleum Geology of the North European Margin*. A. M. Spencer, S. O. Johnsen & A. Mørket (eds). (Graham & Trotman, London): Norwegian Petroleum Society**:** 407-423.

Caine, J. S., James, P. E. & Forster, G. B. (1996). Fault zone architecture and permeability structure. *Geology* 24 (11): 1025-1028.

Chadwick, R. A. (1986). Extension tectonics in the Wessex Basin, southern England. *Journal of the Geological Society of London* 143: 465-488.

Childs, C., Walsh, J. J. & Watterson, J. (1997). Complexity in fault zone structure and implications for fault seal prediction. In: *Hydrocarbon Seals: Importance for Exploration and Production*. P. Møller-Pedersen & A. G. Koestler (eds). Norwegian Petroleum Society (NPF) Special Publications 7**:** 61-72.

Childs, A. D., Nicol, A., Walsh, J. J. & Watterson, J. (1996a). Growth of vertically segmented normal faults. *Journal of Structural Geology* 18: 1389-1398.

Clausen, J. A., Gabrielsen, R. H., Johnsen, E. & Korstgård, J. (2003). Internal fault geometry and clay smear distribution. Examples from field studies and drained ring-shear experiments. *Norwegian Journal of Geology (NJG)*.

Dart, C. J., McClay, K. & Holling, P. N. (1995). 3D analysis of inverted extensional fault systems, southern Bristol Channel basin, UK. In: *Basin Inversion*. J. G. Buchanan & P. G. Buchanan (eds). Geological Society Special Publications 88**:** 393-413.

Davis, G. H. & Reynolds, S. J. (1996). Structural Geology of Rocks and Regions, *John Wiley & Sons, Inc.* p. 776.

Deeks, N. R. & Thomas, S. A. (1995). Basin inversion in a strike-slip regime: the Tornquist Zone, Southern Baltic Sea. In: *Basin Inversion*. J. G. Buchanan, Buchanan, P. G. (eds). Geological Society Special Publication 88**:** 319-338.

Dennis, J. G. (1967). International tectonic dictionary. *American Association of Petroleum Geologists Memoir* 7: p. 196.

Donath, F. A. (1961). Experimental study of shear failure in anisotropic rocks. *Geological Society of America Bulletin* 72: 985-989.

Doré, A. G. (1991). The structural foundation and evolution Mesozoic seaways between Europe and the Arctic. *Palaeogeography, Palaeoclimatologi, Palaeoecology* 87: 441-492.

Doré, A. G., Lundin, E. R., Fichler, C. & Olesen, O. (1997). Patterns of basement structure reactivation along the NE Atlantic margin. *Journal of the Geological Society of London* 154: 85-92.

Eliassen, H. (In prep). Møre-Trøndelag-forkastningskompleks og betydningen av tverrstrukturer på forkastningsonens utvikling på Møre-kysten. Relasjon til Jan Mayen-lineamentet. Unpublished Cand. Scient. thesis, Department of Earth Science, University of Bergen.

EUGEON-S GROUP (1988). Crustal structure and tectonic evolution of the transition between the Baltic Shield and the North German Caledonides (THE EUGEON-S PROJECT). *Tectonophysics* 150: 253-348.

Færseth, R. B. (1996). Interaction between Permo-Triassic and Jurassic extensional fault-blocks during the development of the northern North Sea. *Journal of the Geological Society of London* 153: 931-944.

Fejerskov, M., Myrvang, A. M., Lindholm, C. D. & Bungum, H. (1995). In-situ rock stress pattern of the Norwegian continental shelf and mainland. In: *Proceedings of the Workshop on Rock Stresses in the North Sea, Trondheim, Norway, 13-14 February 1995*. M. Fejerskov & A. M. Myrvang (eds). SINTEF, Rock and Mineral Engineering, Trondheim, Norway**:** 191-201.

Fossen, H. & Gabrielsen, R. H. (1996). Experimental modeling of extensional fault systems by use of plaster. *Journal of Structural Geology* 18: 673-687.

Gabrielsen, R. H. & Braathen, A. (In press). The architecture of fracture lineaments. *Journal of Structural Geology.*

Gabrielsen, R. H. & Clausen, J. A. (2001). Horses and duplexes in extensional regimes: A scale-modeling contribution. In: *Tectonic models: A Volume in Honor of Hans Ramberg.* (Koyi, H. A., Muncktelow (eds). Geological Society of America Memoir 193: 219-233.

Gabrielsen, R. H., Færseth, R. B., Hamar, G. & Rønnevik, H. C. (1984). Nomenclature for the main tectonic features on the Norwegian continental shelf north of the 62nd and parallel. In: *Petroleum Geology of the North European Margin*. A. M. Spencer, S. O. Johnsen, A. Mørket al (eds). Norwegian Petroleum Society (NPF)**:** 41-60.

Gabrielsen, R. H. & Koestler, A. G. (1987). Description and structural implications of fractures in late Jurassic sandstones of the Troll Field, northern North Sea. *Norsk Geologisk Tidsskrift* 67: 371-381.

Gabrielsen, R. H., Odinsen, T. & Grunnaleite, I. (1999). Structuring of the Northern Viking Graben and the Møre Basin; the influence of basement structural grain, and the particular role of the Møre-Trøndelag Fault Complex. *Marine and Petroleum Geology* 16: 443-465.

Gautneb, H. & Roberts, D. (1989). Geology and petrochemistry of the Smøla-Hitra Batholith, Central Norway. *Norges Geologiske Undersøkelse Bulletin* 416: 1-24.

Gibbs, A. D. (1983). Balanced cross-section construction from seismic sections in areas of extensional tectonics. *Journal of Structural Geology* 5: 153-160.

Gibbs, A. D. (1984). Structural evolution of extensional basin margins. *Journal of Structural Geology* 141: 609-620.

Gravesen, P. (1996). Geologisk set. Bornholm. En beskrivelse af områder af national geologisk interesse, *Geografforlaget* p. 208.

Gravesen, P., Rolle, F. & Surlyk, F. (1982). Lithostratigraphy and sedimentary evolution of the Triassic, Jurassic and Lower Cretaceous of Bornholm, Denmark. *Danmarks Geologiske Undersøgelse* Series B (no. 7).

Grønlie, A. & Torsvik, T. H. (1989). On the origin and age of hydrothermal thorium-enriched carbonate veins and breccias in the Møre-Trøndelag Fault Zone, central Norway. *Norsk Geologisk Tidsskrift* 69: 1-19.

Grunnaleite, I. & Gabrielsen, R. H. (1995). Structure of the Møre Basin, mid-Norway continental margin. *Tectonophysics* 252: 221-251.

Holloway, S. & Chadwick, R. A. (1986). The Sticklepath-Lustleigh fault zone: Tertiary sinistral reactivation of a Variscan dextral strike-slip fault. *Journal of the Geological Society of London* 143: 447-452.

Johnsen, E. (1998). Forkastningers forseglingspotensiale, en forkastningsanalyse basert på feltdata fra Bornholm, Malta og Sinaiørkenen, Egypt. *Unpublished Cand. Scient thesis, Geological Institute, University of Bergen*.

Kamerling, P. (1979). The geology and hydrocarbon habitat of the Bristol Channel Basin. *Journal of Petroleum Geology* 2 (1): 75-93.

Kelly, P. G., Sanderson, D. J. & Peacock, D. C. P. (1998). Linkage and evolution of conjugate strike-slip fault zones in limestones of Somerset and Northumria. *Journal of Structural Geology* 20 (11): 1477-1493.

Knipe, R. J. (1997). Juxtaposition and seal diagrams to help analyze fault seals in hydrocarbon reservoirs. *American Association of Petroleum Geologists Bulletin* 81: 187-195.

Knipe, R. J., Fisher, Q. J., Jones, G., Clennell, M. R., Farmer, A. B., Harrison, A., Kidd, B., McAllister, E., Porter, J. R. & White, E. A. (1997). Fault seal analysis: successful methodologies, application and future directions. In: *Hydrocarbon Seals: Importance for Exploration and Production*. P. Møller-Pedersen & A. G. Koestler (eds). Norwegian Petroleum Society (NPF) Special Publication 7**:** 15-40.

Koestler, A. G. & Erhmann, W. U. (1991). Description of brittle extensional features in chalk on the crest of a salt ridge. In: *The geometry of normal faults.* Roberts, A. M. et al. (eds) Geological Society of London Special Publications 56: 113-124.

Kyrkjebø, R., Gabrielsen, R. H., Braathen, A., Dehls, J., Pascal, C. & F., R. T. (2001). Influence of Transfer lineaments, fracture zones and basin master faults on the tectono-sedimenological development of the Mid-Norwegian shelf. *Structural geology laboratory. University of Bergen* 31: p. 73.

Liboriussen, J., Ashton, P. & Tygesen, T. (1987). The tectonic evolution of the Fennoscandian Border Zone in Denmark. *Tectonophysics* 137: 21-29.

Lindholm, C. D., Bungum, H., Villagran, M. & Hicks, E. (1995). Crustal stress and tectonics in Norwegian regions determined from earthquake focal mechanisms. In: *Rock stresses in the North Sea*. M. Fejerskov & A. M. Myrvang (eds). University of Trondheim/SINTEF**:** 77-91.

Losh, S., Eglinton, L., Schoell, M. & Woods, J. (1999). Vertical and lateral fluid flow related to a large growth fault, South Eugene Island Block 330 Field, offshore Louisiana. *American Association of Petroleum Geology Bulletin* 83: 244-276.

Loyd, A. J., Savage, R. J. G., Stride, A. H. & Donovan, D. T. (1973). The geology of the Bristol Channel floor. *Philosophical transactions of the Royal Society* A274: 595-626.

National Map Centre of Great Britain (2002). Map of Kilve Beach. User-defined (313873 m - 315873 m and 144995 m - 1439000 m).

Nielsen, J. K., Hansen, K. S. & Simonsen, L. (1996). Sedimentology and ichnology of the Robbedale Formation (Lower Cretaceous), Bornholm, Denmark. *Bulletin of the Geological Society of Denmark* 43: 115-131.

Nordgulen, Ø., Solli, A. & Sundvoll, B. (1995). Caledonian granitoids in the Frøya-Froan area, central Norway. *Norges Geologiske Undersøkelse Bulletin* 427: 48-51.

Nystuen, J. P. (1989). Rules and recommendations for naming geological units in Norway. *Norsk Geologisk Tidsskrift* 69: p.111.

Oftedahl, C. (1975). Middle Jurassic graben tectonics in mid-Norway. *Norwegian Petroleum Society (NPF)* 1-21.

Pascal, C. & Gabrielsen, R. H. (2001). Numerical modeling og Cenozoic stress patterns in the mid-Norwegian margin and the northern North Sea. *Tectonics* 20 (4): 585-599.

Peacock, D. C. P. (1996). Problems with extrapolating strain between different scales. *Terra Nova* 8: 361-371.

Peacock, D. C. P. & Sanderson, D. J. (1991). Displacements, segment linkage and relay ramps in normal fault zones. *Journal of Structural Geology* 13 (6): 721-733.

Peacock, D. C. P. & Sanderson, D. J. (1992). Effects of layering and anisotropy on fault geometry. *Journal of the Geological Society of London* 149: 793-802.

Peacock, D. C. P. & Sanderson, D. J. (1993). Estimating strain from fault slip using a line sample. *Journal of Structural Geology* 15 (12): 1513-1516.

Peacock, D. C. P. & Zhang, X. (1993). Field examples and numerical modelling of oversteps and bends along normal faults in cross-section. *Tectonophysics* 234: 147-167.

Rattey, R. P. & Hayward, A. B. (1993). Sequence stratigraphy of a filed rift system: the middle Jurassic to Early Cretaceous basin evolution of the Central and Northern North Sea. In: *Petroleum Geology of North-west Europe*. J. R. Parker (ed). Geological Society of London**:** 215-285.

Sellwood, B. W. (1972). Tidal-flat sedimentation in the Lower Jurassic of Bornholm, Denmark. *Palaeogeography, Palaeoclimatology, Palaeoecology* 11: 93-106.

Seranne, M. (1992). Late Palaeozoic kinematics of the Møre-Trøndelag Fault Zone and adjacent areas, central Norway. *Norsk Geologisk Tidsskrift* 72: 141-158.

Shipton, Z. K. & Cowie, P. A. (2003). A conceptual model for the origin of fault damage zone structures in high-porosity sandstone. *Journal of Structural Geology* 25: 333-344.

Sibson, R. H. (1977). Fault rocks and fault mechanisms. *Geological Society of America Special Paper* 303: 183-203.

Skar, T. & et al. (In prep). Fracture distribution around extensional faults, Kilve, SW England.

Steen, Ø., Sverdrup, E. & Hanssen, T. H. (1998). Predicting the distribution of small faults in a hydrocarbon reservoir by combining outcrop, seismic and well data. In: *Faulting, Fault Sealing and Fluid Flow in Hydrocarbon Reservoirs*. G. Jones, Q. J. Fisher & R. J. Knipe (ed). Geological Society of London Special Publications 147**:** 27-50.

Stewart, S. A. & Argent, J. D. (2000). Relationship between polarity of extensional fault array and presence of detachments. *Journal of Structural Geology* 22: 693-711.

Strömberg, A. G. B. (1976). A pattern of tectonic zones in the western part of the East European Platform. *Geologiska Föreningen i Stockholm Förhandlingar* 98: 227-243.

Teleplan (2001). Digital map of Frøya.

Torske, T. (1983). A Fluidization Breccia in Granite at Skaget, Svellingen, Frøya. *Norges Geologiske Undersøkelse* 380: 107-123.

Torsvik, T. H., Sturt, B. A., Ramsay, D. M., Grønlie, A., Roberts, D., Smethurst, M., Atakan, K., Bøe, R. & Walderhaug, H. J. (1989). Palaeomagnetic constraints on the early history of the Møre-Trøndelag Fault Zone, central Norway. In: *Palaeomagnetic Rotations and Continental Deformation*. C. Kissel & C. Laj (eds). Dordrecht: Kluwer Academic Publishers**:** 431-457.

VARV (1977). Geologi på Bornholm. - *VARV Ekskursionsfører* nr. 1: 96 sider.

Vejbæk, O. V., Stouge, S. & Poulsen, K. D. (1994). Palaeozoic tectonic and sedimentary evolution and hydrocarbon prospectivity in the Bornholm area. *Ministry of Environment and Energy, Series A* 34: 4-23.

Whittaker, A. & Green, G. W. (1983). Geology of the country around Weston-super-Mare, memoir for 1: 50,000 geological sheet 279 New series, with part of sheet 263 and 295, *Geological Survey of Great Britain, Institute of Geological Sciences, Her Majesty's Stationary Office, London.* .

Wojtal, S. F. (1994). Fault scaling laws and the temporal evolution of fault systems. *Journal of Structural Geology* 16 (4): 603-612.

Wojtal, S. F. & Mitra, G. (1986). Strain hardening and strain softening in fault zones from foreland thrusts. *Geological Society of America Bulletin* 97: 674-687.

Wojtal, S. F. & Mitra, G. (1988). Nature of deformation in fault rocks from Appalachian thrusts. In: *Geometries and Mechanisms of Thrusting with Special Reference to the Appalachians*. G. Mitra & S. F. Wojtal (eds). Geological Society of America Special Papers 222**:** 17-33.

Woodcock, N. H. & Schubert, C. (1994). Continental strike-slip tectonics. In: *Continental deformation*. P. L. Hancock (ed). Pergamon Press**:** 251-263.

Woodward, N. B., Wojtal, S. F., Paul, J. B. & Zadins, Z. Z. (1988). Partitioning of deformation within several external thrust zones of the Appalachians. *Journal of Geology* 96: 351-361.

Internet address:

http://www.geography.about.com